

UCSF

UC San Francisco Electronic Theses and Dissertations

Title

Protease-activated receptor-2 (PAR2) in epithelial biology

Permalink

<https://escholarship.org/uc/item/2b49z9sm>

Author

Barker, Adrian

Publication Date

2013

Peer reviewed|Thesis/dissertation

Protease-activated receptor-2 (PAR2) in epithelial biology

by

Adrian Barker

DISSERTATION

Submitted in partial satisfaction of the requirements for the degree of

DOCTOR OF PHILOSOPHY

in

Biomedical Sciences

in the

GRADUATE DIVISION

of the

UNIVERSITY OF CALIFORNIA, SAN FRANCISCO

*To my nephews for being the light of my life
To my parents for showing me the way
To Philip, your love knows no bounds*

ACKNOWLEDGEMENTS

Wow, what a journey! First, I'd like to thank my mentor and advisor, Dr. Shaun Coughlin, for giving me the encouragement and wisdom that I needed to succeed in your lab. One thing I will take away from this experience is how powerful collaboration can be. Having encountered labs that have not been willing to collaborate, you are an inspiration and role-model in your willingness to share your resources and knowledge with the scientific community and the academic world is a better place because of it.

To my thesis committee members, Dr. Charly Craik & Dr. Zena Werb. Thank you for the conversations and encouragement. You have given me motivation and kind words in pivotal moments in my career and they have helped me tremendously; more than you'll ever know.

To all the members of the Coughlin lab. We've been through so much together, and many of you have been around since the first day I stepped foot into the lab. Extra special thanks to: Dr. Hilary Clay, for help with the zebrafish work and for fighting for my project when it felt like no one else cared; Dr. Stephen Wilson, for help with any and all things cell culture; Dr. Yao-Wu Zheng, the king of cloning and just a remarkable human being; Dr. Yoga Srinivasan, for sharing your love of books with me; Dr. Yamini Bynagari, for being my go-to person for bouncing ideas off of; and Dr. Antonino Schepis, for the zebrafish knowledge and all of the help with the project over the last year. To the amazing support system for the Coughlin lab: Leonor Patel, for help with everything

literally from A to Z; Aja Bogtong, for the weekly chats (I love seeing the family photos and hearing about your weekend). And an extra special thanks to Marie Demcho-Wagor, for being there for me and for everyone else in the lab. Our lab would not run as smoothly as it does if it wasn't for you and I don't think people tell you this enough.

To all the previous members of the Coughlin lab who have moved on to other endeavors. Some of my most important memories from the lab involve these people: Ivo Cornelissen, Dr. Eric Camerer, Dr. Erica DeCandia, Dr. Gallia Levy, Dr. Jean Regard, & Dr. Dan Palmer. You made the lab social and collaborative and made me realize that Europeans (and Canadians!) know how to have the most fun! Thanks to all of you, I have a network throughout Europe if I ever decide to move back. One extra special thanks to Dr. Marie Terpager. We were really close by the time you left the lab and it was so nice to have a kindred spirit to share in this experience with me. I miss you, Dan, and Sebastian. To my good friend and the most beautiful woman I know, Dr. Joana Borlido. The past year has been incredible and we've shared a very special bond from the very first meeting.

One thing that has kept me sane during this whole process is my devotion to exercise. My life has changed so much in every single way since I joined the gym. Now, I'm a scientist by day and a group fitness instructor by night and it gives me so much fulfillment to give back to our community what I myself was able to receive. To my 02 Athletics family (and especially James Cook): you helped me realize my potential and that there are no limits to what you can do.

I'm where I am now because of all of you. To my Les Mills family: this is a lifestyle and I expect to be doing this for the rest of my life. Thank you for the teaching and learning opportunities, for the amazing support group of instructors, and to the brutal and results-driven programs that you offer. The last few years of my life were spent in so many BodyPump & BodyCombat classes and I'm so happy to have expanded on that repertoire.

Finally, I'd like to thank my family and closest friends. To my parents, Susan and Peter, literally for everything. I can't begin to express how much it means to me that you have been supportive every step of the way. I know I don't tell you this enough but it means everything to me. Thank you! To my amazing younger brother Danny, I'm so proud of all of your accomplishments and am excited to see what your life journey takes you. To Chris & Megan: thank you for the support and for being an important part of my family. To my nephews, Lucas, Brett & Caleb: one of the greatest joys in my life is being able to see you, play with you, and wrestle with you. I hope to give you some cousins soon for you to play with! I love all of you so much!

Thank you to my grandparents and my Uncle Alan and his husband, Nick. Even from afar, you have been the most incredible support system and I love you with all of my heart. I wish we could see each other more frequently. And to my closest friend, Monica Denevan. What a journey, huh? From meeting at the gym, to 02 Athletics bootcamp, and to developing a strong bond that will never be broken. I love our fancy dinners, our wine and martini drinking, our movie nights at Kabuki, our insane workout schedules.

And last but certainly not least, to my fiancé, Philip Thomas. I feel very blessed to have met the person who lights up my life. You mean the world to me and I can't wait to begin our life's journey together. We have so much ahead of us! Thank you for putting up with my crazy teaching schedule and for loving me for me. It is so hard to find someone who will put up with all of your nonsense and you do that with (almost always) a smile on your face. I love you so much!

This dissertation contains data published in the following report:

Camerer E, Barker A, Duong DN, Ganesan R, Kataoka H, Cornelissen I, Darragh MR, Hussain A, Zheng YW, Srinivasan Y, Brown C, Xu SM, Regard JB, Lin CY, Craik CS, Kirchhofer D, Coughlin SR. Local protease signaling contributes to neural tube closure in the mouse embryo. *Dev Cell*. 2010; 18(1):25-38.

Statement from Dr. Shaun Coughlin:

This is to describe Mr. Adrian Barker's contribution to the publication that represents Chapter 2 of his Ph.D. thesis. The study was based on an observation made by postdoctoral fellow Eric Camerer that loss of protease-activated receptor-2 (Par2) and Par1 function led to neural tube defects in mouse embryos and evidence that Par2 is expressed in surface ectoderm at the time and place of neural tube closure. The protease(s) that activate Par2 physiologically were unknown. With Dr. Camerer, Mr. Barker drove the development of a TaqMan-based assay to quantitate ~125 mRNAs encoding all serine proteases and protease-activated receptors (PARs) as well as a subset of protease inhibitors in mouse tissues. This led to the finding that matriptase, prostasin, their inhibitors, and Par2 are co-expressed in most epithelia, suggesting that these molecules might comprise a physiological signaling module. It also enabled confirmation that these genes are expressed at the right time and in the right cell type to contribute to neural tube closure. Mr. Barker adapted the alkaline phosphatase release assay to mouse Par2 and

demonstrated quantitatively that matriptase efficiently cleaves Par2 at its activation site. He also performed cell-based and biochemical assays that demonstrated Par2-dependent matriptase signaling and a "cascade" in which prostasin activates matriptase, which in turn activates Par2. These findings form the rationale and foundation for the work described in Chapter 3 aimed at better demonstrating a physiological role for Par2 activation by matriptase and defining this role in cells and tissues.

Protease-activated receptor-2 (PAR2) in epithelial biology

by

Adrian Barker

Abstract

Protease-activated receptor-2 is a G-protein-coupled receptor involved in inflammatory and pain responses, as well as pathogenesis in the gastrointestinal and cardiovascular systems, among others. Efforts to identify the serine protease(s) involved in activation of Par2 in vivo have so far been unsuccessful. Here we describe novel roles for Par2 in two animal models: mouse and zebrafish, as well as identify matriptase as a key activator of Par2 in vivo.

We report an unexpected role for protease signaling in neural tube closure and formation of the central nervous system. Mouse embryos lacking protease-activated receptor 1 and 2 showed defective hindbrain and posterior neuropore closure and developed exencephaly and spina bifida, important human congenital anomalies. *Par1* and *Par2* were expressed in surface ectoderm, *Par2* selectively along the line of closure. Ablation of $G_{i/z}$ and Rac1 function in these *Par2*-expressing cells disrupted neural tube closure, further implicating G protein-coupled receptors and identifying a likely effector pathway. Cluster analysis of protease and Par2 expression patterns revealed a group of membrane-tethered proteases often co-expressed with Par2. Among these, matriptase activated Par2 with picomolar potency, and hepsin and prostasin activated matriptase. Together, our results suggest a role for protease-activated receptor signaling in

neural tube closure and identify a local protease network that may trigger Par2 signaling and monitor and regulate epithelial integrity in this context.

We also describe a role for Par2 in zebrafish embryos. Hai1a morphants exhibit skin defects including keratinocyte aggregation and shedding, as well as chronic inflammation and ultimately death. Co-knockdown of matriptase or Par2b rescues this phenotype. Further examination of Hai1a morphants reveals keratinocytes that are extruded from the skin, characterized by contraction of an actin-myosin ring around the ejected cell; Par2b knockdown rescues this. Cell extrusion in this context is not apoptosis dependent as extruding cells were negative for caspase-3 and TUNEL stain.

Our data taken together suggests important roles for Par2 in epithelial biology as well as identifies matriptase as an important activator of Par2 in animal models.

TABLE OF CONTENTS

Chapter 1: Introduction

Overview of Project_____	1
G-protein coupled receptors_____	2
Protease-activated receptors_____	3
Type II Transmembrane Serine Proteases_____	5
Matriptase_____	5
Matriptase in normal physiological responses_____	8
Epithelial cell extrusion_____	11
References_____	13

Chapter 2: Local protease signaling contributes to neural tube closure in the mouse embryo

Summary_____	18
Introduction_____	19
Results_____	20
Discussion_____	52
Experimental Procedures_____	60
Acknowledgements_____	71
References_____	72

Chapter 3: Matriptase Orchestrates Epithelial Cell Extrusion in the Zebrafish Embryo in a Protease-Activated Receptor 2-Dependent Manner.

Background_____	78
-----------------	----

Results	79
Discussion	103
Materials and Methods	107
References	112
Chapter 4	
Summary	115
References	120
Chapter 5: Appendix	
List of Taqman primer/probe sets	121
Complete Taqman protease array cluster analysis	126

LIST OF FIGURES

Figure 1.1. Mechanism of Par1 activation_____	4
Figure 1.2. Structure of matriptase_____	7
Figure 1.3. Hai1a is expressed in basal keratinocytes and is required for the proper development of the epidermis_____	10
Figure 1.4. Actin and myosin assemble into a ring during extrusion of apoptotic cells_____	12
Figure 2.1. Targeting the Par locus on mouse chromosome 13: strategy and effects on postnatal survival_____	23
Figure 2.2. Phenotypes associated with combined deficiency of Par2 and Par1_____	24
Figure 2.3. Localized expression of <i>Par2</i> in surface ectoderm and characterization of a surface ectoderm Cre (<i>Grhl3</i> ^{Cre})_____	26
Figure 2.4._____	27
Figure 2.5. Generation of a mouse line expressing Cre recombinase surface ectoderm_____	30
Figure 2.6. Abrogating G _i function and Rac1 expression in surface ectoderm causes neural tube defects_____	34
Figure 2.7. Identification of candidate Par2 activators expressed during neural tube closure_____	37
Figure 2.8. Matriptase with antibody-accessible active site is present on the surface ectoderm ridge at the time of neural tube closure_____	39

Figure 2.9. Par2 cleavage in HaCaT cells by prostaticin and matriptase requires an intact activating cleavage site in Par2_____	44
Figure 2.10. Par2 cleavage and activation by membrane-associated proteases_____	45
Figure 2.11. Evidence for a cascade from prostaticin and hepsin to matriptase to Par2 activation_____	49
Figure 2.12. In a fibroblast cell line, expression of matriptase, but not active site mutant or zymogen conversion site mutant matriptase, expression confers prostaticin-induced Par2 cleavage and signaling_____	50
Figure 3.1. St14 knockdown rescues Hai1 zebrafish morphants_____	82
Figure 3.2. Matriptase knockdown rescues Hai1 morphants_____	83
Figure 3.3. Alignment of zPar2b from cloned sequence and Ensembl published sequence_____	86
Figure 3.4. Zebrafish Par2b is functional in cell culture-based assay_____	87
Figure 3.5. Taqman qRT-PCR data of proteins enriched in keratinocytes of 24 hpf zebrafish embryos_____	88
Figure 3.6. Matriptase is expressed in the skin of zebrafish embryos_____	89
Figure 3.7. Par2b knockdown rescues skin aggregation and shedding in Hai1a morphants_____	91
Figure 3.8. Par2b translation blocking morpholino rescues Hai1 morphants_____	92
Figure 3.9. Par2b splice blocking morpholino rescues Hai1 morphants_____	93
Figure 3.10. Par2b knockdown rescues extravasation of leukocytes_____	94

Figure 3.11. Keratinocytes are extruded from the skin of Hai1a morphants_	97
Figure 3.12. Caspase-3 staining of extruding keratinocytes_____	99
Figure 3.13. Inhibition of apoptosis does not block the Hai1a phenotype__	100
Figure 3.14. Matriptase is active at sites of epithelial cell extrusion_____	102
Figure 4.1. A proposed model of signaling pathway_____	119

Chapter 1

INTRODUCTION

Overview of Project

The epithelium is a deceptively complex tissue, composed of either a single or double cell layer or of multiple cell layers. Once thought of as merely a physical barrier to the environment, the epithelium is, in fact, a highly complex tissue that is incredibly dynamic, exhibiting both internal and external regulation. One can imagine the epithelium as not only the castle wall, but also the sentry that keeps watch from the high tower. When an intruder attempts to invade the castle, the wall acts as a first line of physical defense against such an invasion. There are also mechanisms in place to fortify the castle if stronger defenses are necessary. On the other hand, foreigners to the castle may be scrutinized by the guard sentry before the castle gate is lowered. In much the same way, the epithelium acts as both barrier and sensor of the environment; the epithelium can be regulated in such a way as to allow or disallow certain molecules from entering or leaving.

To further add to the complexity, as is often found in biological systems, the epithelium is not an island unto its own. There is a complex interplay between the epithelium and surrounding tissues. One of the most well-known is that between the epithelium and the immune system (Berin et al., 1999).

When the epithelium misbehaves, the results can be devastating for the organism. The majority of human cancers are epithelial in origin, for instance.

Although this dissertation does not specifically describe roles of epithelium during cancer development, the data is suggestive of potential interplay between normal epithelial biology and cancer biology. Other examples of epithelial pathogenesis include diseases of the digestive tract, including inflammatory bowel disease (IBD) and colitis. Therefore, understanding the biology of the epithelium is critical to our understanding of how complex organisms work, how the disruption of normal cell behavior and processes contribute to pathology, and how we might treat or cure certain epithelial diseases.

In this study, we describe two stories involving epithelial pathology and the study of how epithelial tissues are regulated. The first, in Chapter 2, describes the importance for a G-protein-coupled receptor (GPCR) in regulation of the surface ectoderm during neural tube closure in the mouse embryo. The second story discusses the role of a serine protease in maintenance of the epithelial barrier, and how disruption of this protease causes disease in zebrafish skin. Both stories highlight the importance of the epithelium in normal biological function as well as progression to pathology.

G-protein-coupled receptors

G-protein-coupled receptors (GPCRs) are the largest family of integral membrane proteins, with about 4% of the human genome encoding almost 1000 GPCRs. GPCRs are found in almost every living organism, from a single-celled yeast to the most complex of organisms. GPCRs are involved in practically every important biological function imaginable and from a commercial standpoint,

about 30% of all marketed therapeutics target GPCRs (Kroeze et al., 2003).

Thus, understanding GPCRs is critical for understanding biology, as well as how to treat or cure diseases.

GPCRs are 7-transmembrane protein receptors; they have seven domains that traverse the plasma membrane in a serpentine pattern, typically starting with an extracellular and ending with an intracellular domain. GPCRs are important in signal transduction, the process of cell-cell communication. How a tissue is regulated as well as how this tissue interacts with other tissues oftentimes involves GPCRs so that cells may “talk” to one another (Kobilka, 2007).

Protease-Activated Receptors

The protease-activated receptors (PARs) are a small subfamily of GPCRs with four known members to date, Par1, Par2, Par3, & Par 4. These receptors are commonly referred to as the thrombin receptors as all but Par2 are activated by the coagulation protease, thrombin (Coughlin, 2005).

PARs have a mechanism of activation that is unique amongst GPCRs (Coughlin & Camerer, 2003) (Figure 1.1). They present a protease cleavage site on the ectodomain of the receptor that is recognized by thrombin or another serine protease. The activating protease then cleaves the PAR, generating a new N-terminus that acts as a tethered ligand that in turn, activates the PAR receptor. Thus, activation of a PAR is an irreversible reaction.

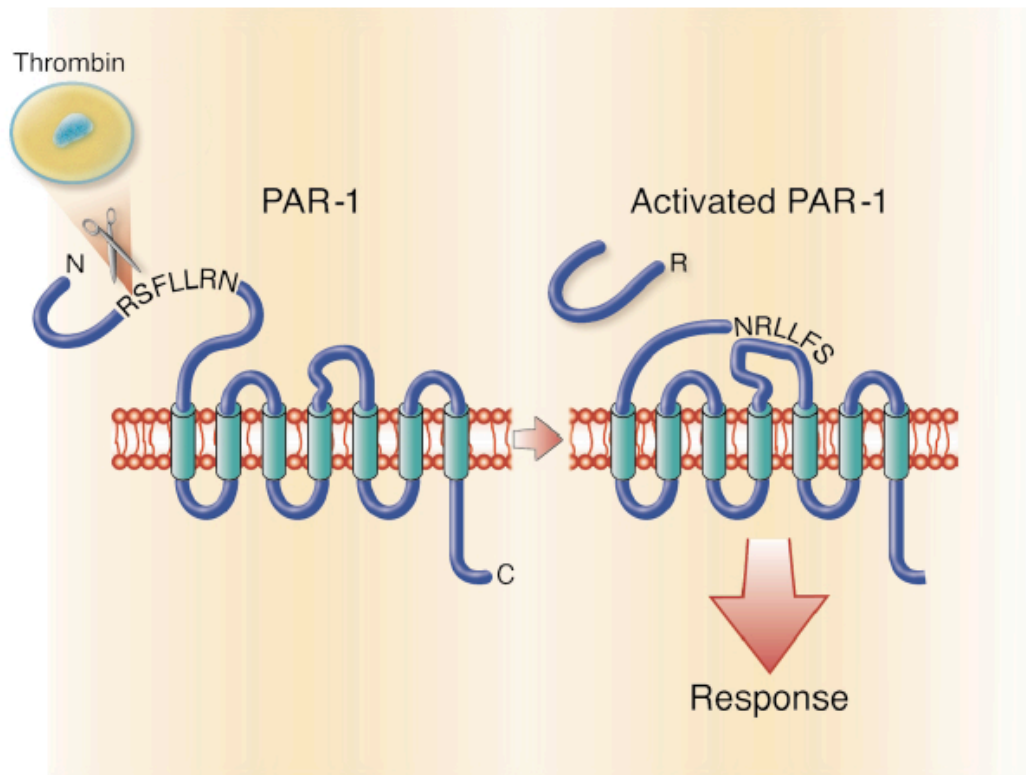


Figure 1.1. Mechanism of Par1 activation. The N-terminus of PAR-1, a seven transmembrane domain G protein–coupled receptor, contains a protease cleavage site that, once cleaved by thrombin, results in a new N-terminus. The new N-terminal sequence, SFLLRN, acts as a tethered ligand and binds intramolecularly to the heptahelical body of the receptor to effect transmembrane signaling and G protein activation. From Coughlin SR & Camerer E, *J Clin Invest*, 2003.

Type-II Transmembrane Serine Proteases (TTSPs)

A subfamily of serine proteases has been recently described: the Type-II Transmembrane Serine Proteases (Bugge et al., 2009). These proteases have the following key elements: an N-terminal transmembrane domain, an extracellular C-terminal serine protease domain containing the catalytic triad of histidine, aspartic acid and serine, and a stem domain that contains a variety of protein domains. There are currently 17 members of the family (Figure 1.2). We became interested in the TTSP matriptase because of previous studies that showed matriptase to be an activator of Par2 in *Xenopus* oocytes (Takeuchi et al., 2000). Oocytes stimulated with soluble matriptase displayed increased Ca^{++} release that was Par2 dependent.

Matriptase

Matriptase (gene name: St14; also known as MT-SP1) is perhaps the most widely studied of the TTSPs and was the first family member to be described. It was originally described as a new gelatinolytic activity in the supernatant of cultured breast cancer cell lines and was eventually cloned and identified (Shi et al., 1993). Matriptase is an 80-90 kDa protein that undergoes complex regulation and processing.

Matriptase contains a short intracellular tail, an N-terminal transmembrane domain, a stem region containing multiple protein domains, and a C-terminal serine protease domain. The function of its intracellular tail is currently unknown. The stem region contains a sperm protein, enterokinase, & agrin (SEA) domain,

two complement C1r/C1s, Uegf, Bmp1 (CUB) domains, and four low-density lipoprotein receptor class A (LDLRa) domains (Bugge et al., 2007) (Figure 1.2). The function of these domains is poorly understood but it is thought that they play a role in proper processing and regulation of the matriptase enzyme (Oberst et al., 2003).

Activation of matriptase is a complex and unique process among serine proteases and is not completely understood. Matriptase undergoes two cleavage events to render an active protease: the first cleavage event occurs at Gly149 in the SEA domain generating a mature inactive (zymogen) form, the second cleavage event occurs at Arg614 in the C-terminal protease domain to form an active enzyme. Both cleavage events must occur to generate a fully active matriptase (Figure 1.2). Cleavage at Gly149 does not release the enzyme from the cell surface; rather, it is believed that non-covalent interactions within the SEA domain anchor the protease to the membrane (Cho et al., 2001). The activation cleavage of matriptase forms a two-chain form of the protein, held together by a disulfide bond. Two commonly used monoclonal antibodies can distinguish between these two forms: M24 (or M32) interacts with one of the LDLRa domains to recognize both forms of the enzyme, whereas M69 interacts with the disulfide bond created by activation cleavage, thus recognizing only the two-chain (“active”) form of the enzyme (Benaud et al., 2001).

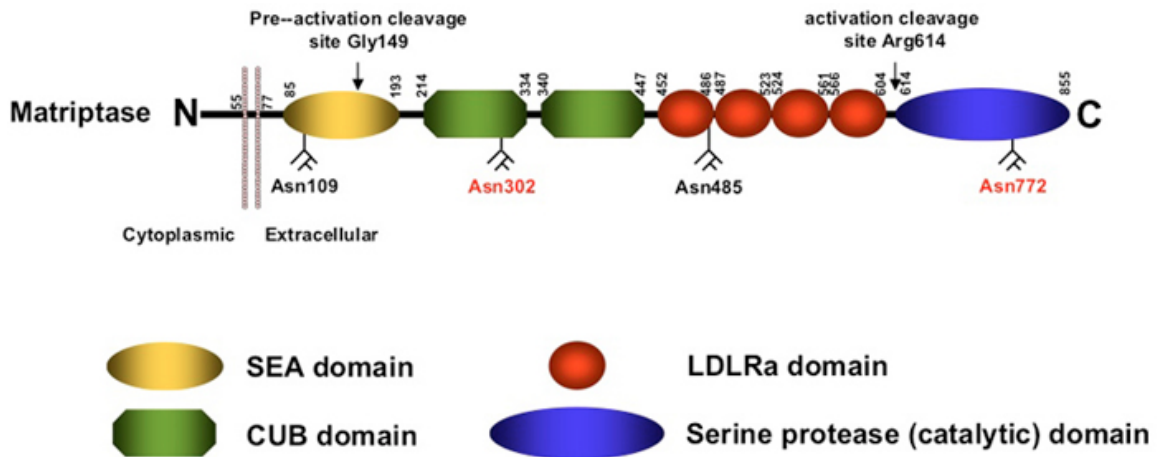


Figure 1.2. **Structure of matriptase.** Matriptase is a type II transmembrane protein consisting of a short cytoplasmic tail (amino acids 1-54), a single pass transmembrane domain (amino acids 56-77), a SEA domain (amino acids 85-193), two CUB domains (amino acids 214-334 and 340-447), four LDLRa domains (amino acids 452-486, 487-523, 524-561, and 566-604), and a C-terminal serine protease domain (amino acids 614-855). Matriptase is proteolytically-activated by an initial cleavage of the SEA domain after Gly149 (arrow), followed by autocatalytic cleavage after Arg614 within the conserved activation cleavage site (arrow). Matriptase is glycosylated at Asn109, Asn302, Asn485, and Asn772. The Asn302 and Asn772 glycans (denoted in red) are required for matriptase activation. From List et al., *Front Biosci*, 2007.

Numerous substrates for matriptase have been described including prostaticin, urokinase plasminogen activator (uPA) (Takeuchi et al., 2000; Lee et al., 2000), epidermal growth factor (EGF) (Chen et al., 2008), hepatocyte growth factor (HGF) (Lee et al., 2000), and Par2 (Takeuchi et al., 2000); however, it is unclear which substrates are relevant in vivo and what roles, if any, these play in physiological or pathophysiological conditions. Matriptase is also known to autoactivate in vitro (Oberst et al., 2003).

The biosynthetic pathway of matriptase is complex and tightly regulated. In the earliest studies describing matriptase, it was observed that matriptase was shed into breast cancer cell-conditioned medium in complex with another

molecule. This was identified as hepatocyte growth factor activator inhibitor-1 (Hai1), a Kunitz-type serine protease inhibitor. Co-expression of matriptase and Hai1 is found in nearly all cell types and tissues (Oberst et al., 2001; Camerer et al., 2010). Interestingly, Hai1 is also important for proper trafficking of matriptase to the plasma membrane (Oberst et al., 2005). In our hands as well as others, we are unable to express matriptase in vitro in the absence of Hai1, either due to improper trafficking or processing of the enzyme or due to toxicity to the cell. In a study examining 54 epithelial ovarian tumors, the ratio of Hai1:matriptase was correlative with tumor stage. Out of 34 stage I/II tumors, 82% were positive for matriptase and 10% were positive for Hai1, with 10% showing coexpression. However, of 20 stage III/IV tumors examined, 11% expressed matriptase and only 1% for Hai1 (Oberst et al., 2002). Thus, it appears that an imbalance between matriptase and Hai1 correlates with tumor stage. This evidence speaks to the importance of this interaction and will be discussed in great detail in this dissertation.

Matriptase in normal physiological responses

In an effort to determine the normal role for matriptase in vivo, matriptase was knocked out in a mouse (St14 KO). The mice appeared grossly normal until gestation, with lethality occurring within 48 hours of birth. St14 KO mice had wrinkly, dry, red skin and presumably died from dehydration due to a compromised epidermal barrier (List et al., 2002). Later studies identified prostasin as a substrate for matriptase as prostasin knockout mice phenocopy the matriptase

knockouts (Leyvraz et al., 2005; Netzel-Arnett et al., 2006). To get around the postnatal lethality in order to study the role of matriptase in older animals, a conditional knockout mouse was made in which exon 2 was flanked with loxP sites; this group knocked out matriptase in the intestinal epithelium using villin-Cre. These mice were significantly smaller in size compared to littermate controls and they typically died within a few weeks to a couple months due to severe dehydration (List et al., 2009). Thus, the evidence suggested that matriptase plays an important role in epithelial barrier integrity.

To study this hypothesis a little further, Buzza et al. used cell culture techniques to study the role of matriptase in Caco2 cells, a human epithelial colorectal adenocarcinoma cell line. When they chemically inhibited or knocked down matriptase using small-interfering RNAs (siRNAs), they found that the Caco2 monolayer was leaky as measured by transepithelial electrical resistance (TEER). They went on to show that these cells deficient for matriptase had enhanced Claudin-2 expression, a cell-cell junction protein that is often associated with a more permissive or “leakier” epithelium (Buzza et al., 2010).

But what about too much matriptase? Are there opposite effects of having an abundance of or uncontrolled matriptase activity? To address this, List et al. created a transgenic mouse overexpressing matriptase specifically in the skin. These mice spontaneously formed squamous cell carcinoma as well as enhanced carcinogen-induced tumor formation, which was rescued by overexpressing Hai1, again highlighting the importance of balancing Hai1:matriptase ratios (List et al., 2005).

In 2007, Carney et al. performed a mutagenesis screen on zebrafish embryos attempting to identify genes that were important in skin development. They identified a number of mutants with skin defects and among these was a mutant for Hai1. The Hai1 mutant showed keratinocyte rounding and shedding which was rescued by knockdown of matriptase, suggesting that the defect was matriptase-dependent. Hai1 mutants also showed chronic inflammatory responses with extravasation of neutrophils to wounded sites, but this was determined to be secondary to the skin defect (Carney et al., 2007).

Thus, numerous studies have linked matriptase and the inhibitor, Hai1, to normal epithelial development as well as pathogenesis.

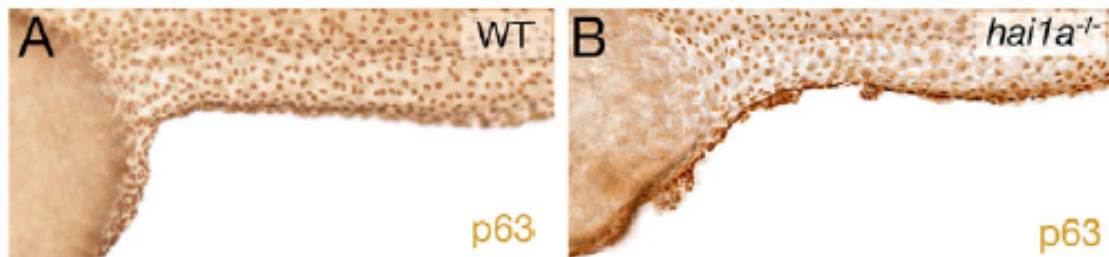


Figure 1.3. Hai1a is expressed in basal keratinocytes and is required for the proper development of the epidermis. (A,B) Lateral views of the trunk of a wild-type sibling (WT; A) and a homozygous hi2217embryo ($hai1a^{-/-}$; B) at 48 hpf, after anti-p63 immunolabeling of basal keratinocytes. From Carney et al., *Development*, 2007.

Epithelial Cell Extrusion

In 2001, the Rosenblatt group was the first to fully appreciate the process known as epithelial cell extrusion. This phenomenon had been described before but not in much detail. When an epithelial cell becomes apoptotic, the Rosenblatt group found that neighboring cells contract an actin-myosin ring around the dying cell and squeeze the cell out of the monolayer. The space left behind by the removed cell is then filled in by the neighboring cells to prevent any holes from forming in the monolayer (Rosenblatt et al., 2001). This same group has been instrumental in defining the cell extrusion pathway in cell culture and in zebrafish embryos. They found that the bioactive lipid mediator, sphingosine-1-phosphate (S1P) is released by the apoptotic cell, binds to the S1P receptor, S1pr2, on neighboring cells to trigger the extrusion pathway (Gu et al., 2011).

Perhaps even more interesting is that live cells also appear to extrude. In a defining study, the Rosenblatt group demonstrated that cell crowding is a trigger for cell extrusion, perhaps as a method to “thin out” a crowded monolayer. These extruded cells were alive and could be plated and grown under culture conditions. They demonstrated that many of the same pathways involved with apoptotic cell extrusion were also important in live cell extrusion (Eisenhoffer et al., 2012).

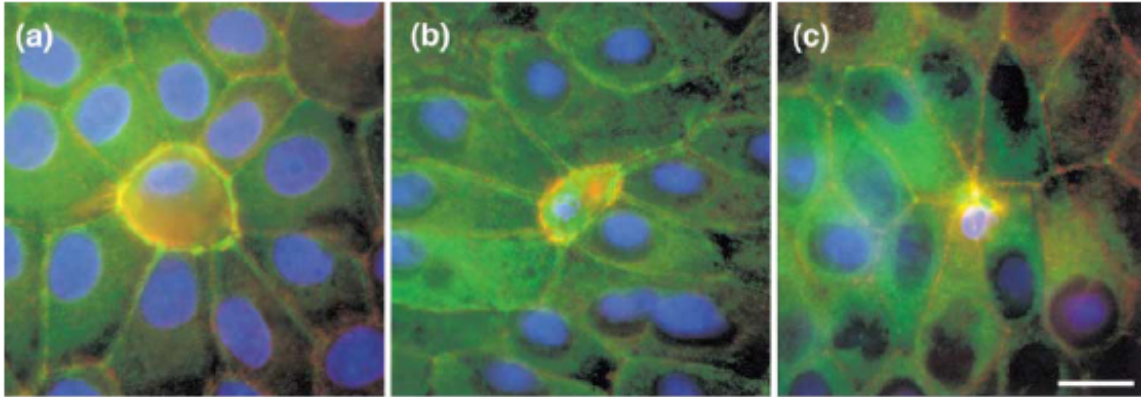


Figure 1.4. Actin and myosin assemble into a ring during extrusion of apoptotic cells. Triple staining of myosin II (green), actin (red), and DNA (blue) shows that actin and myosin II colocalize (yellow) at the interface between the apoptotic cell and its neighbors at **(a)** early, **(b)** middle, and **(c)** late stages of apoptotic cell extrusion. For (a–c), actin and myosin were photographed in the plane of the ring, while DNA was photographed in the plane of the apoptotic nucleus. Note that an apoptotic nucleus moves out of the plane of the other nuclei, as it is extruded from the monolayer. From Rosenblatt et al., *Curr Biol.*, 2001.

In our studies, we have demonstrated that Par2 plays an important role in two distinct models: during neural tube closure in mouse embryos and in skin development in zebrafish embryos. We will show that matriptase triggers Par2-dependent responses in vivo and in vitro. We also define a possible role for matriptase-Par2 in epithelial cell extrusion in zebrafish embryos.

References

- Benaud, C., Dickson, R.B., and Lin, C.Y. (2001). Regulation of the activity of matriptase on epithelial cell surfaces by a blood-derived factor. *Eur J Biochem* 268, 1439-1447.
- Berin, M.C., McKay, D.M., and Perdue, M.H. (1999). Immune-epithelial interactions in host defense. *Am J Trop Med Hyg* 60, 16-25.
- Bugge, T.H., Antalis, T.M., and Wu, Q. (2009). Type II transmembrane serine proteases. *J Biol Chem* 284, 23177-23181.
- Bugge, T.H., List, K., and Szabo, R. (2007). Matriptase-dependent cell surface proteolysis in epithelial development and pathogenesis. *Front Biosci* 12, 5060-5070.
- Buzza, M.S., Netzel-Arnett, S., Shea-Donohue, T., Zhao, A., Lin, C.Y., List, K., Szabo, R., Fasano, A., Bugge, T.H., and Antalis, T.M. (2010). Membrane-anchored serine protease matriptase regulates epithelial barrier formation and permeability in the intestine. *Proc Natl Acad Sci U S A* 107, 4200-4205.
- Carney, T.J., von der Hardt, S., Sonntag, C., Amsterdam, A., Topczewski, J., Hopkins, N., and Hammerschmidt, M. (2007). Inactivation of serine protease Matriptase1a by its inhibitor Hai1 is required for epithelial integrity of the zebrafish epidermis. *Development* 134, 3461-3471.
- Chen, M., Chen, L.M., Lin, C.Y., and Chai, K.X. (2008). The epidermal growth factor receptor (EGFR) is proteolytically modified by the Matriptase-Prostasin serine protease cascade in cultured epithelial cells. *Biochim Biophys Acta* 1783, 896-903.
- Cho, E.G., Kim, M.G., Kim, C., Kim, S.R., Seong, I.S., Chung, C., Schwartz, R.H., and Park, D. (2001). N-terminal processing is essential for release of epithin, a mouse type II membrane serine protease. *J Biol Chem* 276, 44581-44589.
- Coughlin, S.R. (2005). Protease-activated receptors in hemostasis, thrombosis and vascular biology. *J Thromb Haemost* 3, 1800-1814.
- Coughlin, S.R., and Camerer, E. (2003). PARticipation in inflammation. *J Clin Invest* 111, 25-27.
- Eisenhoffer, G.T., Loftus, P.D., Yoshigi, M., Otsuna, H., Chien, C.B., Morcos, P.A., and Rosenblatt, J. (2012). Crowding induces live cell extrusion to maintain homeostatic cell numbers in epithelia. *Nature* 484, 546-549.

Gu, Y., Forostyan, T., Sabbadini, R., and Rosenblatt, J. (2011). Epithelial cell extrusion requires the sphingosine-1-phosphate receptor 2 pathway. *J Cell Biol* *193*, 667-676.

Kobilka, B.K. (2007). G protein coupled receptor structure and activation. *Biochim Biophys Acta* *1768*, 794-807.

Kroeze, W.K., Sheffler, D.J., and Roth, B.L. (2003). G-protein-coupled receptors at a glance. *J Cell Sci* *116*, 4867-4869.

Lee, S.L., Dickson, R.B., and Lin, C.Y. (2000). Activation of hepatocyte growth factor and urokinase/plasminogen activator by matriptase, an epithelial membrane serine protease. *J Biol Chem* *275*, 36720-36725.

Leyvraz, C., Charles, R.P., Rubera, I., Guitard, M., Rotman, S., Breiden, B., Sandhoff, K., and Hummler, E. (2005). The epidermal barrier function is dependent on the serine protease CAP1/Prss8. *J Cell Biol* *170*, 487-496.

List, K., Haudenschild, C.C., Szabo, R., Chen, W., Wahl, S.M., Swaim, W., Engelholm, L.H., Behrendt, N., and Bugge, T.H. (2002). Matriptase/MT-SP1 is required for postnatal survival, epidermal barrier function, hair follicle development, and thymic homeostasis. *Oncogene* *21*, 3765-3779.

List, K., Kosa, P., Szabo, R., Bey, A.L., Wang, C.B., Molinolo, A., and Bugge, T.H. (2009). Epithelial integrity is maintained by a matriptase-dependent proteolytic pathway. *Am J Pathol* *175*, 1453-1463.

List, K., Szabo, R., Molinolo, A., Sriuranpong, V., Redeye, V., Murdock, T., Burke, B., Nielsen, B.S., Gutkind, J.S., and Bugge, T.H. (2005). Deregulated matriptase causes ras-independent multistage carcinogenesis and promotes ras-mediated malignant transformation. *Genes Dev* *19*, 1934-1950.

Netzel-Arnett, S., Currie, B.M., Szabo, R., Lin, C.Y., Chen, L.M., Chai, K.X., Antalis, T.M., Bugge, T.H., and List, K. (2006). Evidence for a matriptase-prostasin proteolytic cascade regulating terminal epidermal differentiation. *J Biol Chem* *281*, 32941-32945.

Oberst, M., Anders, J., Xie, B., Singh, B., Ossandon, M., Johnson, M., Dickson, R.B., and Lin, C.Y. (2001). Matriptase and HAI-1 are expressed by normal and malignant epithelial cells in vitro and in vivo. *Am J Pathol* *158*, 1301-1311.

Oberst, M.D., Chen, L.Y., Kiyomiya, K., Williams, C.A., Lee, M.S., Johnson, M.D., Dickson, R.B., and Lin, C.Y. (2005). HAI-1 regulates activation and expression of matriptase, a membrane-bound serine protease. *Am J Physiol Cell Physiol* *289*, C462-470.

Oberst, M.D., Johnson, M.D., Dickson, R.B., Lin, C.Y., Singh, B., Stewart, M., Williams, A., al-Nafussi, A., Smyth, J.F., Gabra, H., *et al.* (2002). Expression of the serine protease matriptase and its inhibitor HAI-1 in epithelial ovarian cancer: correlation with clinical outcome and tumor clinicopathological parameters. *Clin Cancer Res* 8, 1101-1107.

Oberst, M.D., Williams, C.A., Dickson, R.B., Johnson, M.D., and Lin, C.Y. (2003). The activation of matriptase requires its noncatalytic domains, serine protease domain, and its cognate inhibitor. *J Biol Chem* 278, 26773-26779.

Rosenblatt, J., Raff, M.C., and Cramer, L.P. (2001). An epithelial cell destined for apoptosis signals its neighbors to extrude it by an actin- and myosin-dependent mechanism. *Curr Biol* 11, 1847-1857.

Shi, Y.E., Torri, J., Yieh, L., Wellstein, A., Lippman, M.E., and Dickson, R.B. (1993). Identification and characterization of a novel matrix-degrading protease from hormone-dependent human breast cancer cells. *Cancer Res* 53, 1409-1415.

Takeuchi, T., Harris, J.L., Huang, W., Yan, K.W., Coughlin, S.R., and Craik, C.S. (2000). Cellular localization of membrane-type serine protease 1 and identification of protease-activated receptor-2 and single-chain urokinase-type plasminogen activator as substrates. *J Biol Chem* 275, 26333-26342.

CHAPTER TWO

Local protease signaling contributes to neural tube closure in the mouse embryo

Appeared previously as: Camerer E, Barker A, Duong DN, Ganesan R, Kataoka H, Cornelissen I, Darragh MR, Hussain A, Zheng YW, Srinivasan Y, Brown C, Xu SM, Regard JB, Lin CY, Craik CS, Kirchhofer D, Coughlin SR. Local protease signaling contributes to neural tube closure in the mouse embryo. *Dev Cell*. 2010; 18(1):25-38.

Local Protease Signaling Contributes to Neural Tube Closure in the Mouse

Embryo

Eric Camerer^{1,2,4}, Adrian Barker¹, Daniel N. Duong¹, Rajkumar Ganesan⁵, Hiroshi Kataoka^{1,*}, Ivo Cornelissen¹, Molly R. Darragh³, Arif Hussain¹, Yao-Wu Zheng¹, Yoga Srinivasan¹, Christopher Brown³, Shan-Mei Xu¹, Jean B. Regard^{1,**}, Chen-Yong Lin⁶, Charles S. Craik³, Daniel Kirchhofer⁵, and Shaun R. Coughlin^{1,2}

¹Cardiovascular Research Institute, Departments of ²Medicine and ³Biochemistry, University of California, San Francisco, CA 94158, USA ⁴INSERM Unit 970, Equipe Avenir, Paris Cardiovascular Research Center, 75737 Paris Cedex 15, France. ⁵Department of Protein Engineering, Genentech Inc., South San Francisco, CA 94080, USA. ⁶Department of Biochemistry and Molecular Biology, University of Maryland, Baltimore, MD 21201, USA .

Present address:

*Riken Center for Developmental Biology, Kobe, Japan

**National Institutes of Health, Bethesda, MD 20892-4472, USA

Summary

We report an unexpected role for protease signaling in neural tube closure and formation of the central nervous system. Mouse embryos lacking protease-activated receptor 1 and 2 showed defective hindbrain and posterior neuropore closure and developed exencephaly and spina bifida, important human congenital anomalies. *Par1* and *Par2* were expressed in surface ectoderm, *Par2* selectively along the line of closure. Ablation of $G_{i/z}$ and Rac1 function in these *Par2*-expressing cells disrupted neural tube closure, further implicating G protein-coupled receptors and identifying a likely effector pathway. Cluster analysis of protease and *Par2* expression patterns revealed a group of membrane-tethered proteases often co-expressed with *Par2*. Among these, matriptase activated *Par2* with picomolar potency, and hepsin and prostatic activated matriptase. Together, our results suggest a role for protease-activated receptor signaling in neural tube closure and identify a local protease network that may trigger *Par2* signaling and monitor and regulate epithelial integrity in this context.

Introduction

Protease-activated receptors (PARs) are G protein-coupled receptors (GPCRs) that allow cells to sense specific proteases in their environment (Coughlin, 2000; Vu et al., 1991). Four PARs are found in humans and mice. PARs 1, 3, and 4 mediate cellular responses to the coagulation protease thrombin. PAR2 is not activated effectively by thrombin but can be activated by a variety of serine proteases with trypsin-like specificity including the coagulation proteases tissue factor/factor VIIa and factor Xa (Camerer et al., 2000; Riewald and Ruf, 2001). Studies in cell culture, animal models and humans support the view that, in the adult, PARs and the coagulation cascade couple tissue injury with vascular damage to appropriate cellular responses that regulate hemostasis, inflammation, cell survival and tissue repair (Becker et al., 2009; Camerer et al., 2004; Coughlin, 2000; Coughlin and Camerer, 2003; Guo et al., 2004; Kahn et al., 1999; Sambrano et al., 2001; Vergnolle et al., 2001).

Less is known regarding the roles of PARs and the proteases that activate them in contexts other than tissue injury, particularly in embryonic development. Par1-deficient mouse embryos exhibit partially penetrant lethality at midgestation due to lack of Par1 signaling in endothelial cells (Connolly et al., 1996; Griffin et al., 2001). This phenotype is less penetrant and less severe than that associated with knockout of tissue factor, the trigger for coagulation (Mackman, 2004). Toward testing the possibility that this difference might be due to partially redundant functions of Par1 and other PARs downstream of tissue factor and the coagulation cascade, we generated mice lacking multiple PARs and uncovered

an unexpected phenotype associated with combined knockout of the genes encoding *Par1* and *Par2*: failed neural tube closure. We also characterized a set of membrane-tethered proteases that may comprise a local protease network that activates *Par2* during neural tube closure, and we identified G_i and *Rac* as candidate downstream effectors of *Par2* and other GPCRs in this process. This system appears to operate in the surface ectoderm along the line of closure. Together, our studies identify an unexpected role for local protease/PAR signaling in neural tube closure, a process that is critical for formation of the central nervous system and that goes awry in the congenital anomalies exencephaly and spina bifida.

Results.

Combined deficiency in *Par1* and *Par2* results in defective neural tube closure.

Par1 and *Par2* are just 76kb apart on mouse chromosome 13 (see Experimental Procedures for gene nomenclature). Given this linkage, we generated the *Par1:Par2* double knockout by using homologous recombination to disrupt the *Par1* gene in mouse embryonic stem (ES) cells in which the *Par2* gene had been previously targeted (Camerer et al., 2002). Each recombination inserted a β -galactosidase (*lacZ*) coding sequence at the start codon so as to substitute *lacZ* for *Par1* and *Par2* expression (Griffin et al., 2001) (Figure 2.1a). Crosses of *Par1*^{+/-}:*Par2*^{+/-} mice generated from ES cells in which *Par1* and *Par2* were disrupted on the same chromosome produced live *Par1*^{-/-}:*Par2*^{-/-} offspring at

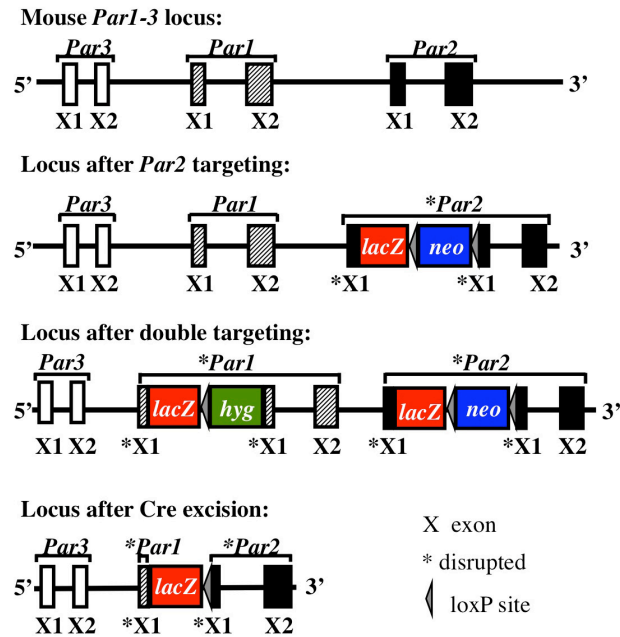
weaning at 4.6-7.6% of the expected Mendelian rate in a mixed 129/BL6 background (Figure 2.1b). In the same genetic background, *Par1*^{+/-} crosses produced *Par1*^{-/-} offspring at ~50% of the expected rate and *Par2*^{+/-} crosses produced *Par2*^{-/-} offspring at ~85% of the expected rate ((Connolly et al., 1996; Damiano et al., 1999; Griffin et al., 2001) and not shown). Thus, combined deficiency of Par1 and Par2 produced much more penetrant embryonic lethality than isolated Par1 or Par2 deficiency. *Par1*^{-/-}:*Par2*^{-/-} embryos showed three different phenotypes, each partially penetrant: midgestational cardiovascular failure beginning at 9.5 dpc as previously described with isolated Par1 deficiency (Connolly et al., 1996; Griffin et al., 2001), exencephaly, and late gestational lethality associated with widespread edema (Figure 2.2a). In the same strain background, exencephaly was not observed in either single knockout and late gestational lethality was seen only infrequently in *Par2*^{-/-} embryos. Thus, these two phenotypes appear to reflect interacting roles of Par1 and Par2 in the developing embryo. Occasional *Par1*^{-/-}:*Par2*^{-/-} mice did survive embryonic development, and these sometimes exhibited spina bifida and curly tail (Figure 2.2a). Exencephaly, spina bifida, and curly tail are all hallmarks of failed neural tube closure (Copp et al., 2003). Thus, *Par1*^{-/-}:*Par2*^{-/-} mice appeared to have an incompletely penetrant defect in closure of both hindbrain and posterior neuropores. Because no role for PARs in the development of the nervous system has been described, we focused on characterizing this phenotype.

Exencephaly was detectable by gross inspection beginning at 11.5 dpc; 17/51 (33%) viable *Par1*^{-/-}:*Par2*^{-/-} embryos exhibited exencephaly after that time

(Figure 2.2a,b). Restoring Par1 expression in endothelial cells with a Tie2p/e-Par1 transgene (Griffin et al., 2001) rescued the midgestational lethality in *Par1*^{-/-}:*Par2*^{-/-} embryos but did not prevent exencephaly (Figure 2.2c), implying that neither loss of Par1 function in endothelial cells nor midgestational cardiovascular failure contributed to the exencephaly phenotype.

Exencephaly is due to defective closure of the hindbrain neuropore. To directly assess neuropore closure, we scored embryos from *Par1*^{-/-}:*Par2*^{-/-} X *Par1*^{+/-}:*Par2*^{+/-} crosses for an open or closed hindbrain neuropore and somite count before genotyping. 22% of *Par1*^{+/-}:*Par2*^{+/-} embryos collected at 9.5 dpc had open hindbrain neuropores compared to 47% of *Par1*^{-/-}:*Par2*^{-/-} embryos (Figure 2.2d). Among embryos that had progressed to the 15-somite stage or beyond, only 4% of controls had open neuropores vs. 32% of mutants (Figure 2.2d,e). The latter frequency is similar to the overall penetrance of exencephaly in the mutants. These results suggest that exencephaly in *Par1*^{-/-}:*Par2*^{-/-} embryos is a result of failed closure of the hindbrain neuropore and that such failure is not simply a result of developmental delay.

A



B

strain	cross	n	+/+;+/+	+/-;+/-	-/-;-/-	-/-;-/- (% expected)**
129/BL6	+/-;+/- x +/-;+/-	266	85	177	4	4.6
129/BL6*	+/-;+/- x +/-;+/-	135	38	91	2	4.7
129/BL6	+/-;+/- x -/-;-/-	99		92	7	7.6
129	+/-;+/- x +/-;+/-	105	34	71	0	0
BL6	+/-;+/- x +/-;+/-	215	79	135	1	1.4
ICR	+/-;+/- x +/-;+/-	48	18	29	1	6.4

*selection markers excised **assuming no loss of double heterozygouts

Figure 2.1, related to Figure 2.2: Targeting the *Par* locus on mouse chromosome 13: strategy and effects on postnatal survival. (A) Diagram of the *Par* locus before and after sequential targeting of *Par2* and *Par1*, and after excision with β -actin-Cre as described in the Mice section in Supplemental Experimental Procedures. (B) Survival of *Par1*:*Par2* double knockouts at postnatal day 14. Live *Par1*^{-/-}:*Par2*^{-/-} mice were observed at roughly 4.6-7.6% of the frequency expected by Mendelian inheritance at P14. This was independent of whether or not the selection markers were excised. Survival was even lower when mice were backcrossed into C57BL6 or 129SVJ inbred strains. The slightly higher number of knockout pups from double knockout/double heterozygous intercrosses may indicate the presence of a survival-enhancing modifier gene transmitted by viable knockout mice. Double knockouts alive at p14 had a normal life expectancy and were fertile.

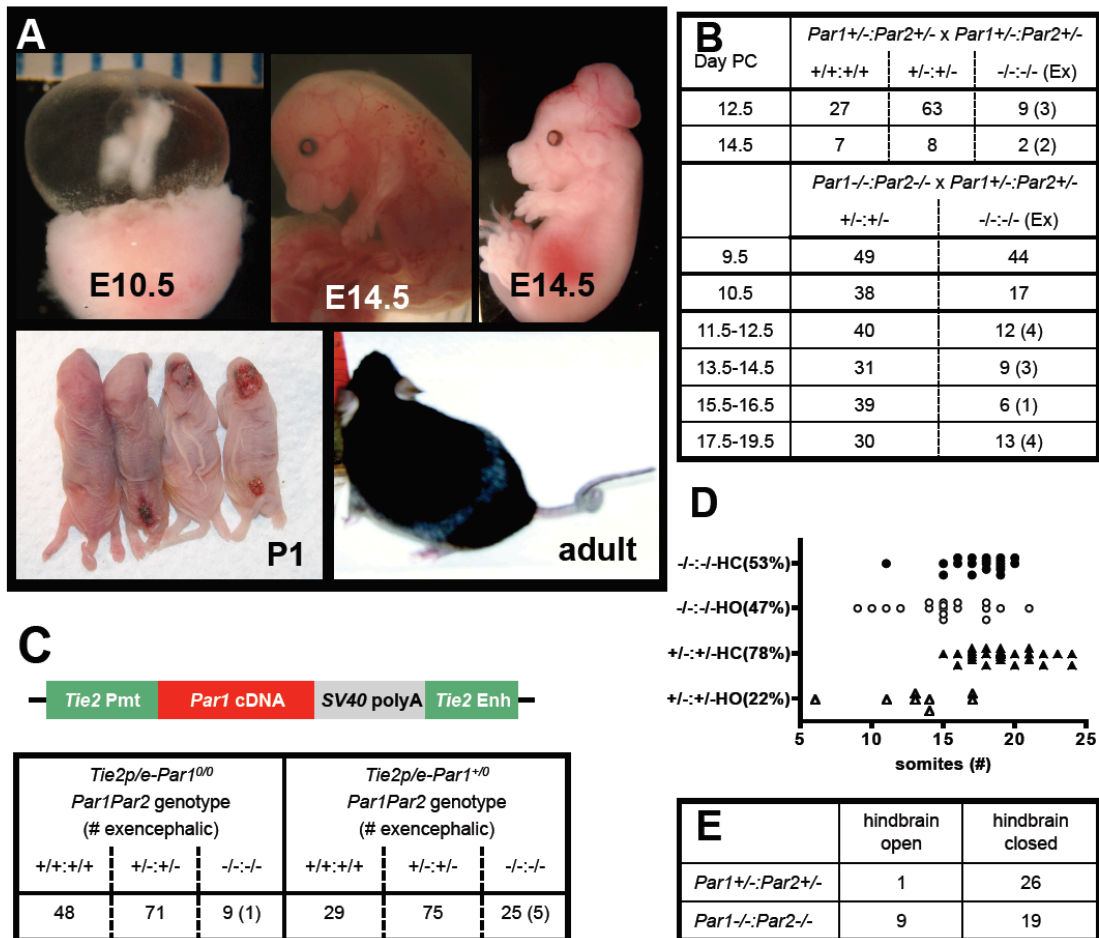


Figure 2.2. Phenotypes associated with combined deficiency of *Par2* and *Par1*. (A) Three phenotypes exhibited by *Par1*^{-/-}:*Par2*^{-/-} embryos: mid-gestational cardiovascular failure (top left); late-gestational death associated with edema (top center) and exencephaly (top right). *Par1*^{-/-}:*Par2*^{-/-} embryos that survived to birth showed exencephaly and spina bifida with incomplete penetrance (lower left; from left to right: curly tail, spina bifida/curly tail, anencephaly, anencephaly and spina bifida/curly tail). A surviving adult with curly tail is at lower right. (B,C) Viability and presence of exencephaly at various gestational ages (B) and in the presence or absence of an endothelial *Par1* transgene (C); # alive (# with exencephaly) is shown. Embryos in (C) were collected at 12.5-14.5 dpc. (D, E) Embryos from *Par1*^{+/-}:*Par2*^{+/-} X *Par1*^{-/-}:*Par2*^{-/-} crosses were collected at 9.5 dpc, scored for an open HO or closed HC hindbrain neuropore and somite count, then genotyped. To visualize the neuropore, embryos were X-gal stained. (E) Results from embryos in (D) with 15 or more somites. See also Figure 2.1.

***Par2* is expressed in the surface ectoderm adjacent to the neuroepithelium at the time and place of neural tube closure.**

A direct role for PARs in neural tube closure would demand expression of the receptors in or around the neural tube at the time of closure. β -galactosidase staining of *Par2-LacZ* knockin embryos revealed expression of *Par2* in the surface ectoderm cells immediately overlying the neuroepithelium at the time and place of fusion (Figure 2.3a,b and Figure 2.4a,b). Such localized *Par2* expression was confirmed by in situ hybridization of wild-type embryos for *Par2* mRNA (Figure 2.3c and Figure 2.4c). By the same measures, *Par1* expression was detected in endocardium, endothelium and a subset of hematopoietic cells but not in surface ectoderm (Figure 2.4d). However, *Par1* mRNA was readily detected by quantitative PCR of RNA from FACS-sorted surface ectoderm cells (see below) suggesting that *Par1* is probably expressed in surface ectoderm at levels below the detection limits of the other techniques. Thus, while we cannot exclude less direct mechanisms, the requirement for knockout of both *Par1* and *Par2* for the appearance of exencephaly may be due to partially redundant functions of these receptors in the surface ectoderm.

Together with the exencephaly phenotype in *Par1^{-/-}:Par2^{-/-}* embryos, the precise expression of *Par2* at the place and time of neural tube closure suggested an unexpected role for local *Par2* signaling in surface ectoderm in neural tube closure. These observations prompted an effort to obtain independent evidence for the importance of GPCR signaling in surface ectoderm during neural tube closure.

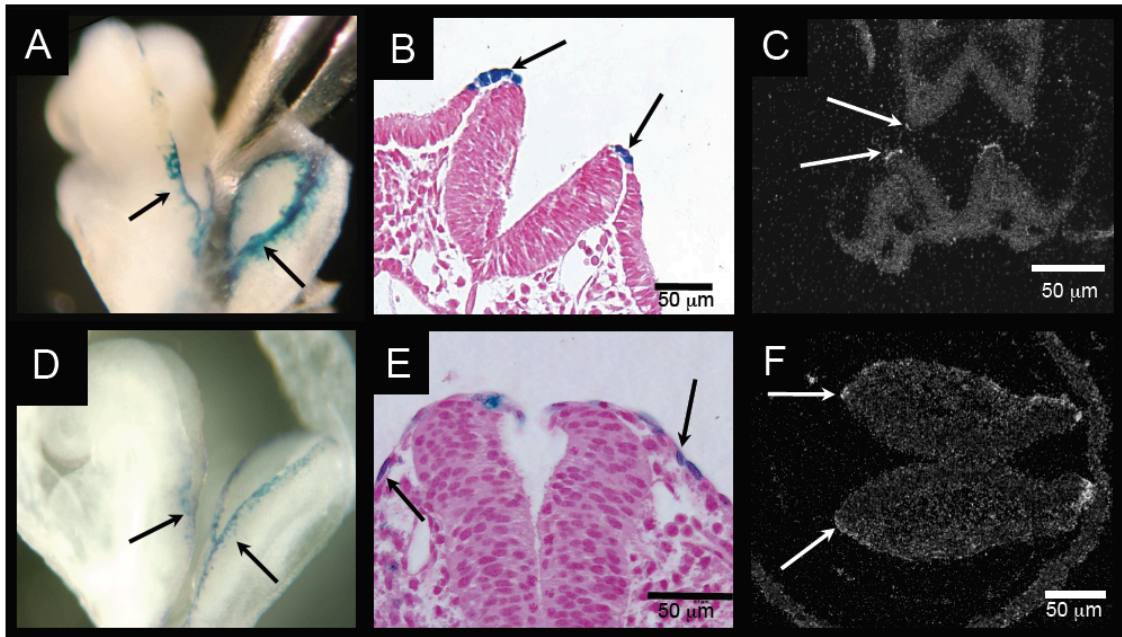


Figure 2.3. Localized expression of *Par2* in surface ectoderm and characterization of a surface ectoderm Cre (*Grhl3*^{Cre}) (A-C) *Par2* expression at the time of neural tube closure. (A,B) X-gal staining of *Par2*-lacZ knock-in embryo in whole mount (A) and cross section (B). In situ hybridization of wild-type embryos for *Par2* mRNA (C). (D, E) LacZ expression from a Cre-IRES-NLSlacZ cassette inserted into the *Grhl3* locus (*Grhl3*^{Cre}). (F) In situ hybridization of wild-type embryo for *Grhl3* mRNA. Sense controls for C and F are in Figure 2.4. Embryos were collected at about 9.25 dpc.

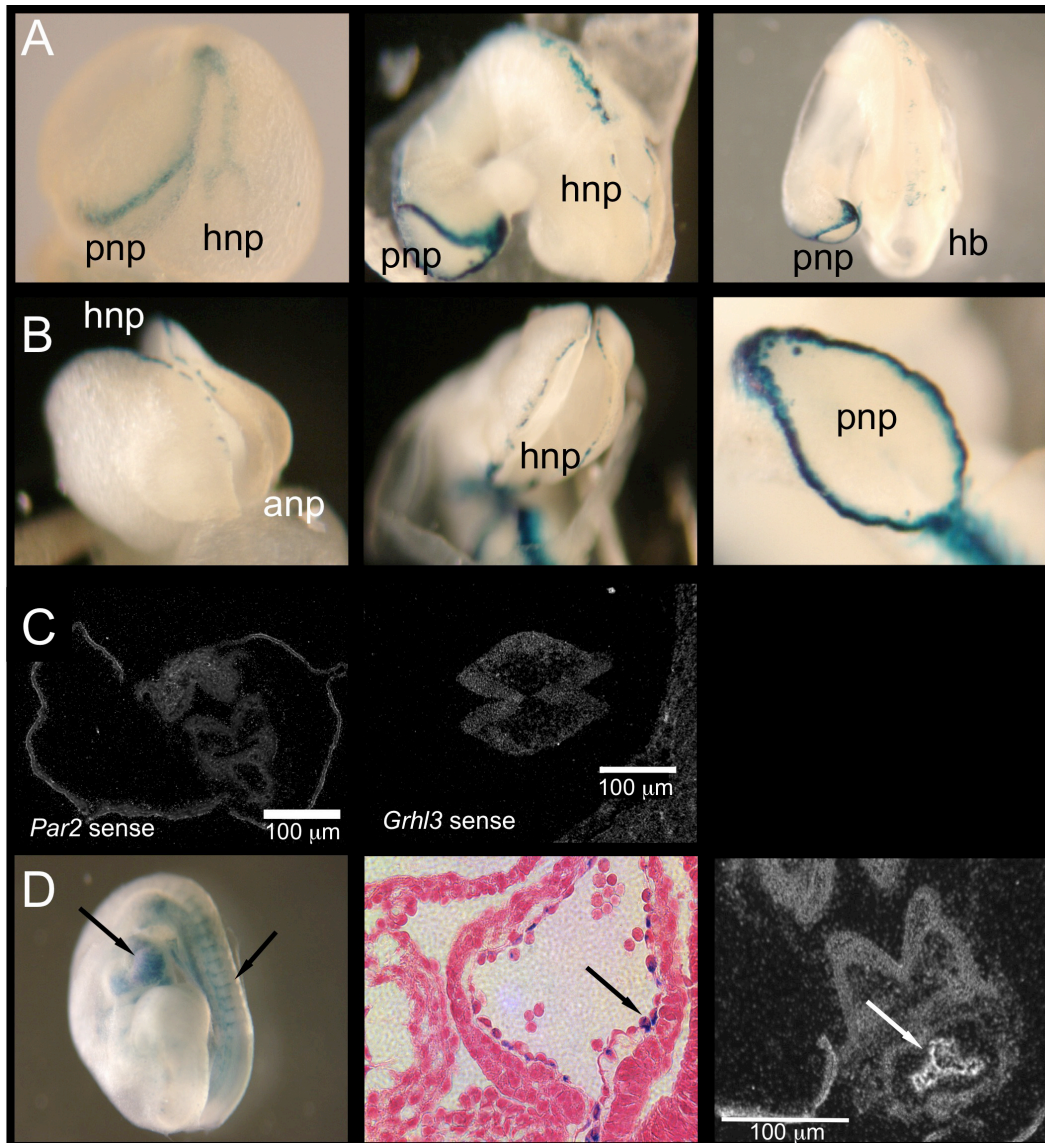


Figure 2.4, related to Figure 2.3: (A, B) LacZ expression from the *Par2* gene in surface ectoderm overlying the neural tube during neural tube closure (A) Left to right: progression of expression from ~8.75 ->9.25 dpc. Staining is seen through intact yolk sack in left image and the hindbrain neuropore is closed in right image. (B) Left to right: close-up of lacZ staining around the anterior (anp), hindbrain (hnp) and posterior (pnp) neuropores. (C) Sense controls for Figure 2C&D. (D) *Par1* expression at midgestation. *Par1* expression at the time of neural tube closure (approximately 9.25 dpc) demonstrated by X-gal staining in whole mount (left) and 5 μ m paraffin sections (center) and by in situ hybridization of 5 μ m paraffin sections (right). Expression in blood vessels, vascular endothelium and endocardium but not in surface ectoderm was detected by these techniques (but *Par1* mRNA was readily detected in surface ectoderm by TaqMan RT-PCR; See Fig. 4 in manuscript). X-gal activity was from a *Par1*^{lacZ} single allele knockin (not *Par1:Par2*). Sense controls (not shown) showed no specific signal.

Surface ectoderm-specific knockout of G_i and Rac1 function, signaling pathways downstream of Par2, causes neural tube defects.

If loss of GPCR function in surface ectoderm is responsible for the neural tube closure defects described above, surface ectoderm-specific knockout of the relevant signaling pathway(s) downstream of GPCRs should also cause neural tube defects. To manipulate genes in surface ectoderm, we generated mice in which a Cre-IRES-NLSlacZ cassette was inserted in the Grainyhead-like-3 (*Grhl3*) gene (Figure 2.5a), hereafter designated *Grhl3*^{Cre/+} mice. *Grhl3* is a transcription factor expressed in surface ectoderm, hindgut endoderm and other epithelial cells in a pattern similar to *Par2* at the time of neural tube closure (Figure 2.3), and loss of *Grhl3* function causes exencephaly and spina bifida in knockout and curly tail (*ct/ct*) mutant mice ((Auden et al., 2006; Gustavsson et al., 2007; Ting et al., 2003); Figure 2.3a-d and Figure 2.5)). X-gal staining of *Grhl3*^{Cre/+} embryos collected at 8.5 dpc confirmed NLSlacZ expression in surface ectoderm along the neural ridge in a pattern that was indistinguishable from *Par2* (Figure 2.3); expression quickly spread laterally from the neural ridge to cover much of the surface ectoderm. In accord, examination of *Grhl3*^{Cre/+} embryos carrying a cytoplasmic lacZ or YFP Cre-excision reporter revealed reporter expression first in the midline then spreading laterally in the surface ectoderm to cover the embryo (Figure S.5b-d). Thus, the *Grhl3*^{Cre} allele drove efficient and relatively tissue-specific excision of floxed sequences in surface ectoderm. *Grhl3*^{Cre/Cre} embryos — effectively *Grhl3* nulls — recapitulated the neural tube defect phenotypes reported for *Grhl3*^{-/-} embryos (Ting et al., 2003), but,

importantly, *Grhl3*^{Cre/+} embryos (effectively *Grhl3* heterozygotes) had no neural tube phenotype in the absence of a relevant floxed target allele.

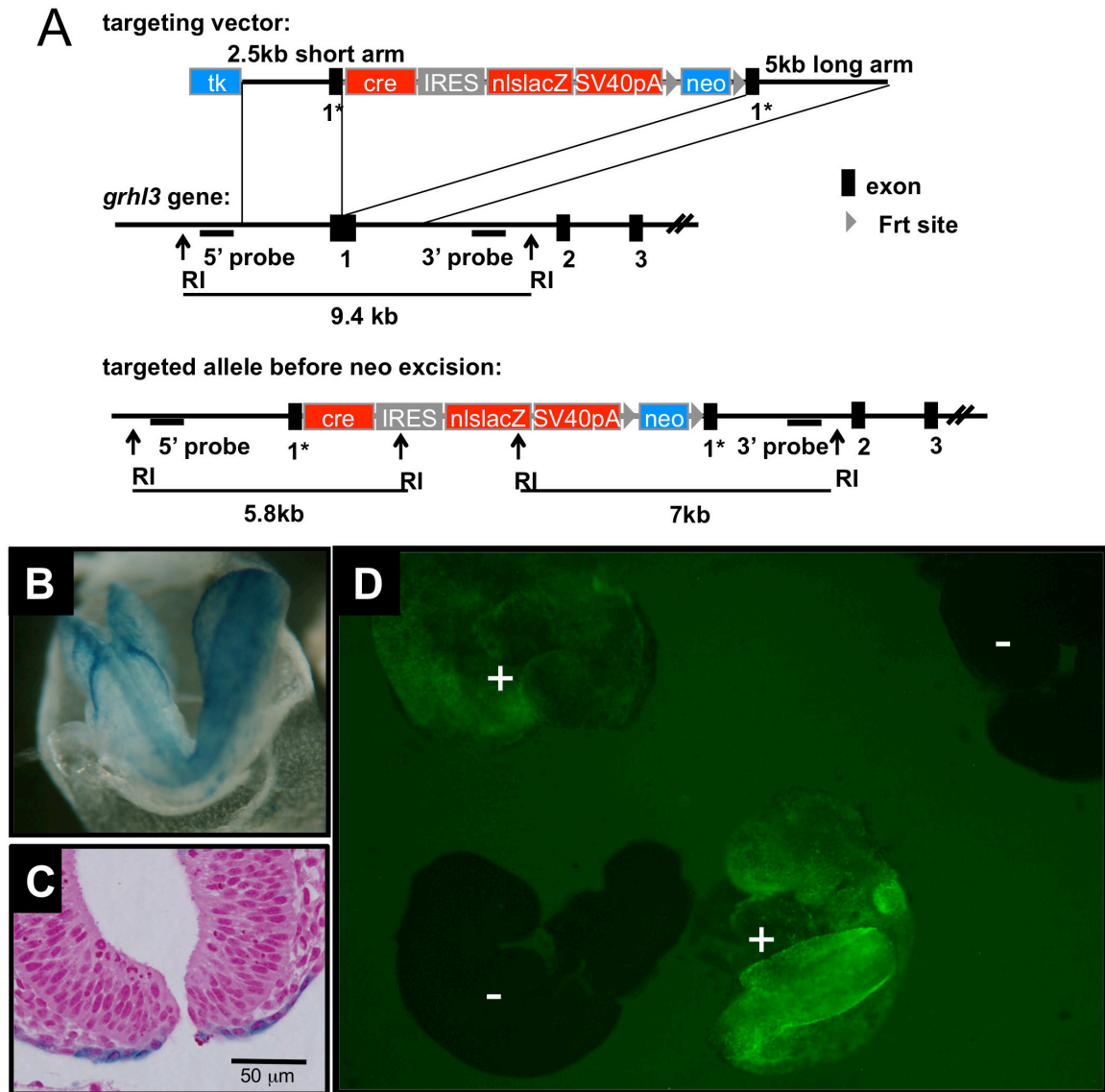


Figure 2.5, related to Figure 2.6: Generation of a mouse line expressing Cre recombinase in surface ectoderm. (A) Diagram of the strategy to generate a surface ectoderm Cre by targeting the *Grhl3* locus on mouse chromosome 4 as described in the Mice section in Supplemental Experimental Procedures. (B-D) Demonstration of Cre activity in surface ectoderm in *Grhl3*^{Cre/+} mice. *Grhl3*^{Cre/+} mice were crossed to mice carrying lacZ and EYFP Cre excision reporter alleles driven from the ROSA26 locus to assess Cre recombinase activity in embryos collected at ~8.75 dpc. Note strong Xgal stain in surface ectoderm around the neuropore of a *Grhl3*^{Cre/+};*ROSA26*^{lacZ/+} embryo (B) and non-nuclear X-gal stain in 5µm sections thereof (C) (the weaker nuclear X-gal stain in the same section is from the Cre-IRES-NLS lacZ driven by the *Grhl3* locus, not from the reporter). Staining was more widespread in B than staining from *Grhl3* locus alone (Figure 2.3d,e). (D) Surface ectoderm fluorescence in surface ectoderm in *Grhl3*^{Cre/+} (+) but not Cre-negative (-) embryos collected at 8.75 dpc from a *Grhl3*^{Cre/+} x *ROSA26*^{YFP/YFP} cross.

Par1 and Par2 can couple to members of the $G_{q/11}$, $G_{i/o/z}$, and $G_{12/13}$, G protein subfamilies (Coughlin, 2000), although Par2 coupling to $G_{12/13}$ may be less effective than Par1 (Vouret-Craviari et al., 2003). Combined deficiency in G_{α_q} and $G_{\alpha_{11}}$ causes embryonic lethality around 11 dpc; neural tube defects were not reported (Offermanns et al., 1998). $G_{\alpha_{13}}$ (gene symbol *Gna13*) is an important GPCR effector in endothelial cells and neural crest during embryonic development, and $G_{\alpha_{13}}$ signaling in neural crest contributes to neural tube closure (Ruppel et al., 2005). To determine whether $G_{\alpha_{13}}$ in surface ectoderm might also contribute to neural tube closure, we generated surface ectoderm-specific $G_{\alpha_{13}}$ knockouts. $Grhl3^{Cre/+};G_{\alpha_{13}}^{ff}$ embryos lived through E14.5 and did not display exencephaly. Addressing possible redundancy with $G_{\alpha_{12}}$, we found that $Grhl3^{Cre/+};G_{\alpha_{13}}^{ff};G_{\alpha_{12}}^{-/-}$ embryos died by E10.5 with turning and other defects but with a closed hindbrain neuropore (not shown). Thus, loss of $G_{\alpha_{12/13}}$ signaling in surface ectoderm is unlikely to account for exencephaly in $Par1^{-/-};Par2^{-/-}$ embryos.

We next addressed the role of the $G_{i/o/z}$ family. Four of the five widely expressed $G_{\alpha_{i/o/z}}$ family members ($G_{\alpha_{i1}}$, $G_{\alpha_{i2}}$, $G_{\alpha_{i3}}$, and G_{α_o}) are inhibited by pertussis toxin; G_{α_z} is pertussis-insensitive. To circumvent redundancy among the $G_{\alpha_{i/o/z}}$ family members, we used a $ROSA26^{PTX}$ conditional allele (Regard et al., 2007) to express pertussis toxin S1 catalytic subunit (PTX) in surface ectoderm by Cre-mediated excision of a Lox-Stop-Lox cassette. Embryos from $ROSA26^{PTX/PTX} \times Grhl3^{Cre/+}$ crosses were collected at 14.5 dpc.

Grhl3^{Cre/+}:*ROSA26*^{PTX/+} embryos showed exencephaly with a penetrance of ~10% (Figure 2.6). The frequency of exencephaly increased to 20% in a $G\alpha_z$ null background. Exencephaly was not observed in mice lacking only $G\alpha_z$ nor in Cre-negative *ROSA26*^{PTX/+}: $G\alpha_z$ ^{-/-} embryos. Posterior neural tube defects — spina bifida and curly tail — were seen in 0%, 18%, and 40% of *Grhl3*^{Cre/+}:*ROSA26*^{PTX/+} embryos in $G\alpha_z$ ^{+/+}, ^{+/-} and ^{-/-} backgrounds, respectively. Thus, PTX S1 expression in surface ectoderm and $G\alpha_z$ deficiency interacted to promote neural tube defects, strongly supporting the notion that these phenotypes are caused by loss of $G_{i/o/z}$ pathway function and hence that G_i signaling in surface ectoderm is required for normal closure of the neural tube. In contrast to *Grhl3*^{Cre/+}:*ROSA26*^{PTX/+}: $G\alpha_z$ ^{-/-} embryos, posterior neural tube defects were rare in *Par1*^{-/-}:*Par2*^{-/-} embryos. *Grhl3* expression in hindgut contributes to posterior neuropore closure (Gustavsson et al., 2007). Although neural tube defects were not detected in *Grhl3*^{Cre/+} embryos, it is possible that haploinsufficiency of *Grhl3* interacts with loss of G_i signaling in hindgut in *Grhl3*^{Cre/+}:*ROSA26*^{PTX/+}: $G\alpha_z$ ^{-/-} embryos to produce such defects. It is also possible that knockout of G_i pathway signaling uncovered a role for G_i -coupled GPCRs in addition to *Par2* and *Par1* in posterior neural tube closure.

Rac is one of several downstream effectors of G_i signaling. Abrogation of *Rac* function impairs dorsal closure of the *Drosophila* embryo cuticle due to an inability of opposing epithelial sheets to migrate and fuse (Harden et al., 1995). *Rac1* is the main *Rac* family member expressed in non-hematopoietic tissues in mice (Sugihara et al., 1998). To determine whether *Rac* function in surface

ectoderm might be necessary for neural tube closure in mouse embryos, we examined *Grhl3*^{Cre/+}:*Rac1*^{ff} embryos collected at 14.5 dpc (Figure 2.6). 58% of *Grhl3*^{Cre/+}:*Rac1*^{ff} embryos displayed exencephaly vs. 0% for Cre-negative *Rac1*^{ff} embryos or Cre-positive embryos with a single wild-type *Rac1* allele (Figure 2.6). As with elimination of *G_{i/o/z}* function in surface ectoderm, we also observed posterior neural tube defects at a high rate (83%). *Grhl3*^{Cre/+}:*Rac1*^{ff} embryos were present at the expected Mendelian frequency, and X-gal staining (for β -gal expressed from the IRESlacZ included with the *Grhl3* Cre knockin) demonstrated that most surface ectoderm cells expressed Cre at this time. Thus, *Rac1* function was not required for survival of surface ectoderm cells. These results are consistent with a model in which Gi-Rac signaling downstream of PARs and other GPCRs in surface ectoderm contributes to neural tube closure.

Neural tube defects are often classified as sensitive or resistant to folate supplementation (Copp et al., 2003). Folate injections of pregnant female mice (Fleming and Copp, 1998) at E7.5 and 8.5 did not affect the penetrance of hindbrain or posterior neural tube defects in *Grhl3*^{Cre/+}:*Rac1*^{ff} embryos collected at 14.5 dpc (Figure 2.6), suggesting that these defects are folate-resistant.



B

	<i>Grhl3^{+/+}</i>		<i>Grhl3^{Cre/+}</i>	
	exenceph (%)	posterior NTD (%)	exenceph (%)	posterior NTD (%)
<i>ROSA26^{PTX/+}:Gα_z^{+/+}</i>	0/15 (0)	0/15 (0)	2/21 (10)	0/21 (0)
<i>ROSA26^{PTX/+}:Gα_z^{+/-}</i>	0/24 (0)	0/24 (0)	1/27 (4)	5/27 (18)
<i>ROSA26^{PTX/+}:Gα_z^{-/-}</i>	0/10 (0)	0/10 (0)	3/15 (20)	6/15 (40)
<i>Rac1^{fl/+}</i>	0/11 (0)	0/11 (0)	0/15 (0)	0/15 (0)
<i>Rac1^{fl/fl}</i>	0/7 (0)	0/7 (0)	7/12 (58)	10/12 (83)
<i>Rac1^{fl/+} (folate)</i>	0/15 (0)	0/15 (0)	0/14 (0)	0/14 (0)
<i>Rac1^{fl/fl} (folate)</i>	1/12 (8)	0/12 (0)	8/13 (62)	10/13 (77)

Figure 2.6. Abrogating G_i function and Rac1 expression in surface ectoderm causes neural tube defects. (A) Exencephaly in *Par1^{-/-}:Par2^{-/-}*, *Grhl3^{Cre/+}:ROSA26^{PTX/+}:Gα_z^{-/-}*, and *Grhl3^{Cre/+}:Rac1^{fl/fl}* embryos collected at 14.5 dpc. Spina bifida and curly tail in *Grhl3^{Cre/+}:ROSA26^{PTX/+}:Gα_z^{-/-}* (lower) and *Grhl3^{Cre/+}:Rac1^{fl/fl}* (both) embryos. (B) Occurrence of neural tube defects (# with NTD/# live (%)) by genotype at 14.5 dpc. See also Figure 2.5.

Identification of candidate Par2-activating proteases in the context of neural tube closure.

Multiple serine proteases can activate Par2 in vitro but its physiological activators are uncertain. Uncovering a necessary role for surface ectoderm Par2 in neural tube closure provided a context in which to search for a Par2-activating protease. Toward identifying candidate proteases, we first asked which extracellular proteases are expressed in the mouse embryo at the time of neural tube closure and which proteases are expressed in tissues in a pattern most like Par2.

We generated TaqMan-type qPCR primer/probe sets for the ~125 genes in mouse predicted to encode a serine protease that would reside in the extracellular compartment (e.g., proteases with signal peptides, or type-2 transmembrane proteins with extracellular protease domain (TTSPs); Appendix 5.1) and used these to quantitate mRNAs in mouse embryos collected at 8.5-9.5 dpc. About 25% of the 125 protease genes examined were expressed above background. We focused first on the ten most abundantly expressed (Figure 2.7a), especially in light of our cluster results (see below). Analysis of RNA from FACS-sorted surface ectoderm cells from *Grhl3*^{Cre/+}:ROSA26^{YFP/+} embryos collected at 8.5-9.5 dpc confirmed expression of nine of these ten in surface ectoderm, and mRNA for four proteases — prostaticin, epitheliasin, matriptase (also known as MT-SP1 and St14), and hepsin — was enriched in surface ectoderm relative to the rest of the embryo (Figure 2.7a).

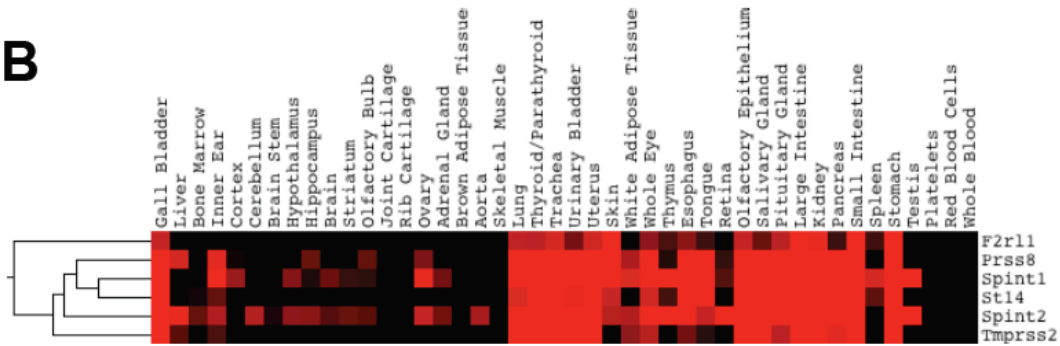
Cluster analysis of the pattern of expression of the 125 proteases and 11 selected inhibitors across 44 different tissues in adult mice revealed matriptase (St14) and prostaticin (Prss8), their Kunitz-type inhibitors Hai-1 and Hai-2 (Spint1 and 2), and epitheliasin (Tmprss2) to be expressed in a pattern most similar to Par2 (F2r1) (Figure 2.7b and Appendix 5.2). Hepsin was broadly expressed and did not specifically cluster with Par2, but hepsin and Par2 were often expressed in the same tissues. Prostaticin, matriptase, hepsin, and epitheliasin are membrane-tethered proteases and hence are likely to function on or near the cell in which they are expressed. These results raised the possibility that matriptase, prostaticin, hepsin and/or epitheliasin might, together with Par2, comprise a local protease signaling system in surface ectoderm. Our previous observation that matriptase can activate Par2 heterologously expressed in *Xenopus* oocytes (Takeuchi et al., 2000) encouraged investigation of this hypothesis.

In situ hybridization confirmed expression of prostaticin, epitheliasin, matriptase, and hepsin mRNA in surface ectoderm of wild-type embryos collected at 8.75 dpc; t-PA and Klk8 hybridization was also detected and was more widespread (Figure 2.7c). Although Masp1 was expressed in surface ectoderm (Figure 2.7a), past studies had suggested that Masp1 was not an effective Par2 activator (not shown). Based on these results, we chose Klk8, prostaticin, tPA, epitheliasin, matriptase and hepsin for further study.

A

protease	Gene symbol	Δ CT abundance relative to control (n=4)	$2^{\Delta\Delta$ CT abundance relative to Par2 (n=4)	$2^{\Delta\Delta$ CT enrichment in surface ectoderm (n=2)
klk8	Klk8	7.3 +/- 0.4	25 +/- 10	1.0 +/- 0.1
prostasin	Prss8	7.7 +/- 1.3	23 +/- 5.9	3.2 +/- 0.9
tPA	Plat	8.7 +/- 0.4	8.9 +/- 6.5	1.0 +/- 0.1
epitheliasin	Tmprss2	9.1 +/- 1.7	9.6 +/- 6.2	1.5 +/- 0.2
masp1	Masp1	9.2 +/- 0.3	4.8 +/- 2.8	1.2 +/- 0.2
polyserase-2	Prss36	9.5 +/- 0.3	5.3 +/- 2.6	1.0 +/- 0.0
matriptase	St14	9.5 +/- 0.5	5.2 +/- 1.9	2.5 +/- 0.2
hepsin	Hpn	9.6 +/- 1.3	6.6 +/- 3.0	2.2 +/- 0.3
cfb	Cfb	10 +/- 0.6	3.3 +/- 1.5	1.1 +/- 0.2
chymopasin	Ctrl	11 +/- 0.5	1.8 +/- 1.3	Undetectable
Par1	F2r	5.5 +/- 0.4	76 +/- 52	1.0
Par2	F2r1	12 +/- 1		5.8

B



C

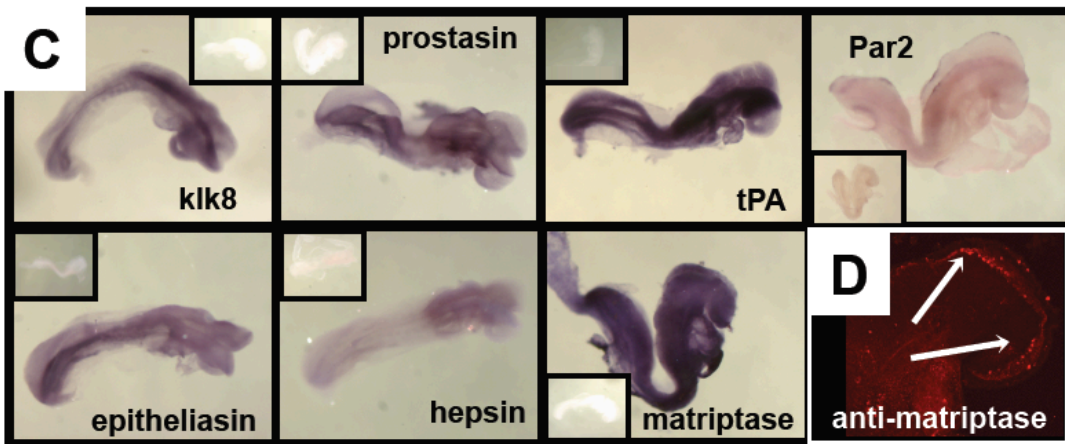


Figure 2.7. Identification of candidate Par2 activators expressed during neural tube closure. (A) Expression of 125 serine proteases predicted to reside in the extracellular space by real-time PCR of RNA from pooled wild-type embryos collected at 8.5-9.5 dpc. The ten most abundantly expressed relative to housekeeping genes (Δ CT), their abundance relative to Par2 ($2^{\Delta\Delta$ CT) and their enrichment in surface ectoderm (expression in YFP-positive surface ectoderm cells sorted from dissociated $\text{Grhl3}^{\text{Cre+/-}}:\text{ROSA26}^{\text{YFP/+}}$ (ROSA26 Lox-STOP-Lox YFP) embryos relative to YFP-negative cells from the same embryos ($2^{\Delta\Delta$ CT)) are shown. (B) Hierarchical cluster analysis was used to compare expression patterns of 125 candidate proteases, 11 select inhibitors and Par2 was measured by real-time PCR of RNA from 44 tissues and circulating cells from adult mice (See Appendix 5.1). The cluster containing Par2, matriptase (St14), prostatic (prss8) and their inhibitors Hai-1 (Spint1) and Hai-2 (Spint2) is shown in TreeView; red intensity indicates increased expression. See Appendix 5.2 for entire cluster analysis. (C) Surface ectoderm expression of mRNA for the indicated candidate proteases and Par2 by whole-mount in situ hybridization of 8.5 dpc embryos; sense controls are in insets. (D) Immunostaining of live 8.5 dpc embryos with E2, an antibody specific for the active form of matriptase. Arrows indicate staining of surface ectoderm overlying the hindbrain neuropore. Close-up is in Figure 2.8.

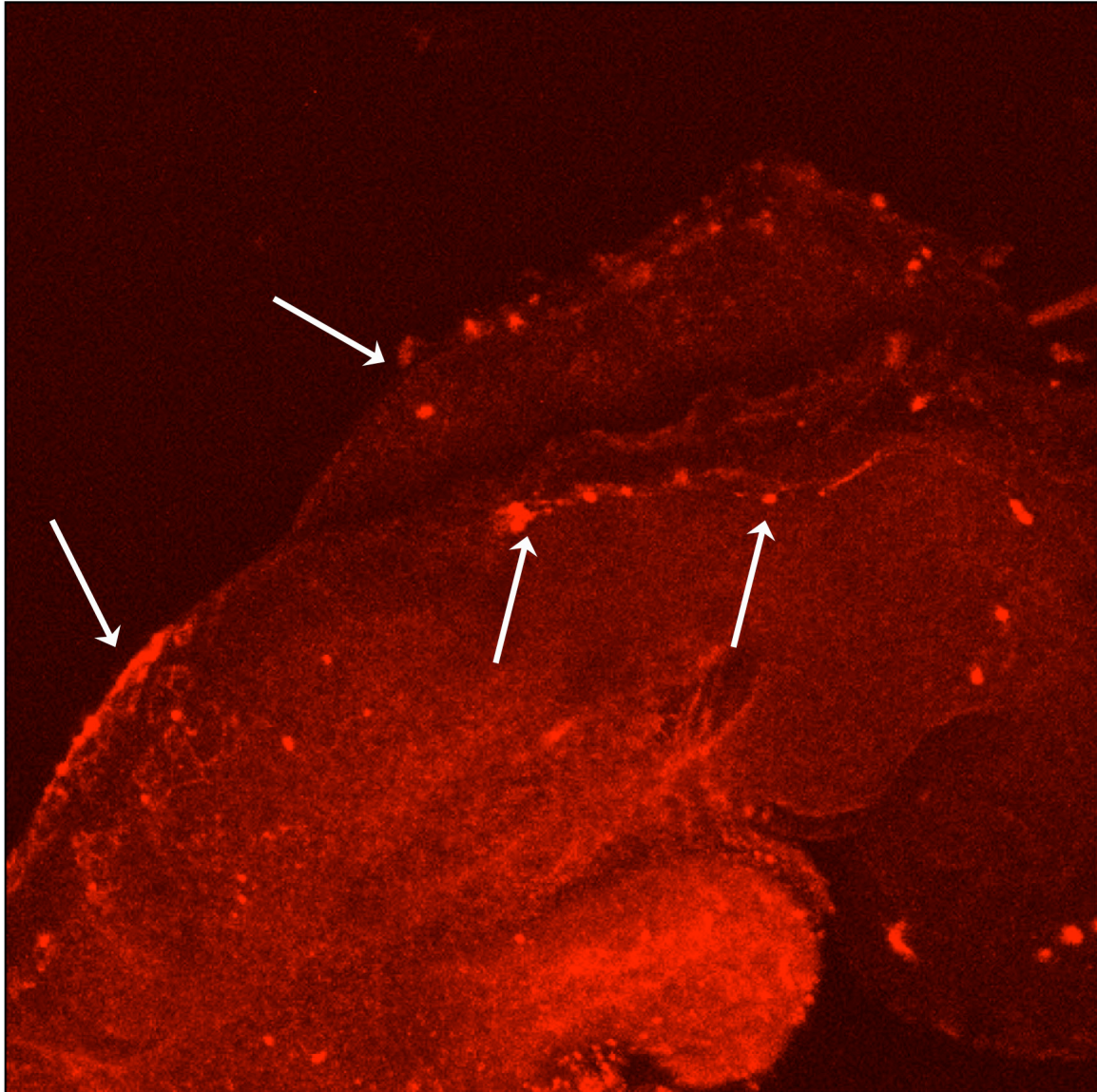


Figure 2.8, related to Figure 2.7: Matriptase with antibody-accessible active site is present on the surface ectoderm ridge at the time of neural tube closure. Embryos collected at 8.75-9.25 dpc were stained with Alexaflour 594-conjugated E2 monoclonal antibody, which specifically recognizes the matriptase active site. Stained embryos were imaged using confocal fluorescence microscopy. A high-resolution image of an embryo stained with E2 as in Figure 2.7d is shown. Image represents a reconstruction from a Z-series collected through the entire depth of the embryo. Note fluorescence localized to the surface ectoderm along the ridge overlying the neural tube and around the open neuropore (arrows).

Par2 cleavage and signaling in response to candidate proteases.

To determine whether these proteases might elicit signaling in cells that express Par2 at natural levels, we examined phosphoinositide (PI) hydrolysis in response to exogenous soluble recombinant proteases added to cultures of HaCaT cells, a keratinocyte-like surface ectoderm lineage cell line that naturally expresses PAR1 and PAR2. At 50 nM, prostatic, matriptase, and hepsin protease domains triggered PI hydrolysis in HaCaT cells; Klk8, t-PA and epitheliasin had no activity (Figure 2.10a). Matriptase was remarkably potent in the HaCaT system, with an EC₅₀ of ~200 pM; EC₅₀ values for prostatic and hepsin were around 20 nM (Figure 2.10b). Responses were blocked by recombinant ecotin or HAI-1 (not shown), both broad-spectrum inhibitors of trypsin-fold serine proteases (Takeuchi et al., 1999), confirming that responses to the recombinant protease preparations were indeed due to protease activity.

To assess the ability of proteases to productively cleave individual PARs, we transiently transfected HaCaT cells with Par1 and Par2 that had alkaline phosphatase (AP) fused to their N-terminal exodomains such that receptor cleavage released alkaline phosphatase into the culture medium (Ludeman et al., 2004). Addition of 10 nM soluble recombinant matriptase to HaCaT cultures expressing AP-Par2 released 90-95% of surface-available (trypsin-releasable) AP within 60 minutes in 3 of 3 separate experiments, 20-60% was released by 10-20 nM prostatic, and hepsin showed some but variable activity in this assay (Figure 2.10c and Figure 2.9, 2.12). None of these proteases released AP activity from cells expressing AP-Par2csm, an AP-Par2 mutant with a two amino

acid change that disrupts its activating cleavage site (Figure 2.9). Thus, exposure to matriptase, prostasin, and hepsin resulted in productive cleavage of Par2 expressed in HaCaT cells.

Unlike AP-Par2, AP release from AP-Par1-transfected HaCaT cells by recombinant matriptase, prostasin, and hepsin was not ablated by mutation of the activating cleavage site in Par1 (not shown). Par1 is subject to nonproductive cleavage and shedding of its N-terminal exodomain by an ADAM17-like metalloproteinase (Ludeman et al., 2004), and prostasin, hepsin and matriptase failed to cause AP release from AP-Par1-transfected HaCaT cells in the presence of the metalloproteinase inhibitor 1,10-phenanthroline (Figure 2.9). AP release from AP-Par2-transfected cells upon addition of prostasin, hepsin and matriptase was unaffected by metalloproteinase inhibition (Figure 2.9). Metalloproteinase-dependent Par1 shedding can be increased by stimulation of protein kinase C (Ludeman et al., 2004). Thus, PAR2 activation of metalloproteinase-dependent Par1 shedding may account for release of AP from AP-Par1 by matriptase, prostasin, and hepsin in the HaCaT system in the absence of metalloproteinase inhibition.

Evidence for a Par2-activating protease “cascade”.

The experiments described above do not speak to whether matriptase, prostasin, and/or hepsin act upon Par2 directly. Toward addressing this question, we first examined the ability of these proteases to trigger Par2 transfection-dependent PI hydrolysis in lung fibroblasts from Par1-deficient mice

(KOLF). In the absence of transfection, KOLF do not express Par2 or other PARs, matriptase, prostatic, hepsin or Hai-1 mRNA as assessed by TaqMan RT-PCR. In accord, even at 50 nM, exogenous matriptase, prostatic, and hepsin did not stimulate PI hydrolysis in untransfected KOLFs (Figure 2.10d). After PAR2 transfection of KOLFs, matriptase triggered signaling as effectively as saturating concentrations of PAR2 agonist peptide and with an EC₅₀ of ~300 pM (Figure 2.10d,e), similar to that found in HaCaT cultures (Figure 2.12b). Matriptase showed no activity in PAR1- or PAR4-transfected KOLFs even at >100x the EC₅₀ for PAR2 (Figure 2.10d and not shown). Similar results were obtained whether mouse or human PAR cDNAs were transfected. Activity at PAR3 was not examined because the mouse homolog of this receptor is incapable of mediating transmembrane signaling (Nakanishi-Matsui et al., 2000).

Surprisingly, in contrast to the case in HaCaT cells, prostatic produced no PI hydrolysis response in KOLFs transfected to express PAR2 or other PARs (Figure 2.10d and not shown). Similarly, only a weak response to hepsin was detected (Figure 2.10d,e). The different protease responsiveness of HaCaT and KOLF cultures suggested that KOLFs might lack a factor that permits, or express an inhibitor that prevents, direct or indirect PAR2 activation by prostatic and hepsin. Quantitative PCR analysis showed that matriptase was expressed by HaCaTs but not by KOLFs. This and the potency of matriptase as a PAR2 activator suggested that activation of the zymogen form of matriptase by prostatic or hepsin might account for the ability of these proteases to activate PAR2 in HaCaT cultures. To test this possibility, we first determined whether

matriptase inhibition would attenuate signaling in response to prostatic and hepsin in HaCaT cultures.

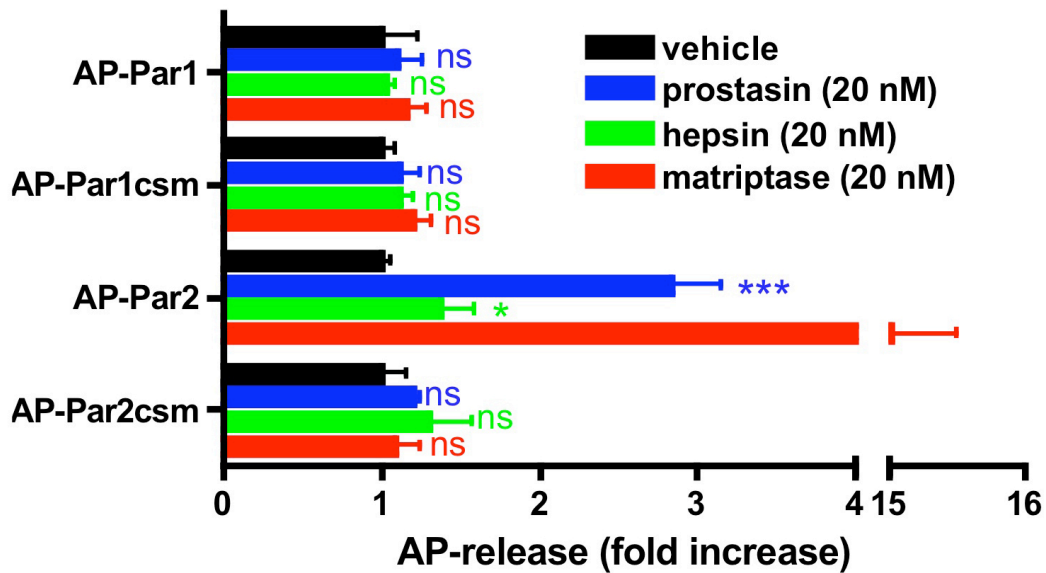


Figure 2.9, related to figure 2.10: Par2 cleavage in HaCaT cells by prostaticin and matriptase requires an intact activating cleavage site in Par2. An ectoderm-derived keratinocyte cell line (HaCaT) was transiently transfected with constructs encoding Par1, Par2 or cleavage site mutants (csm) of the same, all tagged with alkaline phosphatase (AP) fused to their N-terminus. 1,10 Phenanthroline (5 mM) was included in the incubation medium in these studies to prevent metalloprotease-dependent shedding of Par1 (See manuscript). Receptor cleavage was assessed as appearance of AP activity in the culture medium during a one-hour incubation with protease and was expressed as fold increase over AP activity in the medium in the absence of added protease. Note 1) significant increase in AP activity upon incubation of HaCaTs expressing AP-Par2 with prostaticin and matriptase, and 2) lack of activity of these proteases upon AP-Par2_{R38A/S39P} cleavage site mutant (csm), AP-Par1 or AP-Par1csm. AP-Par1 was efficiently cleaved by thrombin and trypsin (not shown). Note also that hepsin some but variable activity activity at AP-Par2. *p<0.05, ***p<0.001, ^{ns}p>0.05 by 2-way ANOVA and Bonferroni's post-test relative to vehicle treatment in the same transfection group. Mean ± standard deviation (n=3) is shown.

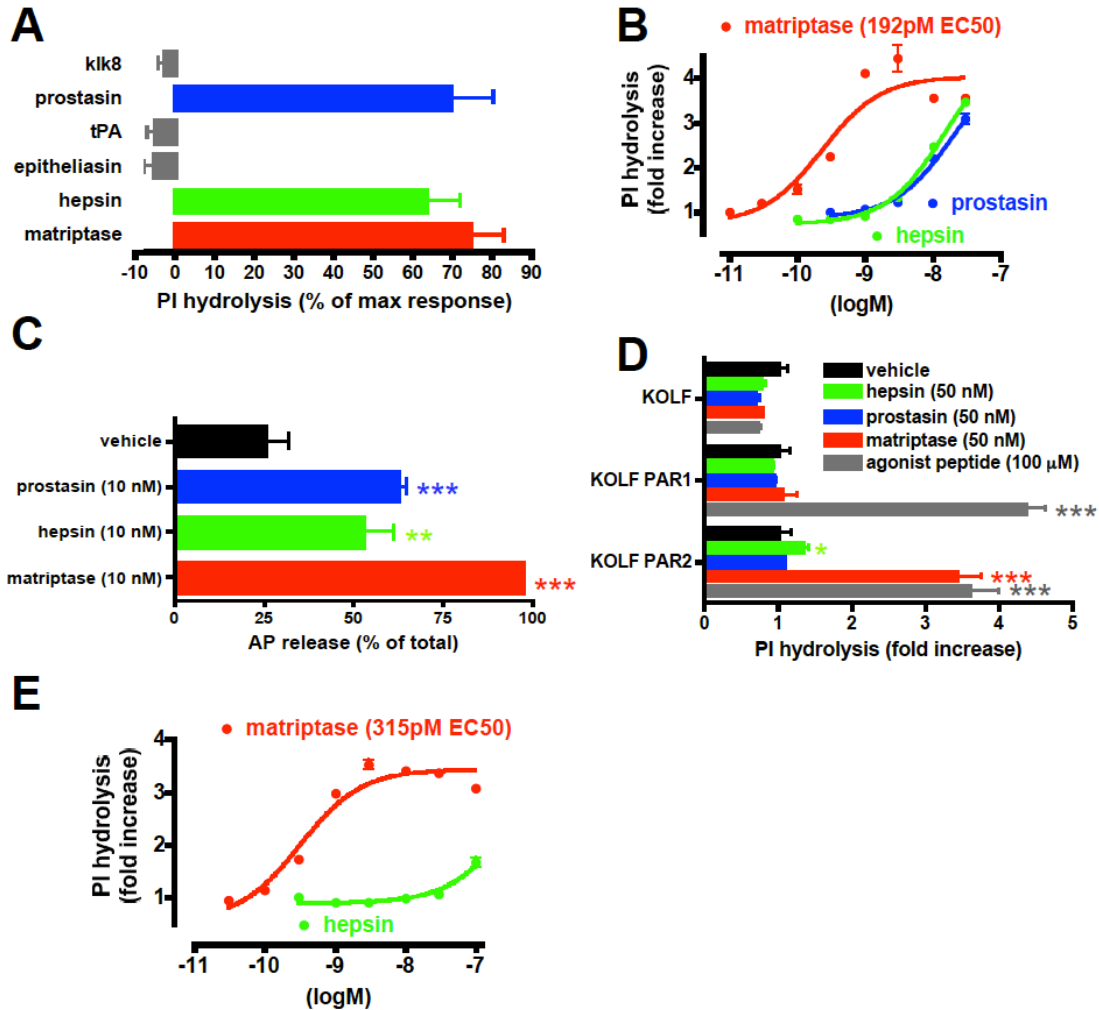


Figure 2.10. Par2 cleavage and activation by membrane-associated proteases. (A,B,E) Protease-triggered phosphoinositide (PI) hydrolysis in response to candidate Par2-activating proteases. (A) PI hydrolysis in HaCaT cultures after addition of soluble recombinant protease domains (50 nM) expressed as % of the response to maximal concentrations of PAR-activating peptides (100 μ M TFLLRN + 100 μ M SLIGRL). (B) Concentration response to protease domains that showed activity in (A). (C) Alkaline phosphatase (AP) release upon addition of soluble protease domains to HaCaTs transiently expressing an N-terminal AP-Par2 fusion protein. See Figure S5 for cleavage site specificity and PAR selectivity. (D) PI hydrolysis triggered by recombinant soluble protease domains or a maximal concentration (100 μ M) of PAR1 or PAR2 peptide agonist (or both peptides for untransfected KOLFs) in KOLFs stably transfected with PAR1 or PAR2. Similar results were obtained in three separate experiments. (E) PI hydrolysis in PAR2-expressing KOLFs, concentration response to matriptase and hepsin.

E2, a potent and highly selective antibody inhibitor to matriptase (Farady et al., 2008; Sun et al., 2003), blocked the ability of prostatic and hepsin to trigger phosphoinositide hydrolysis in HaCaT cultures (Figure 2.11a). E2 at the same concentration had no effect on signaling by factor Xa (Figure 2.11a), which can directly activate PAR2, nor did E2 inhibit the activity of 10nM prostatic or hepsin in amidolytic assays (not shown). These results suggested that prostatic and hepsin activated Par2 in HaCaTs by an indirect mechanism that was matriptase-dependent. To further probe this possibility, we examined Par2 cleavage in KOLFs with and without co-expression of matriptase. Hai-1 was co-expressed with matriptase in these experiments because matriptase expression in the absence of its inhibitor appeared to be toxic (not shown). In contrast to soluble recombinant matriptase, addition of soluble recombinant prostatic to KOLFs expressing AP-Par2 or AP-Par2 plus Hai-1 did not trigger AP release. However, soluble recombinant prostatic did release AP from KOLFs expressing AP-Par2 and Hai-1 plus matriptase but not active site mutant matriptase nor a matriptase mutated at the site required for proteolytic processing of the matriptase zymogen to the active form (Figure 2.11b and 2.12). Thus, Par2 cleavage by prostatic required expression of matriptase with an intact active site and an intact zymogen conversion site, consistent with a model in which prostatic activates Par2 by activating matriptase zymogen co-expressed in the same or nearby cells. Similar results were obtained with hepsin, but hepsin also showed weak direct activity at Par2 (Figure 2.12).

Purified recombinant matriptase can spontaneously cleave itself from zymogen to active form (Takeuchi et al., 1999), but how matriptase is activated in vivo and how such activation is regulated is unknown. To probe the state of matriptase heterologously expressed in KOLFs and naturally expressed in HaCaT cells and to further test the model that such matriptase can be activated by prostatic and hepsin, we utilized specific antibodies that distinguish two-chain, active matriptase from its zymogen form (Benaud et al., 2001; Wang et al., 2009). The fact that active matriptase migrates in a complex with Hai1 on non-reducing SDS-PAGE was also exploited to detect formation of active matriptase (Oberst et al., 2003).

Lysates of KOLFs transfected with Hai-1 plus vector or matriptase were analyzed by immunoblot with M69 and M24 antibodies; M69 recognizes the processed active form and M24 recognizes both zymogen and active forms (Wang et al., 2009). In the absence of added protease, matriptase and Hai-1 co-transfection resulted in the appearance of a 70 kDa band recognized by M24 but not M69, consistent with expression of matriptase in its zymogen form (Figure 2.11c, lane 4). Treatment with soluble recombinant active matriptase, prostatic, or hepsin caused the appearance of a matriptase transfection-dependent ~120 kDa band recognized by M69, consistent with appearance of active matriptase complexed with Hai-1 (Figure 2.11c, lanes 5-7). Prostatic was consistently the most active in this regard. The intensity of the 70kDa zymogen band recognized by M24 was concomitantly decreased, consistent with conversion of matriptase zymogen to its active form. The 65kDa band in the M69 blots likely represents

the truncated soluble recombinant matriptase, which is not recognized by M24. Exogenous matriptase, prostatic, and hepsin treatment also converted a matriptase active site mutant to a form recognized by M69 and Hai-1, suggesting that matriptase activity and autoactivation are not required to convert matriptase from its zymogen to its two-chain form in this system (Figure 2.11c, lanes 9-11). These results are consistent with a model in which prostatic and hepsin cleave and convert matriptase zymogen expressed on the surface of KOLFs to its active form.

Similar results were obtained in HaCaT cells that naturally express matriptase and HAI1. In lysates of untreated HaCaTs, matriptase was mainly in the zymogen form (Figure 2.11d, lanes 1-2, ~70 kDa band in M24 panel). Addition of soluble recombinant active matriptase, prostatic or hepsin caused the appearance of the active form of matriptase migrating in complex with Hai-1 (Figure 2.11d, lanes 3-8, ~120 kDa band in M69 panel). This band was also recognized by Hai-1 immunoblot (not shown). Again, prostatic was the most active of the three proteases tested in this assay. Taken together, our results are consistent with the notion that prostatic and hepsin activate the zymogen form of matriptase on KOLF and HaCaT cells.

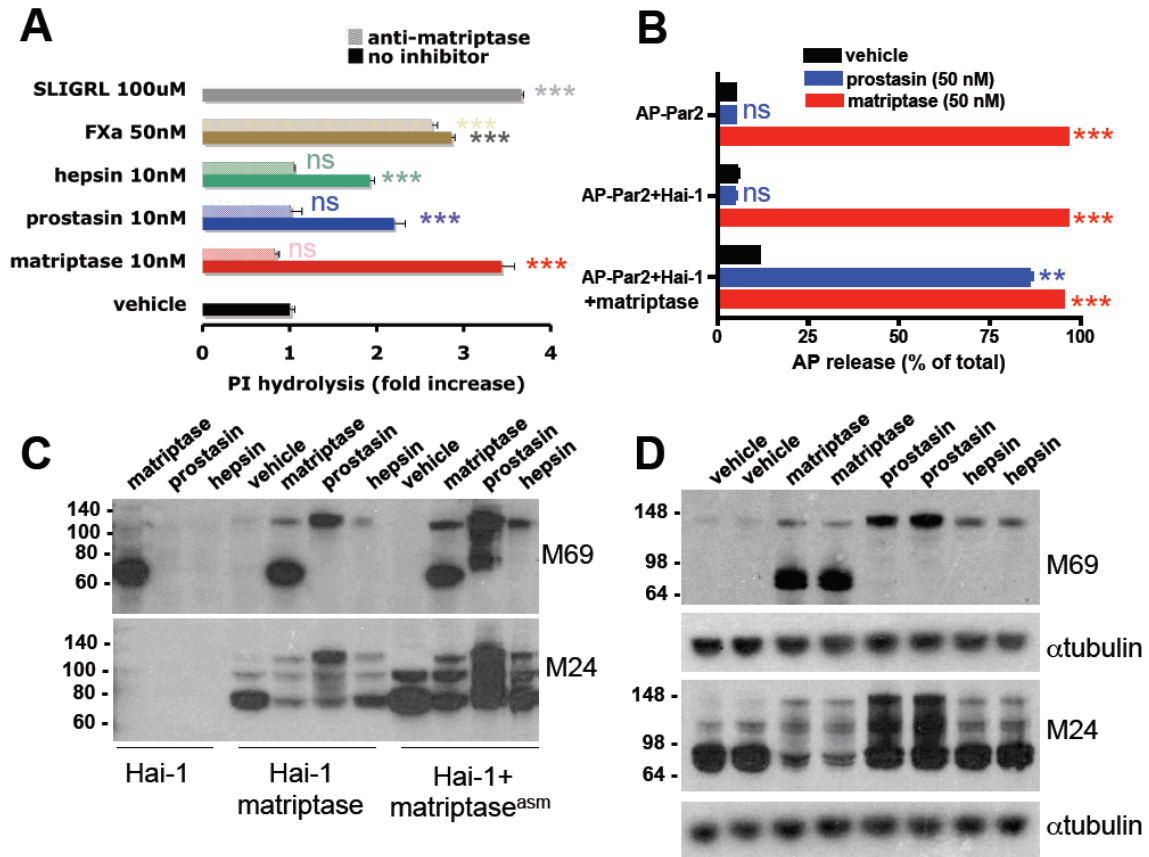


Figure 2.11. Evidence for a cascade from prostatic and hepsin to matriptase to Par2 activation. (A) Inhibition of protease-triggered PI hydrolysis in HaCaT by E2 (2 μ M), an active site-blocking antibody to matriptase. (B) Par2 cleavage by prostatic in KOLF cells transiently transfected with expression vectors for mouse AP-Par2, Hai-1 and full-length matriptase as indicated. AP release in response to addition of soluble recombinant prostatic or matriptase (50nM) was measured. (C) Immunoblot analysis of matriptase processing by prostatic and hepsin in KOLF cells transfected with Hai-1 alone or Hai-1 plus matriptase or matriptase active site mutant (asm) expression vectors. Cultures were treated with the soluble recombinant protease domains (50 nM) indicated at top; lysates were immunoblotted with M69 and M24 matriptase antibodies, which recognize the active processed form and total matriptase, respectively. (D) Conversion of endogenously expressed matriptase zymogen to its active form by prostatic and hepsin in HaCaT cultures. Cultures were treated with the indicated soluble recombinant protease domains and cell lysates analyzed as in (C). Tubulin blot served as a loading control. See also Figure 2.12.

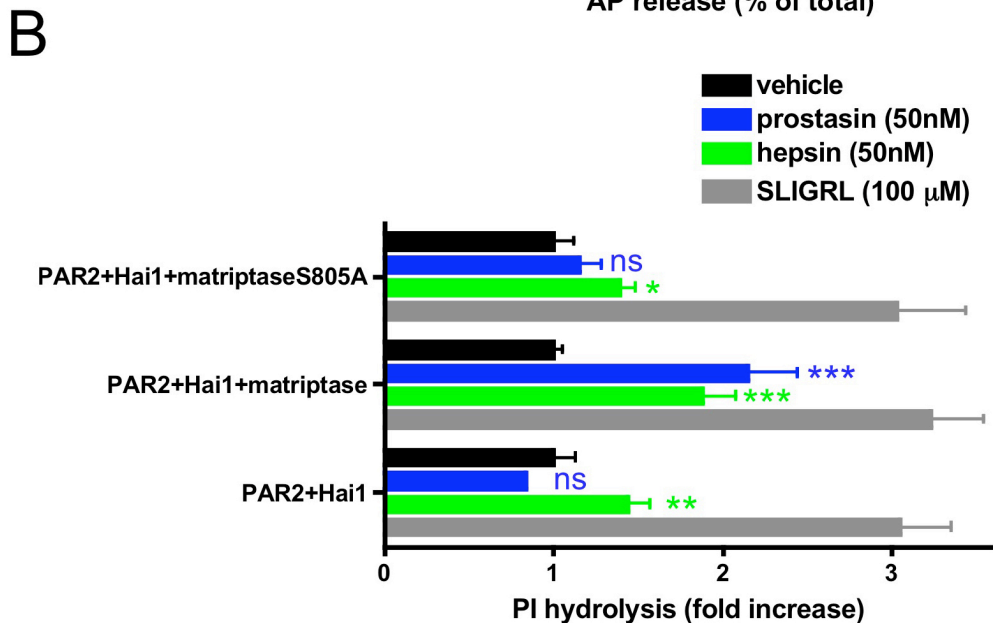
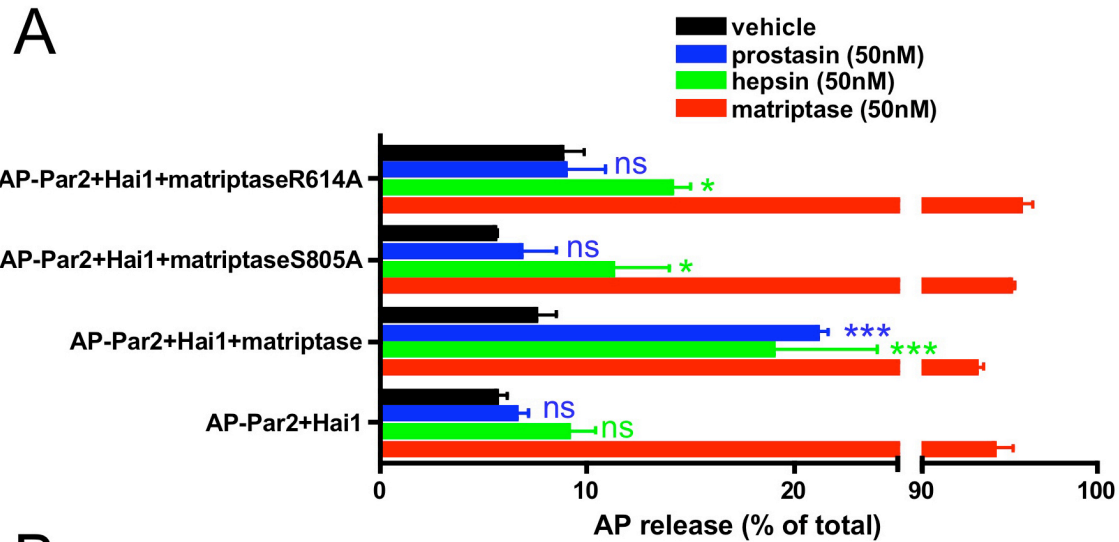


Figure 2.12, related to figure 2.11: In a fibroblast cell line, expression of matriptase, but not active site mutant or zymogen conversion site mutant matriptase, expression confers prostaticin-induced Par2 cleavage and signaling. (A) Par1 knockout lung fibroblasts (KOLF), which do not normally express any of the PARs, proteases or inhibitors studied here, were transiently transfected so as to express AP-Par2, the matriptase inhibitor Hai-1, and full-length wild-type matriptase, active site mutant matriptase (S805A), or zymogen-conversion site mutant matriptase (R614A). AP release in response to added proteases was measured as in Figure 2.9, except that results are expressed as % of AP-Par2 cleaved (defined as AP released by test protease/(amount release by test protease + amount released by subsequent incubation with 50nM trypsin for 5 min.). Note that AP release upon addition of active prostaticin occurred in cultures transfected with wild-type matriptase, but not in cultures lacking matriptase nor in cultures transfected with the matriptase mutants. Note also that hepsin showed some matriptase-independent and some matriptase-dependent activity at AP-Par2. (B) KOLFs were transfected as in A) and phosphoinositide (PI) hydrolysis in

response to added proteases was measured. Note prostatic response in cells expressing wild-type matriptase but not in controls. * $p < 0.05$, ** $p < 0.01$, *** $p < 0.001$, ^{ns} $p > 0.05$ by 2-way ANOVA and Bonferroni's post-test relative to vehicle treatment in the same transfection group. Results shown are mean \pm standard deviation (n=3).

Evidence for the presence of active matriptase at the time and place of neural tube closure.

The results outlined above suggest a model in which matriptase and Par2 are co-expressed in the surface ectoderm, with matriptase becoming activated locally in a manner that activates Par2 and supports normal closure of the neural tube. Matriptase is co-expressed with its inhibitors, Hai1 and 2 (Figure 2.7; see also (Kirchhofer et al., 2003; List et al., 2005; Szabo et al., 2008)), and with its candidate activators prostatic and hepsin. When and where active matriptase is made available to cleave substrates in vivo is unknown (List et al., 2006). To determine whether active matriptase is present at the same time and place as Par2 during neural tube closure, we utilized E2 (Farady et al., 2008) conjugated to Alexafluor 594 to stain live mouse embryos collected at 8.5 dpc (Figure 4D and Figure S5). Antibody bound to surface ectoderm in a distribution similar to that of Par2 expression. A control fluorescently labeled antibody showed no such anatomically specific binding. These results suggest that the matriptase active site is present on surface ectoderm cells at the time and place of neural tube closure, consistent with the model described above.

Discussion

PARs function in the context of responses to injury in the adult and contribute to cardiovascular development in the embryo. Our results show an unexpected role for PARs and protease signaling in regulating neural tube closure in the mouse embryo. Our results also suggest that matriptase and other

membrane-tethered proteases co-expressed with Par2 may comprise a local protease network that activates Par2 in this context. This paradigm for autocrine/paracrine PAR activation raises interesting questions regarding the roles of local protease signaling in regulating epithelia, and the observation that Par2 and other Gi-coupled GPCRs in surface ectoderm contribute to neural tube closure in mice may lead to insights into the complex mechanisms underlying human neural tube defects.

A role for PARs and Gi signaling in neural tube closure

During neural tube closure in rodents, surface ectoderm is the first structure to close the gap between the opposing sides of the open neural tube at the level of the hindbrain neuropore; at most other levels, the neuroepithelium is the site of initial closure (Geelen and Langman, 1979; Waterman, 1976). Exencephaly in *Par1^{-/-}:Par2^{-/-}*, *Grhl3^{Cre/+}:ROSA26^{PTX/+}*, and *Grhl3^{Cre/+}:Rac1^{fl/fl}* embryos suggests that disruption of GPCR, Gi, and Rac1 signaling in surface ectoderm hampers neural tube closure where surface ectoderm closure is an early event, but posterior neural tube defects in *Grhl3^{Cre/+}:ROSA26^{PTX/+}* and *Grhl3^{Cre/+}:Rac1^{fl/fl}* embryos suggest that Gi pathway signaling in surface ectoderm also contributes where the surface ectoderm closes after the neuroepithelium. Events during neural tube closure include fusion of the neuroepithelium, fusion of the surface ectoderm, de-adhesion of the neuroepithelium from the surface ectoderm and separation of the closed ectoderm from the neural tube, differentiation and migration of neural crest cells between these structures, and extensive remodeling of the extracellular matrix (Geelen and Langman, 1979;

Greene and Copp, 2009; Schoenwolf and Smith, 1990; Waterman, 1976; Zohn and Sarkar, 2008). Par2, G_i and Rac regulate multiple cellular events including reorganization of the actin cytoskeleton, lamellipod formation, cell spreading, polarization and migration, integrin and cadherin function, and other cellular processes. Which of these accounts for the phenotypes described herein remains to be determined.

The similarity of the *Grhl3* and *Par2* expression patterns prompted us to use *Grhl3* to drive Cre recombinase expression for surface ectoderm-specific excision of floxed alleles. Intriguingly, the 5' region of *Par2* contains several potential Grhl3 binding sites. Gel shift assays confirmed that these sites bind protein in a sequence-specific manner, but decreased *Par2* expression in surface ectoderm was not detected in *Grhl3* nulls (not shown). Whether *Grhl3* participates in the control of *Par2* expression and whether and how these genes might interact to contribute to neural tube closure remains to be determined. Regardless, Grhl3-Cre should be useful for excision of floxed alleles selectively in surface ectoderm.

Candidate Par2-activating proteases during neural tube closure

The finding that Par2 contributes to neural tube closure raised the question of what this receptor senses biochemically and physiologically. An answer requires identifying the protease(s) that activates Par2 in this context. Proteases reproducibly shown to cleave PARs productively have been extracellular serine proteases. Accordingly, we focused on secreted, GPI-linked,

and integral membrane proteins with an extracellular serine protease domain that are expressed in embryos at the time of neural tube closure as candidate Par2 activators. Analysis of Par2 and protease expression patterns, abundance in embryos collected at 8.5-9.25 dpc, expression in surface ectoderm at this time, and functional testing all pointed to matriptase as a strong candidate Par2 activator during neural tube closure.

Matriptase is a type-2 transmembrane protein with a serine protease domain at its extracellular carboxyl terminal. We previously identified matriptase as a potential Par2 activator based on its P1-P4 substrate sequence preference and found that recombinant matriptase protease domain activated Par2 heterologously expressed in *Xenopus* oocytes (Takeuchi et al., 2000). However, the EC_{50} for Par2-dependent signaling in this system was relatively high (>10 nM), and there was no obvious context in which to determine whether matriptase was a physiological Par2 activator. In the current study, recombinant matriptase productively cleaved and activated Par2 expressed in mammalian cells with an EC_{50} in the 200-300 pM range. Whether the difference in EC_{50} s in the *Xenopus* and mammalian systems is due to differences in temperature (25 vs. 37 °C), protease inhibitors, or other factors is unknown. Regardless, the impressive potency of soluble recombinant matriptase for Par2 activation in mammalian cells and the fact that the matriptase protease domain is normally tethered to the cell surface suggests that matriptase might be a physiological activator of Par2 in cells that express both protease and receptor. Detection of matriptase mRNA in surface ectoderm (Figure 2.7a,c) and binding of a matriptase active site-specific

antibody to the surface ectoderm cells near the closing neural tube (Figures 2.7c and 2.8) suggests that active matriptase may indeed co-exist with Par2 in vivo at a place and time consistent with a role in neural tube closure.

Matriptase did not show agonist activity for Par1, and the protease(s) that might activate Par1 in its possible back-up role in neural tube closure is unknown. No neural tube defects were reported in the matriptase knockout mice (List et al., 2002), but none would be expected if Par1 were activated by a matriptase-independent mechanism.

A local network of membrane-tethered proteases may trigger Par2 signaling

Several observations suggest that prostasin, which is GPI-linked to the cell surface, might interact with matriptase and contribute to Par2 activation. Prostasin is co-expressed with matriptase as well as Hai-1 and Hai-2, Kunitz-type inhibitors for both proteases, in many tissues (List et al., 2007) including surface ectoderm at the time of neural tube closure (Figure 2.7), and knockouts of the prostasin and matriptase genes in mouse exhibit similar phenotypes (defective skin development and barrier function) (Leyvraz et al., 2005; List et al., 2002). Both proteases are also tightly co-expressed with Par2 (Figure 2.10 and (Bhatt et al., 2007)). While soluble recombinant matriptase appeared to activate Par2 directly, soluble recombinant prostasin activated Par2 indirectly by a matriptase-dependent mechanism (Figures 2.10 and 2.11). The simplest model consistent with these and other data is that prostasin converts matriptase from a zymogen

form to an active form that can in turn activate Par2. In accord with this model, we recently observed that, like loss of matriptase inhibition (Szabo et al., 2009b), overexpression of either proprostasin or Par2 in mouse skin led to ichthyosis and that Par2 deficiency rescued skin abnormalities caused by proprostasin overexpression (Frateschi S, Camerer E, Coughlin SR, Hummler E and colleagues, submitted for publication). Par2 dependence of matriptase gain-of-function phenotypes was not addressed (Szabo et al., 2009b).

Although hepsin was expressed more broadly than matriptase, proprostasin and Par2, it was expressed in surface ectoderm during neural tube closure, and, like proprostasin, a soluble recombinant hepsin that included its protease domain showed matriptase-dependent signaling activity (Figure 2.10, 2.11). Hepsin is a type-2 transmembrane protein with an extracellular protease domain, and cell surface-localized hepsin might well be an effective matriptase activator.

Epitheliasin, another type-2 transmembrane protein with an extracellular protease domain that was expressed in surface ectoderm during neural tube closure, was often co-expressed with matriptase and Par2 (Figure 2.7). We did not detect epitheliasin-triggered signaling activity in either HaCaTs or matriptase and PAR2-expressing KOLFs, but PAR2-dependent signaling in LNCaP cells has been reported (Wilson et al., 2005). Epitheliasin might use an indirect mechanism to activate PAR2 in LNCaP cells that requires components present in LNCaP cells but absent in the HaCaT and KOLF systems.

Consistent with the mechanism proposed above for matriptase-dependent Par2 activation by proprostasin, our data suggest that matriptase naturally

expressed in HaCaT s or co-expressed with Hai-1 in KOLFs exists predominantly in the zymogen form and is converted to the active form upon addition of active prostaticin or hepsin (Figure 2.11c,d). Thus, Par2 activation in surface ectoderm cells that also express matriptase might be regulated at the level of matriptase activation. How matriptase activation is regulated in vivo is unknown. While our results suggest that prostaticin can activate matriptase, there is strong evidence that matriptase is necessary for normal prostaticin activation, at least in skin (Netzel-Arnett et al., 2006). Together, these observations raise the possibility that prostaticin might function both downstream and upstream of matriptase to constitute a positive feedback loop. Ready examples of this paradigm exist in the coagulation cascade, in which the effector protease thrombin activates upstream coagulation factors that mediate thrombin generation to amplify thrombin production and propagate coagulation in space and time (Broze, 1995).

Possible physiological roles for membrane-tethered protease/Par2 signaling

Intriguingly, while matriptase and prostaticin are often expressed in the same epithelial cell, they may sort to distinct membrane compartments, with matriptase directed basolaterally and prostaticin apically (Godiksen et al., 2008; Wang et al., 2009). Could it be that a prostaticin-matriptase-Par2 network has evolved to sense breaks in epithelial barrier function, in which loss of cell-cell junctions allows mixing of compartments such that the proteases make contact, activate and trigger activation of Par2 and other effectors? And/or might this

system function at the edges of closing epithelial sheets or in immature epithelium, where junctions and apical-basal polarity have not yet been established such that protease interaction and activation is permitted? Our detection of active matriptase predominantly at the edges of the surface ectoderm during neural tube closure is consistent with models that include such localized protease activation.

It was recently reported that deficiency of the protease inhibitor Hai-2 causes neural tube closure defects in mouse embryos that were partially rescued by concomitant matriptase deficiency (Szabo et al., 2009). If matriptase activates Par2, how might matriptase gain-of-function and Par2 loss-of-function yield similar phenotypes? Gain of matriptase function might result in increased cleavage of other physiological substrates and/or cleavage of non-physiological substrates to disrupt neural tube closure by a mechanism unrelated to Par2 activation. Alternatively, loss of matriptase inhibition might disrupt normal spatial and temporal control of Par2 activation and/or excess matriptase activity might downregulate Par2, effectively causing loss of Par2 function. Either mechanism might disrupt the precise tissue remodeling that occurs during neural tube closure (Massa et al., 2009). Regardless, this report supports the notion that matriptase is normally expressed and active in or around the closing neural tube, consistent with the model outlined above.

Might the paradigm of membrane-tethered or locally secreted proteases acting via Par2 to regulate epithelial function extend beyond neural tube closure? Expression profiling confirms a tight link in expression of Par2, matriptase,

prostasin, and epitheliasin across epithelial organs in adult mice, suggesting a potential functional link in adult biology as well. There are several reported roles for these proteases in regulating external barriers and in tumor progression where Par2 might be explored as a candidate effector (Bhatt et al., 2007; Klezovitch et al., 2004; Leyvraz et al., 2005; List et al., 2002; List et al., 2009; List et al., 2005). Like prostasin and matriptase, overexpression of Par2 in skin leads to hyperkeratosis, stratum corneum detachment and itching (EC and SRC, unpublished observations). Similar phenotypes have been reported for overexpression of Klk7 (Hansson et al., 2002), and excessive Klk5 activity secondary to loss of Kazal-type related inhibitor (Lektl; encoded by the Spink5 gene) has been suggested to drive stratum corneum detachment in Netherton syndrome in a PAR2-dependent manner (Briot et al., 2009). KLK5 has been reported as a PAR2 activator (Oikonomopoulou et al., 2006); we have confirmed this finding, whereas KLK7 appears to induce matriptase-dependent activation of Par2 like prostasin (not shown). PAR2 has a complex role in inflammation in the gastrointestinal tract (Vergnolle, 2000); tryptase, trypsin and Xa have been proposed activators in this context, but type-2 transmembrane serine proteases are highly expressed in gut epithelium and might well play a role. Together with our results, these observations support exploration of the notion that local networks of membrane-tethered proteases and Par2 might contribute to the regulation of epithelial function in homeostasis and disease.

Experimental Procedures

Nomenclature. Gene names are italicized. Human genes and proteins are in capital letters (*ST14*, ST14); mouse has first letter capitalized (*St14*, St14). Protease-activated receptors are designated by their commonly used designation Par1, Par2, etc. (their HUGO gene names are F2r, F2r1, etc.). PARs is used to refer to the family generically. Genes encoding Grhl3; the G protein α subunits $G\alpha_{12}$, $G\alpha_{13}$, and $G\alpha_z$; and matriptase are designated *Grhl3*; *G α_{12}* , *G α_{13}* , and *G α_z* ; and *St14*, respectively. HUGO gene names for $G\alpha_{12}$, $G\alpha_{13}$, and $G\alpha_z$ are *Gna12*, *Gna13* and *Gnaz*, respectively.

Mice, timed matings and gross analysis of mouse embryos. Experiments were performed in accordance with protocols approved by the UCSF internal animal use and care committee. The morning a vaginal plug was detected was considered 0.5 days post coitus (dpc). For embryo collection, yolk sack and placenta were removed intact, scored as below, then embryos were removed, examined and photographed. Before 12.5 dpc, viability was scored by the presence or absence of a heartbeat. At or after 12.5, the presence of pulsation in vitelline or umbilical vessels or response to pinch was used. In some cases, embryos and deciduas were fixed en bloc and processed for paraffin embedding and sectioning.

X-gal staining and in situ hybridization. Embryos were fixed, processed for X-gal staining (Griffin et al., 2001), then imaged or paraffin embedded, sectioned at 5 μ m and counterstained with Nuclear Fast Red. For in situ hybridization, 9.0 dpc embryos were fixed in 4% paraformaldehyde, washed and dehydrated. In situ

hybridization was performed in whole mount or on 5 μ m paraffin sections (Henrique et al., 1995; Soifer et al., 1994); images were acquired.

Cell Culture and cell signaling assays. HaCaTs and vector- and PAR-transfected KOLFs were grown in DMEM with 10% FBS, 100 units/ml penicillin, and 100 μ g/ml streptomycin (Camerer et al., 2000). KOLF, KOLF_{PAR2} or HaCaTs were transiently transfected with pSPORT6 (Open Biosystems) and pCDNA3 (Invitrogen) expression vectors carrying cDNAs for matriptase, matriptase_{S805A}, Hai-1 and/or human or mouse PARs by electroporation (Amaxa Inc) or using Mirus transfection reagent (Mirus). The next day, the cells were washed and incubated in SFM (serum-free DMEM with 20 mM HEPES and 0.1% bovine serum albumin (BSA)) with 2 μ Ci/mL *myo*-[³H]inositol overnight, then washed again and incubated with SFM for 2 hours prior to the addition of agonist and LiCl for 90 minutes. Cells were then extracted and released inositol phosphates measured (Camerer et al., 2000).

Receptor cleavage assay. AP-*Par1* and AP-*Par2* encoding secreted human placental alkaline phosphatase (SEAP) fused to the mouse PAR N-terminal with an intervening linker region containing the FLAG epitope were generated (Ludeman et al., 2004). Briefly, the coding regions of *Par1* and *Par2* C-terminal to the signal peptidase site were PCR amplified and ligated into the HpaI (5') and XbaI (3') sites of pCMV-SEAP (Tropix/Applied Biosystems) such that the SEAP stop codon was removed and SEAP was joined to each Par via an SGASGA

linker. PCR-based site directed mutagenesis was used to generate Par2_{R38A/S39P} and Par1_{R41A/S42P} cleavage site mutants and to generate the matriptase_{S805A} in which the active site serine was replaced by alanine (Takeuchi et al., 1999).

KOLF and HaCaT cells were transiently transfected with human or mouse matriptase, matriptase_{S805A}, and/or Hai-1 together with AP-Par1 or AP-Par2 or their cleavage site mutants. The next day, cells were washed and incubated in serum-free M199 with 25 mM HEPES and 0.1% BSA for two hours, treated with the indicated proteases for 60 minutes, and conditioned medium was assayed for alkaline phosphatase activity (Ludeman et al., 2004). The amount of intact receptor remaining on the cell surface and still available for cleavage after treatment with test proteases was determined by washing cells, then treating with trypsin (50 nM; Sigma) for an additional 5 minutes, at which time conditioned medium was collected and AP again measured. Data is presented as fold increase or % of total AP released (AP released by test protease/(same + remaining surface AP released by trypsin)). For HaCaT cell studies, 1,10 phenanthroline (5 mM) was added to the incubation medium to inhibit metalloprotease-dependent non-productive PAR shedding (Ludeman et al., 2004).

Matriptase immunoblot. Cells were treated as indicated, washed twice with ice-cold Tris-buffered saline (TBS) then lysed in 1X Laemmli sample buffer. Lysates were analyzed by SDS/PAGE under non-boiling, non-reducing conditions, then blotted onto nitrocellulose membranes. Membranes were

incubated with mouse monoclonal antibodies for active (M69) or total (M24) matriptase (Wang et al., 2009), then with horseradish peroxidase-conjugated goat anti-mouse IgG (Invitrogen) and chemiluminescence detection reagents (GE Healthcare).

Mice. Wild type C57BL/6 mice, Rac1 conditional knockouts (Rac1^{ff} (Glogauer et al., 2003)) and β -Galactosidase (Rosa26R;Rosa26^{lacZ}) Cre excision reporter mice were purchased from Jackson Laboratory (JAX; Bar Harbor, ME). Rosa26^{EYFP} reporter mice were from N. Killeen (UCSF, CA), β -actin-Cre from J. Miyazaki (Osaka University Medical School, Osaka), β -actin-FLP from S.M. Dymecki (Carnegie institute of Washington, Baltimore), the G_{12} and G_z knockout alleles were from M. Simon (California Institute of Technology, Pasadena, CA) and L.F. Brass (University of Pennsylvania School of Medicine, Philadelphia, PA), respectively (Offermanns et al., 1997; Yang et al., 2000). Generation of *Par1*^{lacZ}, *Par2*^{lacZ}, *Tie2 p/e-Par1*, and conditional G_{13} knockout and PTX inducible (ROSA26^{PTX}) mice has been described (Camerer et al., 2002; Griffin et al., 2001; Regard et al., 2007; Ruppel et al., 2005).

To generate the *Par1:Par2* double knockout, DNA containing the mouse Par1 and Par2 genes was obtained from a bacterial artificial chromosome (BAC) from a 129/SvJ mouse genomic library (Kahn et al., 1998). The *Par1* and *Par2* gene loci were sequentially targeted by lacZ knockin strategies as previously described for *Par1* and *Par4* alleles (Griffin et al., 2001; Sambrano et al., 2001). Briefly, a Kozak sequence immediately preceding a bacterial LacZ gene was inserted in

frame at the first ATG of each *Par* gene, thus simultaneously interrupting gene function and generating a reporter for gene expression. We first targeted *Par2* exon 1 in RF8 embryonic stem cells (129/SvJ) with a LacZ-PGK-Neo^R cassette (Camerer et al., 2002). After positive selection for integration (neomycin) and negative selection to ensure homologous recombination (thymidine kinase), correct targeting was confirmed by southern blotting with 5' and 3' probes. A correctly targeted ES line was then re-targeted by replacing the ATG and codons 2 to 4 of *Par1* exon 1 with a LacZ-PGK-Hygro^R cassette. LoxP sites were inserted at both recombined loci such that excision would remove the selectable markers and, when both targeting events had occurred on the same chromosome, the sequence between *Par1* and *Par2* (Figure 2.1). Double targeting of the same chromosome was confirmed by transfecting targeted clones with a Cre recombinase/puromycin vector, enriching for Cre expressing cells with puromycin, and then amplifying a PCR product that would only be produced in clones in which loxP sites from both targeting vectors were inserted in cis on the same chromosome (Figure 2.1). Chimeric males were generated by injecting doubly targeted ES cells into C57BL/6 blastocysts, and effects of gene deletion was addressed in offspring of F1 *Par1*^{+/-}:*Par2*^{+/-} mice. Importantly, since *Par1* and *Par2* are positioned within 100kb of each other on the same chromosome, segregation was never observed between mutant alleles (i.e. *Par1*^{+/-}:*Par2*^{+/-} intercrosses would only yield *Par1*^{+/+}:*Par2*^{+/+}, *Par1*^{+/-}:*Par2*^{+/-}, and *Par1*^{-/-}:*Par2*^{-/-} offspring). Some *Par1*^{+/-}:*Par2*^{+/-} mice were crossed with mice bearing a β-actin-Cre recombinase to excise the *neo* and *hygro* cassettes and

the 76 kb of genomic sequence between the *Par* genes. Excision was confirmed by Southern blotting. This intervening sequence does not contain known genes, and exencephaly was observed regardless of excision arguing that it is not secondary to introduction of the selectable marker cassettes. The studies described here were done with mice that had not been crossed with β -actin-Cre recombinase to exclude the possibility that unknown functional elements within the excised region might affect phenotypes.

To generate the *Grhl3*^{Cre} mouse line (Figure 2.13), we introduced a cDNA encoding P1 bacteriophage Cre recombinase in frame into the start ATG of the *Grhl3* gene as predicted by the Ensembl database (www.ensembl.org). To facilitate detection of expression directly, and later, to address the effects of Cre-mediated excision on target cells, an internal ribosomal entry sequence (IRES) followed by a nuclear localization signal and lacZ gene (Shah et al., 2004) were introduced downstream of the Cre gene. An FRT-flanked Neo cassette (Pappu et al., 2007) was positioned 5' of the Cre, and a thymidine kinase (tk) cassette was positioned outside the homologous arms (amplified by PCR from E14 ES cell DNA) for negative selection. The targeting construct was introduced into E14 ES cells (129SVJ) by electroporation, and, after positive and negative selection, homologous recombination was confirmed by Southern blotting with probes positioned both 5' and 3' of the homologous arms. Chimeric males derived from blastocyst injections of positive clones into C57BL/6 recipients were mated with C57 FLPe females to remove the neo gene.

Reagents. The agonist peptides TFLLRNPNDK (PAR1-specific) and SLIGRL (PAR2-specific) and AYPGKF (PAR4-specific) were from Anaspec (San Jose, CA). Recombinant mouse and human matriptase, hepsin, prostasin, Kik5 and Kik8 were purchased from R&D systems (Minneapolis, MN) or produced as previously described (Fan et al., 2005; Moran et al., 2006; Takeuchi et al., 1999). Active site inhibition was as described (Tripathi et al., 2008). Trypsin was from Sigma (St. Louis, MO), tPA from Abcam (Cambridge, MA), human FXa from Hematologic Technologies (Essex Junction, VT) and epitheliasin a kind gift from Peter Nelson (University of Washington, Seattle, WA).

Generation, validation and use of a qRT-PCR array to identify new Par agonist proteases. We focused on trypsin-like serine proteases because 1) productive cleavage of PARs takes place after a P1 arginine or lysine immediately amino-terminal of the tethered ligand, and proteases with such specificity are usually in the trypsin family, and 2) PAR-activating proteases described to date have been trypsin-like serine proteases. The exception to this is MMP-1 (Boire et al., 2005), and we have been unable to replicate this report. Accordingly, proteins in the Pfam protein database (pfam.sanger.ac.uk) containing a trypsin domain were chosen; proteases that did not have a signal peptide or a transmembrane domain were eliminated as were proteases described in the literature as intracellular, inactive, or without activity toward substrates with a P1 arginine or lysine. TaqMan primer/probe sets (5' FAM/3' BHQ) for real-time PCR were designed for each of the 125 remaining proteases plus 11 select inhibitors using Primer Express software (Applied Biosystems) and

cDNA sequences from the Ensembl database (<http://www.ensembl.org/>), and were purchased from Biosearch Technologies (Novato, CA). Of the primer-probe sets employed, 121 amplified products from at least one RNA source. Whether the 4 genes for which expression was not detected (*Gzme*, *Klk4*, *Mcpt9* and *Tessp3*) are expressed only in cell types not examined or represent pseudogenes or a failure of the specific primer-probe sets used is not known. mRNA isolation, first strand synthesis, Taqman qPCR, normalization of protease Ct data to housekeeping genes using the Δ Ct method, and conversion to fold-increase over abundance of each protease mRNA in mixed tissues using the $\Delta\Delta$ Ct method was as described (Regard et al., 2008). Dilution studies revealed that the amount of qRT-PCR product was proportional to the amount of starting material. TA cloning (Invitrogen) and sequencing of 10% of qPCR amplicons showed all to be the expected products.

Application of this qPCR array to assess protease expression in mid-gestational wild-type embryos and across mouse tissues using this qPCR array was as described (Regard et al., 2008). To generate surface ectoderm cDNA for qPCR, embryos were collected at E8.75-E9.5 embryos from *Grhl3*^{Cre/+} male, *ROSA26*^{EYFP/EYFP} female crosses. EYFP-positive embryos were identified by immunofluorescence microscopy and separated, digested for 15 minutes with collagenase/dispase (Roche), homogenized with an insulin syringe and purified through a 100 μ m cell strainer. A FACSAria cell sorter (Beckton Dickinson) was used to separate EYFP-positive cells from EYFP-negative cells. The fraction of EYFP-positive cells ranged from approximately 1% at E8.75 to 6% at E9.5,

consistent with our observation that *Grhl3*^{Cre} excision of EYFP or lacZ reporter lines began in the surface ectoderm cells over the ridge of the fusing neuroectoderm at E8.75 and spread to most of surface ectoderm by E9.5 (Figure 2.13). RNA was isolated from EYFP-positive cells and, for comparison, EYFP-negative cells for cDNA synthesis and qPCR as described above.

Whole-mount staining of live mouse embryos for active matriptase. Wild-type embryos were harvested at E8.75-E9.25, incubated in 10% goat serum for 15 minutes and subsequently in M199 with 0.1% BSA and 25mM HEPES, pH 7.4 with an Alexafluor 594 conjugated anti-matriptase antibody (200nM; EB9/E2 scFv (Farady et al., 2008; Sun et al., 2003)), irrelevant antibody or dye alone for 45 minutes at room temperature. Embryos were washed five times in PBS, fixed in 4% paraformaldehyde for 20 minutes, and imaged on an MRC-1024 laser scanning confocal microscope (Biorad Laboratories). Images represent combined Z-series slices through the entire depth of the embryos. Control embryos incubated either with dye alone or with an irrelevant antibody at the same concentrations as the conjugated anti-matriptase antibody did not show specific staining in surface ectoderm.

Statistical analysis. Phenotype frequencies were analyzed by Chi-Square. Phosphoinositide hydrolysis and AP release assays were analyzed by one- or two-way ANOVA followed by t-test for individual comparisons. Bonferroni correction for planned multiple comparisons was included when appropriate.

Single, double and triple asterisks (*) indicate $p < 0.05$, 0.01 and 0.001 compared to vehicle control, respectively; not significant (ns) indicates $p > 0.05$. The findings reported in Figures 2.10 and 2.11 were reproduced at least twice. Data shown are mean \pm SD. N was 3 or greater except for 6B (n=2).

Acknowledgements: S.R.C., C.S.C. and co-workers are funded by the National Institutes of Health. Eric Camerer is funded by an INSERM Avenir Fellowship. Daniel Kirchhofer and Rajkumar Ganesan are employees of Genentech, Inc. Linda Prentice, Lydia-Marie Joubert, Jinny Wong, Leonor Patel, Cherry Concengco, Khushboo Kaushal, Ganesh Elongavan, and Jay Dietrich for technical support; Brian Black, Orion Weiner, Takashi Mikawa, Sarah DeVal, Pooja Agarwal for advice; Nirao Shah for the IRES-NLSlacZ construct; Mel Simon, Skip Brass, David Kwiatkowski, Jun-ichi Miyazaki, Nigel Killeen and Susan Dymecki for mouse lines; and Henry Bourne for critical reading of the manuscript.

References

Auden, A., Caddy, J., Wilanowski, T., Ting, S.B., Cunningham, J.M., and Jane, S.M. (2006). Spatial and temporal expression of the Grainyhead-like transcription factor family during murine development. *Gene Expr Patterns* 6, 964-970.

Becker, R.C., Moliterno, D.J., Jennings, L.K., Pieper, K.S., Pei, J., Niederman, A., Ziada, K.M., Berman, G., Strony, J., Joseph, D., *et al.* (2009). Safety and tolerability of SCH 530348 in patients undergoing non-urgent percutaneous coronary intervention: a randomised, double-blind, placebo-controlled phase II study. *Lancet* 373, 919-928.

Benaud, C., Dickson, R.B., and Lin, C.Y. (2001). Regulation of the activity of matriptase on epithelial cell surfaces by a blood-derived factor. *Eur J Biochem* 268, 1439-1447.

Bhatt, A.S., Welm, A., Farady, C.J., Vasquez, M., Wilson, K., and Craik, C.S. (2007). Coordinate expression and functional profiling identify an extracellular proteolytic signaling pathway. *Proc Natl Acad Sci U S A* 104, 5771-5776.

Briot, A., Deraison, C., Lacroix, M., Bonnart, C., Robin, A., Besson, C., Dubus, P., and Hovnanian, A. (2009). Kallikrein 5 induces atopic dermatitis-like lesions through PAR2-mediated thymic stromal lymphopoietin expression in Netherton syndrome. *J Exp Med* 206, 1135-1147.

Broze, G.J., Jr. (1995). Tissue factor pathway inhibitor and the revised theory of coagulation. *Annu Rev Med* 46, 103-112.

Camerer, E., Duong, D.N., Hamilton, J.R., and Coughlin, S.R. (2004). Combined deficiency of protease-activated receptor-4 and fibrinogen recapitulates the hemostatic defect but not the embryonic lethality of prothrombin deficiency. *Blood* 103, 152-154.

Camerer, E., Huang, W., and Coughlin, S.R. (2000). Tissue factor- and factor X-dependent activation of protease-activated receptor 2 by factor VIIa. *Proc Natl Acad Sci U S A* 97, 5255-5260.

Camerer, E., Kataoka, H., Kahn, M., Lease, K., and Coughlin, S.R. (2002). Genetic evidence that protease-activated receptors mediate factor Xa signaling in endothelial cells. *J Biol Chem* 277, 16081-16087.

Connolly, A.J., Ishihara, H., Kahn, M.L., Farese, R.V., Jr., and Coughlin, S.R. (1996). Role of the thrombin receptor in development and evidence for a second receptor. *Nature* 381, 516-519.

Copp, A.J., Greene, N.D., and Murdoch, J.N. (2003). The genetic basis of mammalian neurulation. *Nat Rev Genet* 4, 784-793.

Coughlin, S.R. (2000). Thrombin signalling and protease-activated receptors. *Nature* 407, 258-264.

Coughlin, S.R., and Camerer, E. (2003). PARticipation in inflammation. *J Clin Invest* 111, 25-27.

Damiano, B.P., Cheung, W.M., Santulli, R.J., Fung-Leung, W.P., Ngo, K., Ye, R.D., Darrow, A.L., Derian, C.K., de Garavilla, L., and Andrade-Gordon, P. (1999). Cardiovascular responses mediated by protease-activated receptor-2 (PAR-2) and thrombin receptor (PAR-1) are distinguished in mice deficient in PAR-2 or PAR-1. *J Pharmacol Exp Ther* 288, 671-678.

Farady, C.J., Egea, P.F., Schneider, E.L., Darragh, M.R., and Craik, C.S. (2008). Structure of an Fab-protease complex reveals a highly specific non-canonical mechanism of inhibition. *J Mol Biol* 380, 351-360.

Fleming, A., and Copp, A.J. (1998). Embryonic folate metabolism and mouse neural tube defects. *Science* 280, 2107-2109.

Geelen, J.A., and Langman, J. (1979). Ultrastructural observations on closure of the neural tube in the mouse. *Anat Embryol (Berl)* 156, 73-88.

Godiksen, S., Selzer-Plon, J., Pedersen, E.D., Abell, K., Rasmussen, H.B., Szabo, R., Bugge, T.H., and Vogel, L.K. (2008). Hepatocyte growth factor activator inhibitor-1 has a complex subcellular itinerary. *Biochem J* 413, 251-259.

Greene, N.D., and Copp, A.J. (2009). Development of the vertebrate central nervous system: formation of the neural tube. *Prenat Diagn* 29, 303-311.

Griffin, C.T., Srinivasan, Y., Zheng, Y.W., Huang, W., and Coughlin, S.R. (2001). A role for thrombin receptor signaling in endothelial cells during embryonic development. *Science* 293, 1666-1670.

Guo, H., Liu, D., Gelbard, H., Cheng, T., Insalaco, R., Fernandez, J.A., Griffin, J.H., and Zlokovic, B.V. (2004). Activated protein C prevents neuronal apoptosis via protease activated receptors 1 and 3. *Neuron* 41, 563-572.

Gustavsson, P., Greene, N.D., Lad, D., Pauws, E., de Castro, S.C., Stanier, P., and Copp, A.J. (2007). Increased expression of Grainyhead-like-3 rescues spina bifida in a folate-resistant mouse model. *Hum Mol Genet* 16, 2640-2646.

Hansson, L., Backman, A., Ny, A., Edlund, M., Ekholm, E., Ekstrand Hammarstrom, B., Tornell, J., Wallbrandt, P., Wennbo, H., and Egelrud, T.

(2002). Epidermal overexpression of stratum corneum chymotryptic enzyme in mice: a model for chronic itchy dermatitis. *J Invest Dermatol* 118, 444-449.

Harden, N., Loh, H.Y., Chia, W., and Lim, L. (1995). A dominant inhibitory version of the small GTP-binding protein Rac disrupts cytoskeletal structures and inhibits developmental cell shape changes in *Drosophila*. *Development* 121, 903-914.

Henrique, D., Adam, J., Myat, A., Chitnis, A., Lewis, J., and Ish-Horowicz, D. (1995). Expression of a Delta homologue in prospective neurons in the chick. *Nature* 375, 787-790.

Kahn, M.L., Nakanishi-Matsui, M., Shapiro, M.J., Ishihara, H., and Coughlin, S.R. (1999). Protease-activated receptors 1 and 4 mediate activation of human platelets by thrombin. *J Clin Invest* 103, 879-887.

Kirchhofer, D., Peek, M., Li, W., Stamos, J., Eigenbrot, C., Kadkhodayan, S., Elliott, J.M., Corpuz, R.T., Lazarus, R.A., and Moran, P. (2003). Tissue expression, protease specificity, and Kunitz domain functions of hepatocyte growth factor activator inhibitor-1B (HAI-1B), a new splice variant of HAI-1. *J Biol Chem* 278, 36341-36349.

Klezovitch, O., Chevillet, J., Mirosevich, J., Roberts, R.L., Matusik, R.J., and Vasioukhin, V. (2004). Hepsin promotes prostate cancer progression and metastasis. *Cancer Cell* 6, 185-195.

Leyvraz, C., Charles, R.P., Rubera, I., Guitard, M., Rotman, S., Breiden, B., Sandhoff, K., and Hummler, E. (2005). The epidermal barrier function is dependent on the serine protease CAP1/Prss8. *J Cell Biol* 170, 487-496.

List, K., Bugge, T.H., and Szabo, R. (2006). Matriptase: potent proteolysis on the cell surface. *Mol Med* 12, 1-7.

List, K., Haudenschild, C.C., Szabo, R., Chen, W., Wahl, S.M., Swaim, W., Engelholm, L.H., Behrendt, N., and Bugge, T.H. (2002). Matriptase/MT-SP1 is required for postnatal survival, epidermal barrier function, hair follicle development, and thymic homeostasis. *Oncogene* 21, 3765-3779.

List, K., Hobson, J.P., Molinolo, A., and Bugge, T.H. (2007). Co-localization of the channel activating protease prostasin/(CAP1/PRSS8) with its candidate activator, matriptase. *J Cell Physiol* 213, 237-245.

List, K., Kosa, P., Szabo, R., Bey, A.L., Wang, C.B., Molinolo, A., and Bugge, T.H. (2009). Epithelial integrity is maintained by a matriptase-dependent proteolytic pathway. *Am J Pathol* 175, 1453-1463.

List, K., Szabo, R., Molinolo, A., Sriuranpong, V., Redeye, V., Murdock, T., Burke, B., Nielsen, B.S., Gutkind, J.S., and Bugge, T.H. (2005). Deregulated matriptase causes ras-independent multistage carcinogenesis and promotes ras-mediated malignant transformation. *Genes Dev* 19, 1934-1950.

Ludeman, M.J., Zheng, Y.W., Ishii, K., and Coughlin, S.R. (2004). Regulated shedding of PAR1 N-terminal exodomain from endothelial cells. *J Biol Chem* 279, 18592-18599. Epub 12004 Feb 18524.

Mackman, N. (2004). Role of tissue factor in hemostasis, thrombosis, and vascular development. *Arterioscler Thromb Vasc Biol* 24, 1015-1022.

Massa, V., Greene, N.D., and Copp, A.J. (2009). Do cells become homeless during neural tube closure? *Cell Cycle* 8, 2479-2480.

Nakanishi-Matsui, M., Zheng, Y.W., Sulciner, D.J., Weiss, E.J., Ludeman, M.J., and Coughlin, S.R. (2000). PAR3 is a cofactor for PAR4 activation by thrombin. *Nature* 404, 609-613.

Netzel-Arnett, S., Currie, B.M., Szabo, R., Lin, C.Y., Chen, L.M., Chai, K.X., Antalis, T.M., Bugge, T.H., and List, K. (2006). Evidence for a matriptase-prostasin proteolytic cascade regulating terminal epidermal differentiation. *J Biol Chem* 281, 32941-32945.

Oberst, M.D., Williams, C.A., Dickson, R.B., Johnson, M.D., and Lin, C.Y. (2003). The activation of matriptase requires its noncatalytic domains, serine protease domain, and its cognate inhibitor. *J Biol Chem* 278, 26773-26779.

Offermanns, S., Zhao, L.P., Gohla, A., Sarosi, I., Simon, M.I., and Wilkie, T.M. (1998). Embryonic cardiomyocyte hypoplasia and craniofacial defects in G alpha q/G alpha 11-mutant mice. *EMBO J* 17, 4304-4312.

Oikonomopoulou, K., Hansen, K.K., Saifeddine, M., Vergnolle, N., Tea, I., Blaber, M., Blaber, S.I., Scarisbrick, I., Diamandis, E.P., and Hollenberg, M.D. (2006). Kallikrein-mediated cell signalling: targeting proteinase-activated receptors (PARs). *Biol Chem* 387, 817-824.

Regard, J.B., Kataoka, H., Cano, D.A., Camerer, E., Yin, L., Zheng, Y.W., Scanlan, T.S., Hebrok, M., and Coughlin, S.R. (2007). Probing cell type-specific functions of Gi in vivo identifies GPCR regulators of insulin secretion. *J Clin Invest* 117, 4034-4043.

Riewald, M., and Ruf, W. (2001). Mechanistic coupling of protease signaling and initiation of coagulation by tissue factor. *Proc Natl Acad Sci U S A* 98, 7742-7747.

Ruppel, K.M., Willison, D., Kataoka, H., Wang, A., Zheng, Y.W., Cornelissen, I., Yin, L., Xu, S.M., and Coughlin, S.R. (2005). Essential role for Galpha13 in endothelial cells during embryonic development. *Proc Natl Acad Sci U S A* 102, 8281-8286.

Sambrano, G.R., Weiss, E.J., Zheng, Y.W., Huang, W., and Coughlin, S.R. (2001). Role of thrombin signalling in platelets in haemostasis and thrombosis. *Nature* 413, 74-78.

Schoenwolf, G.C., and Smith, J.L. (1990). Mechanisms of neurulation: traditional viewpoint and recent advances. *Development* 109, 243-270.

Soifer, S.J., Peters, K.G., O'Keefe, J., and Coughlin, S.R. (1994). Disparate temporal expression of the prothrombin and thrombin receptor genes during mouse development. *Am J Pathol* 144, 60-69.

Sugihara, K., Nakatsuji, N., Nakamura, K., Nakao, K., Hashimoto, R., Otani, H., Sakagami, H., Kondo, H., Nozawa, S., Aiba, A., *et al.* (1998). Rac1 is required for the formation of three germ layers during gastrulation. *Oncogene* 17, 3427-3433.

Sun, J., Pons, J., and Craik, C.S. (2003). Potent and selective inhibition of membrane-type serine protease 1 by human single-chain antibodies. *Biochemistry* 42, 892-900.

Szabo, R., Hobson, J.P., Christoph, K., Kosa, P., List, K., and Bugge, T.H. (2009). Regulation of cell surface protease matriptase by HAI2 is essential for placental development, neural tube closure and embryonic survival in mice. *Development* 136, 2653-2663.

Szabo, R., Hobson, J.P., List, K., Molinolo, A., Lin, C.Y., and Bugge, T.H. (2008). Potent inhibition and global co-localization implicate the transmembrane Kunitz-type serine protease inhibitor hepatocyte growth factor activator inhibitor-2 in the regulation of epithelial matriptase activity. *J Biol Chem* 283, 29495-29504.

Takeuchi, T., Harris, J.L., Huang, W., Yan, K.W., Coughlin, S.R., and Craik, C.S. (2000). Cellular localization of membrane-type serine protease 1 and identification of protease-activated receptor-2 and single-chain urokinase-type plasminogen activator as substrates. *J Biol Chem* 275, 26333-26342.

Takeuchi, T., Shuman, M.A., and Craik, C.S. (1999). Reverse biochemistry: use of macromolecular protease inhibitors to dissect complex biological processes and identify a membrane-type serine protease in epithelial cancer and normal tissue. *Proc Natl Acad Sci U S A* 96, 11054-11061.

Ting, S.B., Wilanowski, T., Auden, A., Hall, M., Voss, A.K., Thomas, T., Parekh, V., Cunningham, J.M., and Jane, S.M. (2003). Inositol- and folate-resistant neural

tube defects in mice lacking the epithelial-specific factor Grhl-3. *Nat Med* 9, 1513-1519.

Vergnolle, N. (2000). Review article: proteinase-activated receptors - novel signals for gastrointestinal pathophysiology. *Aliment Pharmacol Ther* 14, 257-266.

Vergnolle, N., Wallace, J.L., Bunnett, N.W., and Hollenberg, M.D. (2001). Protease-activated receptors in inflammation, neuronal signaling and pain. *Trends Pharmacol Sci* 22, 146-152.

Vouret-Craviari, V., Grall, D., and Van Obberghen-Schilling, E. (2003). Modulation of Rho GTPase activity in endothelial cells by selective proteinase-activated receptor (PAR) agonists. *J Thromb Haemost* 1, 1103-1111.

Vu, T.K., Hung, D.T., Wheaton, V.I., and Coughlin, S.R. (1991). Molecular cloning of a functional thrombin receptor reveals a novel proteolytic mechanism of receptor activation. *Cell* 64, 1057-1068.

Wang, J.K., Lee, M.S., Tseng, I.C., Chou, F.P., Chen, Y.W., Fulton, A., Lee, H.S., Chen, C.J., Johnson, M.D., and Lin, C.Y. (2009). Polarized epithelial cells secrete matriptase as a consequence of zymogen activation and HAI-1-mediated inhibition. *Am J Physiol Cell Physiol* 297, C459-470.

Waterman, R.E. (1976). Topographical changes along the neural fold associated with neurulation in the hamster and mouse. *Am J Anat* 146, 151-171.

Wilson, S., Greer, B., Hooper, J., Zijlstra, A., Walker, B., Quigley, J., and Hawthorne, S. (2005). The membrane-anchored serine protease, TMPRSS2, activates PAR-2 in prostate cancer cells. *Biochem J* 388, 967-972.

Zohn, I.E., and Sarkar, A.A. (2008). Modeling neural tube defects in the mouse. *Curr Top Dev Biol* 84, 1-35.

CHAPTER THREE:

Matriptase Orchestrates Epithelial Cell Extrusion in the Zebrafish Embryo in a Protease-Activated Receptor 2-Dependent Manner.

Background

Protease-activated receptors (PARs) are G protein-coupled receptors that mediate cellular responses to extracellular proteases. Among the four PARs found in mammals, PAR1, PAR3 and PAR4 mediate cellular responses to the coagulation protease thrombin to orchestrate hemostasis, inflammation and other physiological responses to tissue injury. These same receptors also contribute to vascular integrity and remodeling during embryonic development (Coughlin, 2005). The physiological activators of PAR2 are uncertain and its roles in vivo have been incompletely explored. PAR2 is co-expressed with the membrane-tethered protease matriptase and its inhibitors, Hai1 and Hai2, in most epithelia (Camerer et al., 2010). Matriptase, a type-2 integral membrane protein, displays a trypsin-like serine protease domain at its extracellular carboxyl terminal. The P4-P1' amino acid sequence of the activating cleavage site of PAR2 is favorable for cleavage by matriptase, and exposure of cultured cells expressing PAR2 to even subnanomolar concentrations of soluble recombinant matriptase protease domain leads to PAR2 cleavage and activation (Takeuchi et al., 2000; Camerer et al., 2010). Overexpression of matriptase (List et al., 2005), the matriptase

activator prostaticin or PAR2 (Frateschi et al., 2011) in mouse skin leads to hyperplasia and defective barrier function, and matriptase is necessary for the normal barrier function of skin and gut epithelium (List et al., 2002; List et al., 2009; Buzza et al., 2010). The mechanisms and roles of matriptase and PAR2 in regulating epithelial functions are incompletely understood.

Given the activities of matriptase and PAR2 described above and their co-expression in epithelial tissues and cell types, we sought to determine whether matriptase might be a physiological activator of PAR2 and to identify the role of any such activation in regulating epithelial cell function. We report evidence that PAR2 contributes to matriptase-dependent extrusion of cells from skin of zebrafish embryos. Our results suggest that local protease signaling may help orchestrate extrusion of cells from epithelial sheets, a highly organized program that maintains epithelial barrier function while jettisoning apoptotic, damaged or infected cells.

Results.

The skin of the zebrafish embryo provides a useful model system for the study of epithelial remodeling in vivo. The skin is readily visualized, useful transgenic lines are in hand, and microinjection of zebrafish embryos with antisense morpholino oligonucleotides, cRNA, or transgenes enables convenient manipulation of gene expression. Lessons learned by study of zebrafish skin will likely extend to other epithelia and other species, a notion supported by our studies and others.

Deficiency of the matriptase inhibitor Hai1a in zebrafish embryos causes abnormal skin development characterized by aggregation of keratinocytes on the surface of the skin, most prominently between the yolk sac and yolk sac extension; this is associated with an increase in free cells or debris in the chorionic cavity (Carney et al., 2007; Mathias et al., 2007). Tissue infiltration by neutrophils is present, but the skin phenotype is neutrophil-independent. Knockdown of matriptase expression rescues these phenotypes, suggesting that Hai1a deficiency results in matriptase-dependent abnormalities in zebrafish skin (Carney et al., 2007).

We first established that zebrafish embryos injected with a Hai1a translation-blocking morpholino oligonucleotide (MO) exhibited the skin phenotype described for the Hai1a mutant (*hi2217*) including the appearance of cell aggregates on the surface of skin, free cells in the chorionic cavity, and extravascular neutrophils (Figure 3.1). Importantly, the number of aggregates appearing, the amount of debris in the chorionic cavity and the survival rate were dependent upon morpholino dose. As with the Hai1a mutant *hi2217*, the phenotypes associated with Hai1a morpholino injection were rescued by injection of a matriptase translation-blocking morpholino (Figures 3.1 a,b; Figure 3.2). When subjected to blind scoring, 89% of Hai1a morphants had a severe phenotype compared to only 2% of Hai1a:St14 double morphants. Conversely, 90% of Hai1a:St14 double morphants had a mild or normal phenotype, compared to 0% of Hai1a morphants. These results support the notion that increased matriptase protease activity accounts for the Hai1a morphant phenotype and

provided a platform for examining necessary roles of potential substrates of matriptase in this system.

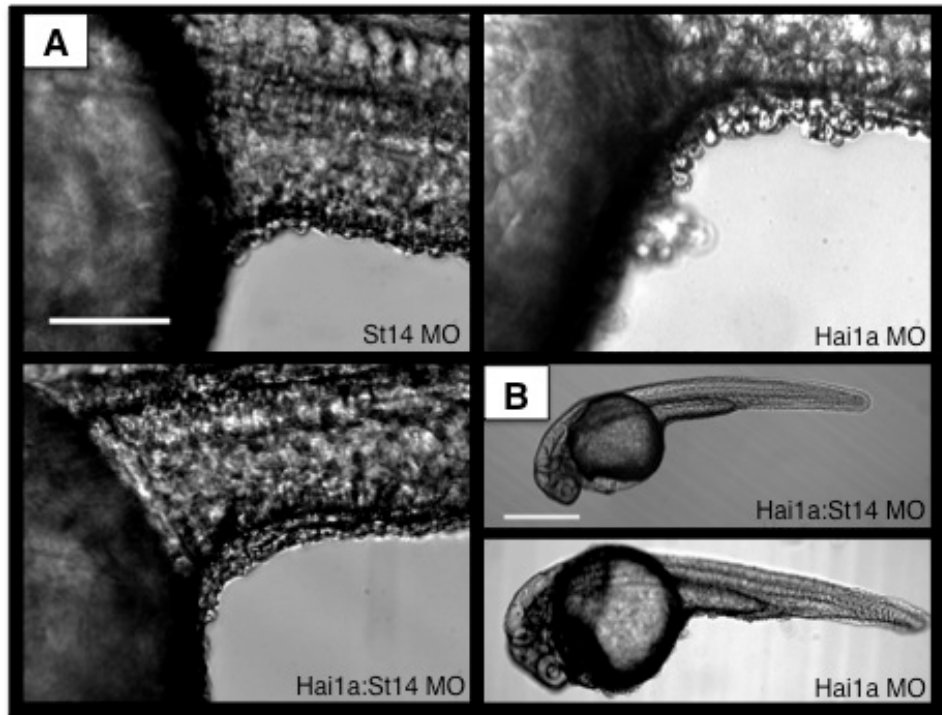


Figure 3.1. St14 knockdown rescues Hai1 zebrafish morphants. (A) Representative images of 24 hpf zebrafish embryos injected with St14, Hai1, or a combination of St14 & Hai1 MOs. Images focus on the intersection of the yolk sac and yolk sac extension where cell shedding is most prominent. Images are DIC at 20X magnification. Scale bar = 100 μ m. (B) DIC images at 4X magnification depicting representative 24 hpf zebrafish embryos injected with Hai1 or Hai1 & St14 morpholinos. Scale bar = 500 μ m.

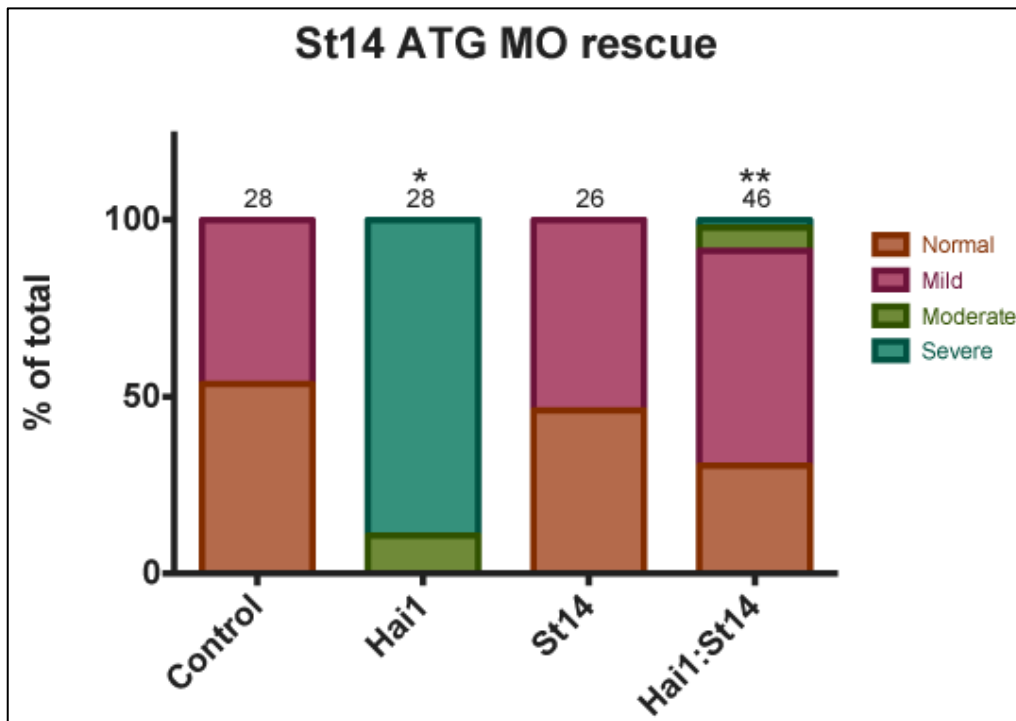


Figure 3.2. Matriptase knockdown rescues Hai1 morphants. Quantification of zebrafish morphants at 48hpf. Embryos were blind scored. Each embryo was given a score of either normal, mild, moderate, or severe based on severity of phenotype. * $p < 0.01$, ** $p < 0.005$

Zebrafish Par2b can be activated by matriptase and, like matriptase and Hai1a, is expressed in the skin of the zebrafish embryo

Two *f2r1* genes, *f2r1.1* and *f2r1.2*, encode two Par2 homologs, Par2a and Par2b, in zebrafish. We cloned both Par2a and Par2b from zebrafish cDNA. The predicted cleavage site for trypsin-like proteases in Par2a is NWDR/G, however, the corresponding peptide agonist did not elicit a Par2-dependent response in cell culture (Xu et al., 2007). The predicted amino acid sequence of the Par2b that we cloned from the AB/TL zebrafish strain used for these studies was significantly different from that published in Ensembl, consistent with previous observations (Xu et al., 2007) and perhaps due to strain differences. Although the sequence of the protease cleavage site of the Par2b homologs was different (KNGR/M and GKGR/S; Figure 3.3), both contained P4-P1' residues favorable for cleavage by matriptase (Takeuchi et al., 2000). Zebrafish Par2b indeed conferred signaling by phosphoinositide (PI) hydrolysis assay in response to recombinant matriptase protease domain or trypsin when heterologously expressed in a mouse lung fibroblast cell line that does not endogenously express PARs (Figure 2.4).

Matriptase and Hai1a have both been shown by in situ hybridization to be expressed in zebrafish skin (Carney et al., 2007). A previous study examined expression of Par2b in zebrafish skin by in situ hybridization (Xu et al., 2011). Par2b was expressed in the pronephric duct, the liver, pharynx, and gut of a 24 hpf zebrafish embryo, however, expression in keratinocytes was not described. We asked whether Par2b was expressed in zebrafish skin by using a semi-

quantitative Taqman qRT-PCR assay. Primer/probe sets were designed to zebrafish matriptase, Hai1a and Par2b as well as the keratinocyte markers keratin-4 and keratin-8, and a neural marker, cdh2. Using the transgenic zebrafish line Tg(krt4:Scp140-Venus)^{cy22} which expresses the F-actin-binding peptide LifeAct fused to Venus fluorescent protein under the control of the zebrafish keratin-4 promoter (not published, Dr. Hsiao, Chung Yuan Christian University, Taiwan), we sorted fluorescent keratinocytes from non-fluorescent cells and measured mRNA levels for genes of interest in each. Hai1a, matriptase, and Par2b mRNAs were highly expressed and enriched in keratinocytes at 24hpf (Figure 3.5) as were the keratinocyte markers, keratin 4 & keratin 8. The housekeeping gene, beta-actin, was used as an endogenous control. By comparison, the neural marker Cadherin 2 (a.k.a. n-Cadherin; cdh2) was not enriched in keratinocytes. We confirmed expression of matriptase in zebrafish skin by in situ hybridization (Figure 3.6). Given co-expression of matriptase, Hai1a, and Par2b in keratinocytes at the relevant time in development, we asked whether Par2b might contribute to the matriptase-dependent phenotypes associated with decreased Hai1a expression in skin.

MAVSESYRILLFLACVIFASAQPGK-NGRMMIVIQDDAGHIFVDQITRETLQSSLTTFVM	Actual
MAVSESYRILLFLACVIFASAQPG GR ++VIQ+DAGH+FVDQI RETLQSSLTTFVM	Ensembl
MAVSESYRILLFLACVIFASAQPGTGKGRSLVVIQNDAGHMFVDQIARETLQSSLTTFVM	Ensembl
PIIYIIVFVVLPTNAMAIYVLLFRSKKVHPPAAIYMGNLALADLMFVIWTPPKIAYHLKG	Actual
PIIYIIVFVVLPTNAMAIYVLLFRSKKVHPPAAIYMGNLALADLMFVIWTPPKIAYHLKG	Ensembl
PIIYIIVFVVLPTNAMAIYVLLFRSKKVHPPAAIYMGNLALADLMFVIWTPPKIAYHLKG	Ensembl
DNWTYGEEMCKVSVGFFYGNMYCSILFITCLSVQRYWVCAHPLTQQRKDNRLAIIISVCV	Actual
+NWTYGEEMCKVSVGFFYGNMYCSILFITCLSVQRYWVCAHPLTQQR+DNRLAIIISVCV	Ensembl
NNWTYGEEMCKVSVGFFYGNMYCSILFITCLSVQRYWVCAHPLTQQRDNRLAIIISVCV	Ensembl
WVFIGVSTTPLYLYNQTAQLQDLNITTCHDVNIITKKSFDNRNAFLDVQEPYFFMVMAG	Actual
WVFIGVSTTPLYLYNQT QLQDLNITTCHDVNIITKKSFD+ NAFLDVQEPYFFMVMAG	Ensembl
WVFIGVSTTPLYLYNQTVQLQDLNITTCHDVNIITKKSFDNHNNAFLDVQEPYFFMVMAG	Ensembl
LVFFVPMVVIIVAYVLLLRSLGNSSVKGSAGKSRKRAVILIVTVLITFLVCFIPSNAMLV	Actual
LVFFVPMVVI+AYVLLLRSLGNSSVKGSAGKSRKRAVILIVTVLITFLVCFIPSN MLV	Ensembl
LVFFVPMVVIIMAYVLLLRSLGNSSVKGSAGKSRKRAVILIVTVLITFLVCFIPSNVMLV	Ensembl
VHYSLMRNNSFNASYGFYLKALCIASLNSCLD	Actual
VHYSL+RNNSFNASYGFYL ALCIASLNSCLD	Ensembl
VHYSLLRNNSFNASYGFYLTALCIASLNSCLD	Ensembl

Figure 3.3. Alignment of zPar2b from cloned sequence and Ensembl published sequence. Par2b was cloned from TL/AB cDNA, inserted into pCS2+ vector, and sequenced. Actual sequence is shown aligned with that pulled from Ensembl database (Tubingen strain). Predicted tethered ligand is shown in red (MMIVIQ versus SLVVIQ).

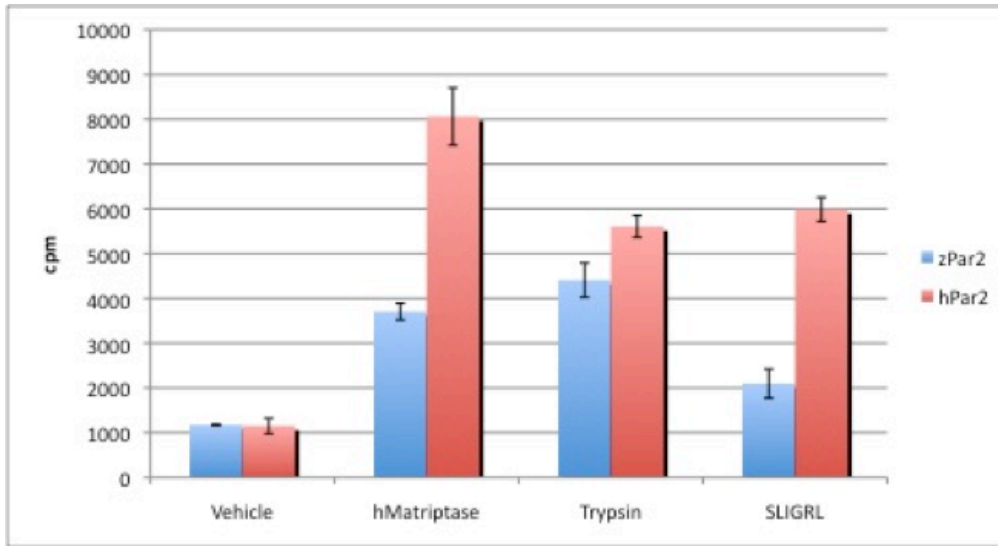


Figure 3.4. Zebrafish Par2b is functional in cell culture-based assay.

Phosphoinositide (PI) hydrolysis assay in KOLF cell line. KOLFs were transfected with human Par2 or zebrafish Par2b, treated with vehicle, recombinant human matriptase (50nM), soluble bovine trypsin (50nM), or the mouse Par2 peptide agonist, SLIGRL for 90 minutes. Tritiated inositol phosphates were measured in a liquid scintillation counter and are expressed as counts per minute (cpm).

Protein	Gene Symbol	Abundance relative to beta-actin (10-dCt)	Enrichment in GFP+ keratinocytes ($2^{-\Delta\Delta Ct}$)
Par1	F2r	0.0	0.0
Par2b	F2rl1	8.2	59.8
Hai1a	Spint1	7.4	13.1
Hai2	Spint2	8.8	46.4
Matriptase	St14a	6.7	13.3
Prostasin	Prss8	5.7	21.3
Epitheliasin	Tmprss2	0.0	0.6
Tmprss4	Tmprss4	6.5	48.0
Keratin 4	Krt4	15.6	117.2
Keratin 8	Krt8	10.8	7.0
Cadherin 2	Cdh2	1.1	0.0

Figure 3.5. Taqman qRT-PCR data of proteins enriched in keratinocytes of 24 hpf zebrafish embryos. GFP+ keratinocytes were FACS sorted from dissociated zebrafish embryos at 24hpf. mRNA was extracted and Taqman qRT-PCR was performed. Abundance relative to beta-actin endogenous control (10-dCt) and enrichment in GFP+ keratinocytes relative to GFP- cells were calculated ($2^{-\Delta\Delta Ct}$).

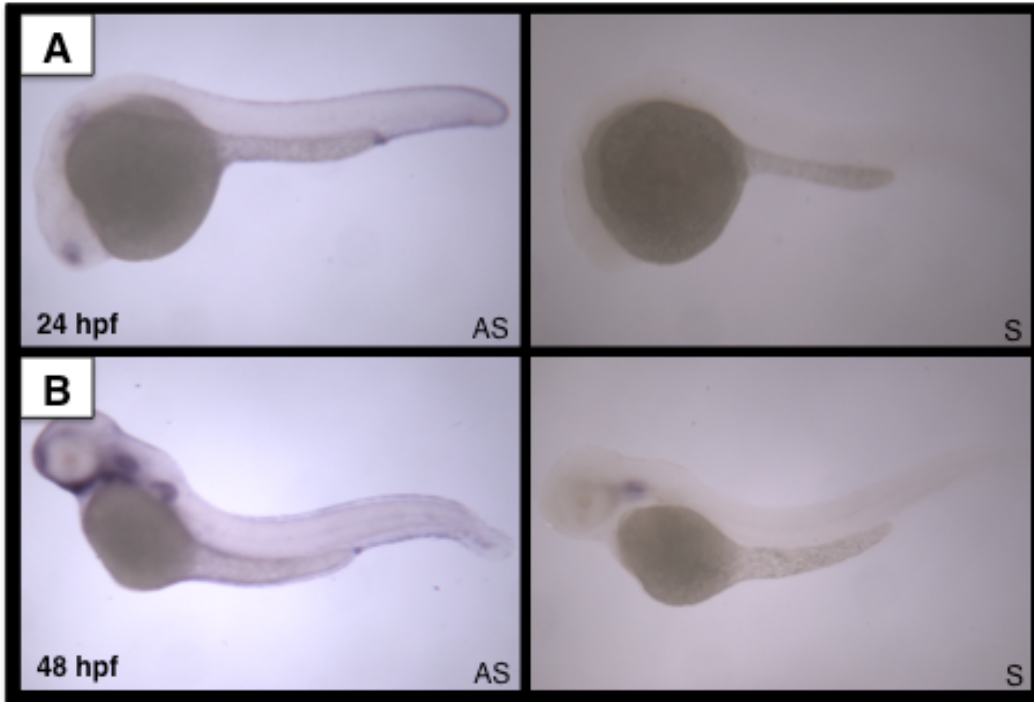


Figure 3.6. Matriptase is expressed in the skin of zebrafish embryos. In situ hybridization for matriptase at A. 24 hpf and B. 48 hpf. Left panels show antisense (AS) probe staining. Notice the dark purple staining in the outer layer of cells of both embryos. Right panels show sense (S) probe controls. Notice the absence of staining suggesting specificity of the AS probe.

Par2b is necessary for the Hai1 morphant phenotype

To determine whether Par2b activation might contribute to the matriptase-dependent Hai1a morphant phenotype described above, we first asked whether morpholino-mediated knockdown of Par2b expression might revert this phenotype. Embryos co-injected with Hai1a MO and a Par2b MO directed against the translational start site of the zebrafish Par2b mRNA showed a substantial decrease in skin aggregates & shedding and decreased extravascular leukocytes compared to Hai1a morphants co-injected with control MO (Figure 3.7). Embryos injected with Par2b MO by itself were indistinguishable from controls. Semiquantitative scoring of phenotypes done blind to treatment revealed that only 8% Hai1a:Par2b morphants had a severe phenotype compared to 56% of embryos injected with Hai1a and control MOs ($p < 0.01$). In accord, 46% Hai1a:Par2b morphants had a mild phenotype compared to only 6% of Hai1a:control morphants ($p < 0.01$) (Figure 8). Similar results were obtained using an independent MO directed against the exon 1-intron 1 splice junction of Par2b (Figure 3.9). Extravasation of leukocytes seen in Hai1a morphants was also rescued by concurrent Par2b knockdown (Figure 3.10). These results suggest that Par2 function plays a necessary role in the matriptase-dependent Hai1a phenotype.

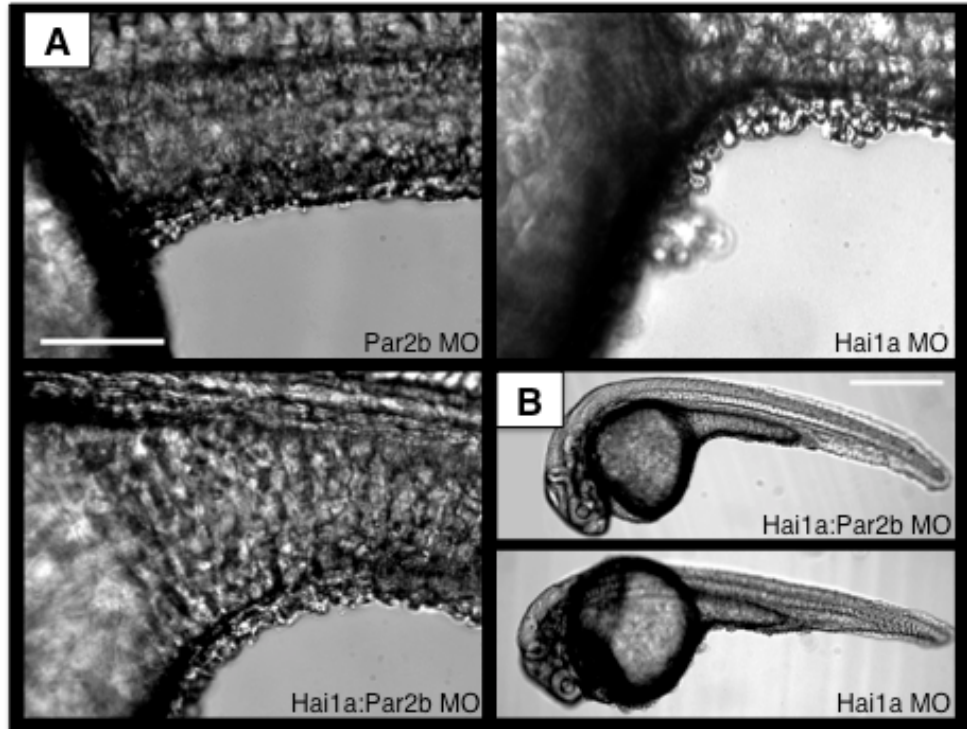


Figure 3.7. Par2b knockdown rescues skin aggregation and shedding in Hai1a morphants. Hai1a morphants were co-injected with a translational blocking morpholino to Par2b. DIC images of 24 hpf zebrafish embryos. A. 20X magnification of the boundary between the yolk sac and yolk sac extension. B. 4X magnification showing whole embryos.

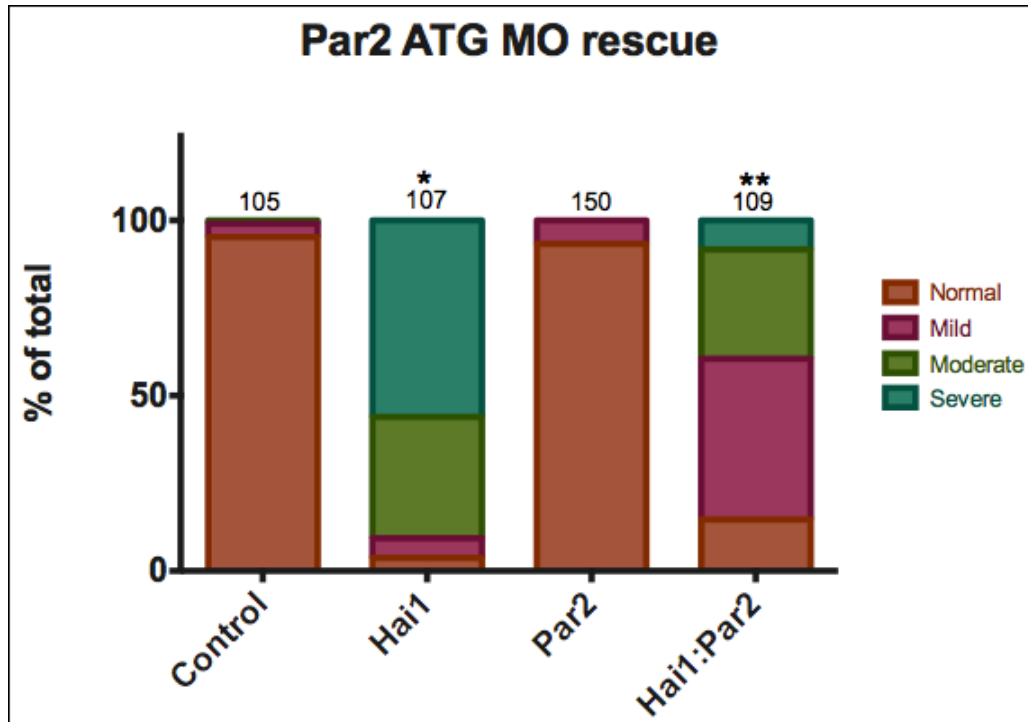


Figure 3.8. Par2b translation blocking morpholino rescues Hai1 morphants. Quantification of zebrafish morphants at 48hpf. Embryos were blind scored. Each embryo was given a score of either normal, mild, moderate, or severe based on severity of phenotype. * $p < 0.01$, ** $p < 0.005$

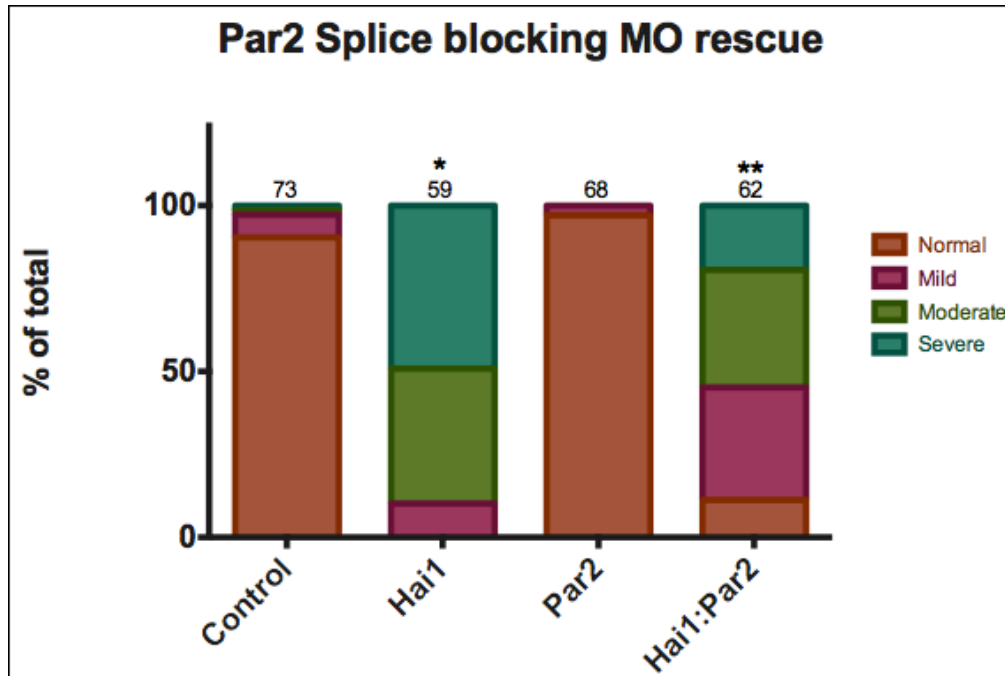


Figure 3.9. Par2b splice blocking morpholino rescues Hai1 morphants. Quantification of zebrafish morphants at 48hpf. Embryos were blind scored. Each embryo was given a score of either normal, mild, moderate, or severe based on severity of phenotype. * $p < 0.01$, ** $p < 0.005$

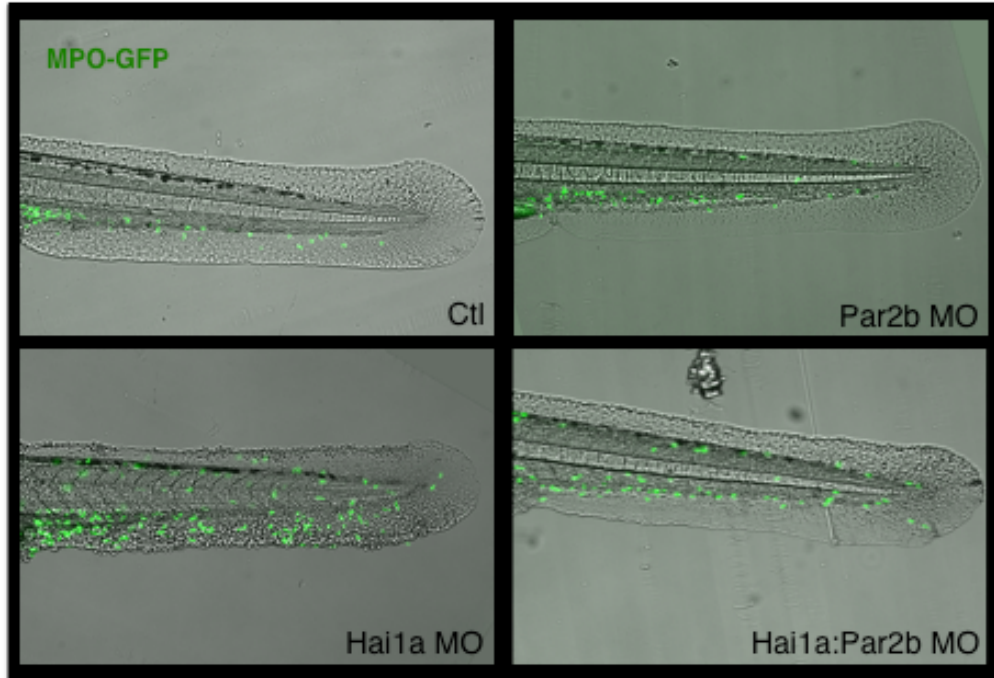


Figure 3.10. Par2b knockdown rescues extravasation of leukocytes. Images are of MPO-GFP transgenic zebrafish embryos at 48hpf showing leukocytes (green) extravasating to affected areas of the zebrafish tail. Leukocytes migrate out of the vasculature of Hai1a morphants but are largely found within the vasculature in Hai1a:Par2b double morphants.

Epithelial cell extrusion in skin of Hai1 morphants.

To better characterize the process underlying accumulation of keratinocyte aggregates on the skin of Hai1a morphants, we used the transgenic zebrafish line Tg(krt4:Scn.Abp140-Venus)^{cy22} to visualize actin organization and keratinocyte shape and movement. Fluorescence imaging for LifeAct-GFP in Hai1a morphant zebrafish embryos at 28-30 hpf revealed increased heterogeneity of epithelial cell size and shape and the formation of epithelial rosettes and rings of condensed F-actin around cells that were rounding (Figure 3.11). Condensed F-actin was also observed at “corners” where three or more epithelial cells met (Figure 3.11). Time-lapse imaging studies of Hai1a MO: Tg(krt4:Scn.Abp140-Venus)^{cy22} embryos revealed that rounding cells were often extruded from the skin (Figure 3.11). Cells were extruded both individually and as groups. Interestingly, some cells that appeared to be extruding later flattened back into the monolayer and became indistinguishable from non-affected cells (Figure 3.11). Extrusion occurred most frequently at the junction of the yolk sac and yolk sac extension but was also observed along the length of the ventral, dorsal and anterior ventral parts of the caudal fin fold and overlying the head region. The latter sites were only apparent in the Tg(krt4:Scn.Abp140-Venus)^{cy22} embryos and were not identified by DIC microscopy as clumping of keratinocytes. Extrusion was not seen in control embryos.

Keratinocyte extrusion in Hai1a morphants is Par2b-dependent.

In time-lapse studies, Hai1a morphants had an average of 6.5 +/- 4.2 extrusion events between 28 and 44 hpf, while Hai1a:Par2b double morphants had 0.1 +/- 0.3. Hai1a morphants co-injected with a control MO were indistinguishable from Hai1a morphants, and embryos injected with Par2b alone were indistinguishable from wild-type. While less pronounced than that seen in Hai1a morphants, increased LifeAct fluorescence was noted at cell corners in Hai1a:Par2b morphants compared to controls. Similarly, keratinocyte size and shape in Hai1a:Par2b morphants were closer to that seen in controls compared to these features in Hai1a morphants. Observations were similar in Tg(krt4:nlsEGFP)cy34, a transgenic zebrafish line expressing nuclear-tagged EGFP specifically in the skin (Chen et al., 2011). This line allows us to observe the nucleus of keratinocytes in real-time. Extruding cells were observed as nuclei moving apically out of the plane of the yolk sac and ultimately being released into the media. Counts of dividing EGFP-positive nuclei did not reveal an increase in proliferation of keratinocytes in Hai1a morphants vs. control in the time period examined.

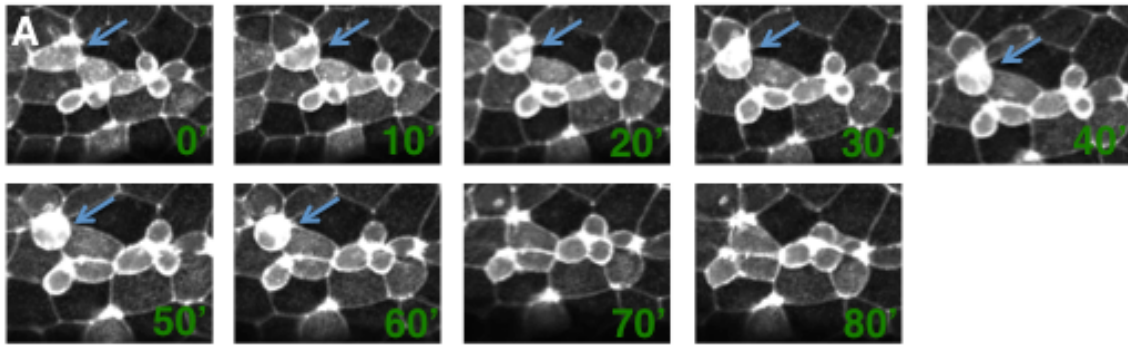


Figure 3.11. Keratinocytes are extruded from the skin of Hai1a morphants. Laser scanning confocal microscopy of ~30hpf *krt4-lifect-Venus* transgenic zebrafish embryos injected with Hai1a morpholino. GFP+ cells are frequently extruded from the tail of the zebrafish embryo, starting as a cell in the monolayer, rounding up and moving apically out of the plane of the monolayer until released into the water (blue arrow). Images are Z projections every ten minutes showing the evolution of an extruding cell.

Cell extrusion is independent of apoptosis

Epithelial cells that are undergoing cellular death by apoptosis undergo extrusion from the monolayer presumably as a protective mechanism against barrier disruption (Rosenblatt et al., 2001). However, living epithelial cells can also undergo extrusion in response to cell crowding (Eisenhoffer et al., 2012). We therefore sought to determine whether keratinocyte extrusion in Hai1a morphants might be secondary to apoptosis.

Hai1a mutants are known to show increased keratinocyte apoptosis as early as 24 hpf (Carney et al., 2007). Accordingly, we first determined whether keratinocytes extruding from the skin of Hai1a morphants were apoptotic as measured by TUNEL staining and by immunostaining for cleaved and activated caspase-3. While some extruding keratinocytes were positive for active caspase-3, the majority of extruding cells were negative. Those keratinocytes

that did stain for active caspase were usually fully rounded and separated or nearly separated from the epithelium, while keratinocytes that showed less rounding and continued association with the monolayer were negative (Figure 3.12). Overall, these results suggest that apoptosis can occur during or after extrusion but may represent a parallel or secondary process, perhaps anoikis, rather than a cause of extrusion.

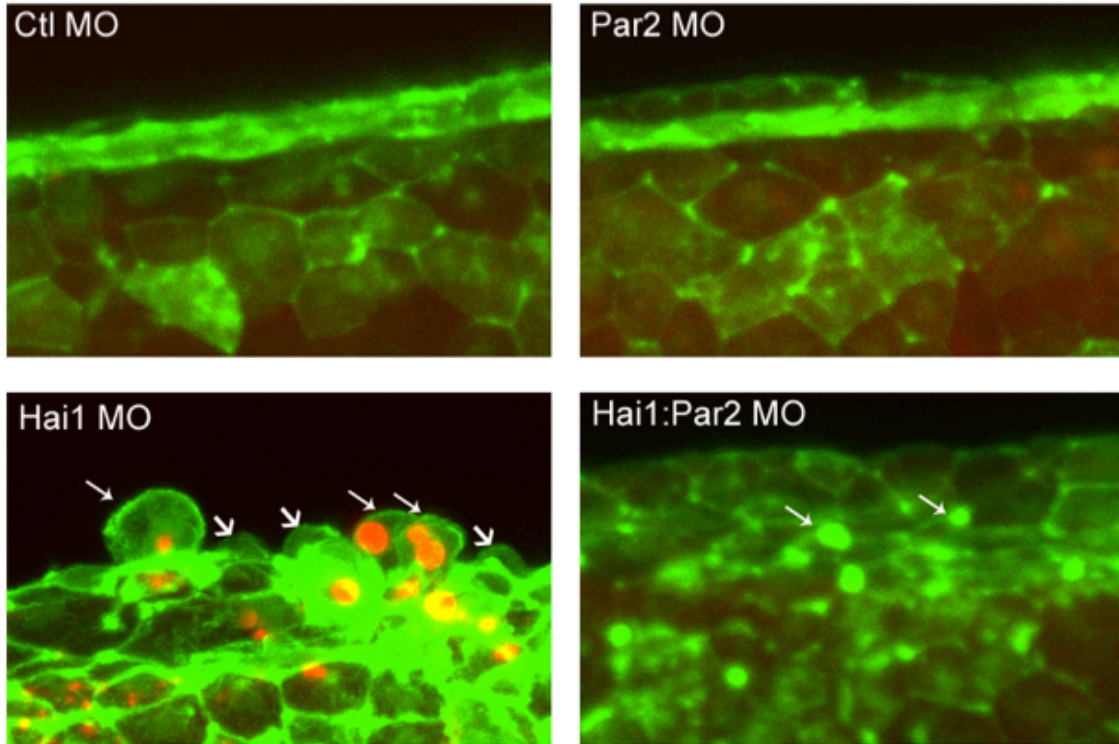


Figure 3.12. Caspase-3 staining of extruding keratinocytes. Zebrafish embryos (*krt4*-*lifeact*-Venus) were injected with control, Hai1a, Par2b, or Hai1a:Par2b morpholinos. At 24 hpf, embryos were fixed and stained for cleaved caspase-3 (red). Level of caspase-3 staining is dependent upon stage of extrusion: rounded, more extruded cells show staining (long arrows) whereas cells just beginning to round that remain within the plane of the skin are negative for caspase-3 (short arrows). Notice the accumulation of actin (green) at cell-cell boundaries, even in Hai1:Par2 MO, although extrusion phenotype is rescued. Images are 20X laser scanning confocal imaging.

To further address the question of apoptosis dependence, we treated zebrafish embryos with a caspase-3 inhibitor, z-VAD-FMK (300uM) at 24 hpf for 12 hours. If the Hai1a morphant phenotype is dependent upon apoptosis, then blocking apoptosis should rescue the phenotype. Hai1a morphants treated with z-VAD-FMK were grossly indistinguishable from untreated Hai1a morphants (Figure 3.13).

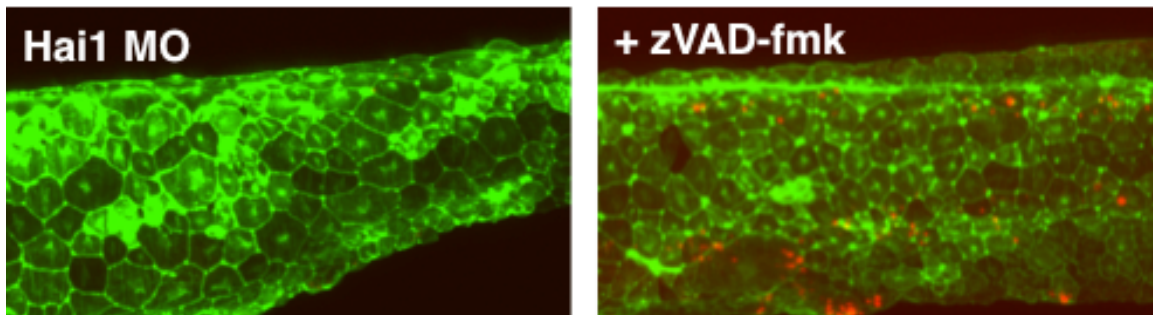


Figure 3.13. Inhibition of apoptosis does not block the Hai1a phenotype. Hai1a zebrafish morphants (*krt4-lifect-Venus*) were treated with the caspase-3 inhibitor, zVAD-fmk, for 12 hours and then fixed and subjected to TUNEL staining. Notice the absence of caspase-3 staining (red) of extruding keratinocytes with (right panel) and without (left panel) zVAD-fmk. Some embryos exhibited punctate red staining (right panel) throughout the embryo; it is unclear as to what these represent but it does not appear to be in the keratinocytes.

Matriptase is active at sites of epithelial cell extrusion.

The observation that cell extrusion in Hai1a morphant embryos was prevented by knocking down matriptase expression suggests that matriptase activity contributes to this phenotype. To determine whether matriptase is indeed active at sites of epithelial cell extrusion, we localized matriptase in cultures of Caco-2 cells, an epithelial cell line derived from a human colon carcinoma. Caco-2 cells were grown to confluence and then subjected to short-wave UV

irradiation to induce apoptosis. Immunostaining with M69, a monoclonal antibody specific for the two-chain, active form of human matriptase (Benaud et al., 2001) (Figure 3.14, green), and an antibody to active caspase-3 (Figure 3.14, red) was used to identify active matriptase and apoptotic cells. Interestingly, we saw an abundance of staining for two-chain matriptase surrounding apoptotic cells at both early stages (characterized by cleaved caspase-3 positive staining and rounding of the cell) and late stages (characterized by cleaved caspase-3 positive staining and apical location of the cell in relation to the monolayer) of extrusion (Figure 3.14). This suggests that matriptase is both expressed and active at sites of epithelial cell extrusion.

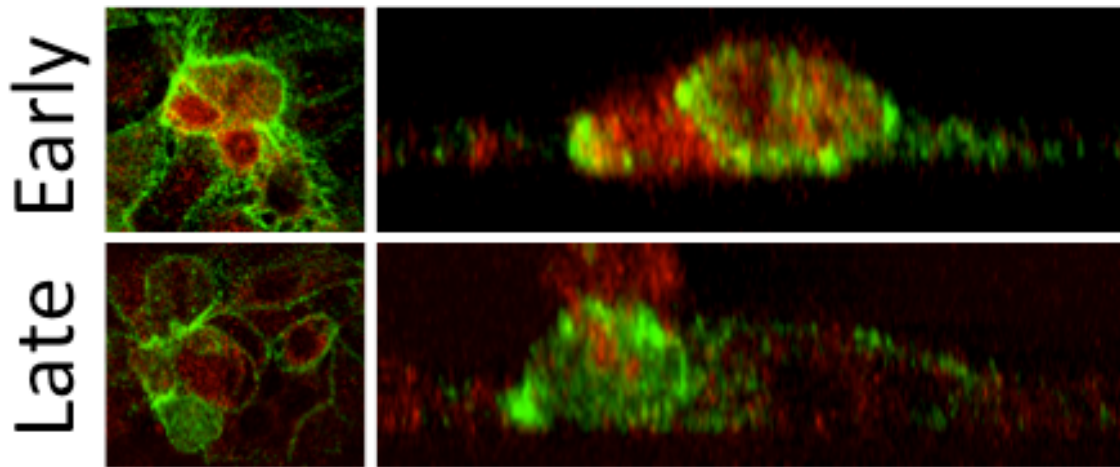


Figure 3.14. Matriptase is active at sites of epithelial cell extrusion. Caco-2 monolayers were exposed to $120\text{mJ}/\text{cm}^2$ of short-wave UV to induce apoptosis. Cells were fixed two hours post-irradiation and stained for active matriptase (M69 antibody – green) or cleaved-caspase 3 (red). Figure shows two examples of epithelial cell extrusion: early and late-stage. Matriptase is active at cell-cell boundaries of apoptotic, extruding cells.

Discussion

In this chapter, we have described uncontrolled epithelial cell extrusion in Hai1a morphants that is rescued by knockdown of either matriptase or Par2b. Combined with our past results demonstrating that matriptase is a potent activator of Par2b in vitro, these results support the notion that Par2b can be activated by matriptase in vivo.

Matriptase is a known regulator of epithelial biology

Previous gain- and loss-of-function studies suggest that matriptase is an important regulator of epithelial barrier integrity. Keratinocyte accumulation and shedding in Hai1a mutant zebrafish embryos was prevented by knockdown of matriptase (Carney et al., 2007). Matriptase knockout mice exhibit skin barrier defects that lead to death within 48 hours of birth. This lethality was attributed to severe dehydration due to impaired skin development (List et al., 2002). Conditional loss of matriptase in adult mice leads to severe growth impairment and ultimately death from fluid loss (List et al., 2009). In cell culture, matriptase knockdown or inhibition results in an increase in epithelial permeability concurrent with an increase in expression of the “leaky” junction protein, claudin-2 (Buzza et al, 2010). These data together suggest that matriptase plays a role in both the formation of and the regulation of the epithelial barrier. But exactly what role matriptase plays in this regulation and what substrates are acted upon by matriptase is unknown. Our data begin to shed some light on this role.

Par2b is an in vivo mediator of matriptase function

Previous studies from our lab demonstrated that recombinant matriptase protease domain is a potent activator of Par2 in cell culture experiments (Takeuchi et al, 2000; Camerer et al., 2010). However, multiple trypsin-like proteases show similar activity (albeit not as potently as matriptase). One might predict that matriptase is likely to be a physiological activator of Par2 in vivo because matriptase protease domain tethered to the cell membrane should cleave and activate Par2b expressed on the same epithelial cell even more effectively than exogenous soluble matriptase protease domain. However, it is also possible that subcellular compartmentalization or positioning of these components would preclude their interaction (Godiksen et al., 2008).

Our results suggest that, at least in the case of matriptase gain-of-function, Par2 can indeed mediate actions of matriptase in vivo. Our model utilized knockdown of the endogenous matriptase inhibitor, Hai1a, to disinhibit matriptase in the zebrafish embryo. This maneuver should lead to increased matriptase activity at sites where matriptase is normally expressed and activated. Surprisingly, we were able to rescue all of the phenotypes associated with Hai1a knockdown with concurrent knockdown of Par2b. This is, to our knowledge, the first evidence that Par2b can mediate the effects of matriptase on epithelia in vivo.

The results described above are consistent with our previous finding that over-expression of the matriptase activator prostasin and Par2 in mouse skin led to indistinguishable phenotypes including hyperplasia, ichthyosis, and

inflammation, and all effects of prostasin overexpression were rescued by knockout of Par2 (Frateschi et al., 2011).

Interestingly, knockout of Par2 failed to rescue phenotypes in Hai1 knockout mice, which exhibit a placental labyrinth defect, and Hai2 knockout mice, which have neural tube defects (Szabo et al., 2009). Whether this reflects differences between skin, placenta, and developing neural tube, gain of function of other proteases and/or an important role for cleavage of matriptase substrates other than Par2 is not known.

How does Par2 participate in epithelial cell extrusion?

During epithelial cell extrusion, a Rho-kinase dependent actin-myosin ring forms around the departing cell. Contraction of this ring is thought to squeeze the departing cell out of the epithelium while bringing the remaining cells into proximity to maintain barrier function (Rosenblatt et al., 2001). What role does Par2 play in this process?

Par2 can couple to Gi/o/z, G12/13, or Gq/11 signaling (Coughlin, 2000) G12/13 signals to Rho kinase and Gi couples to Rac. Thus, it is possible that activation of Rac and Rho by Gi and G12/13 contributes to organization and contraction of the actin-myosin ring that mediates cell extrusion.

What about other regulators of epithelial cell extrusion?

Other regulators of epithelial cell extrusion have been identified, most notably sphingosine-1-phosphate (S1P), a bioactive lipid. Apoptotic MDCK cells were shown to release S1P upon initiation of apoptosis that acted on the S1pr2 receptor on neighboring cells, leading to cell extrusion; this could be blocked by

inhibition of S1pr2 (Gu et al., 2011). Tantalizing data suggest that there may be a connection between S1P, matriptase and actin dynamics. Cells treated with S1P under culture conditions show localization of both matriptase and actin to cell-cell junctions as well as activation of matriptase; however, it is unknown as to whether S1P receptors play a role and what signaling mechanism is used. The authors did not show any epithelial cell extrusion in this system (Benaud et al., 2002; Hung et al., 2004).

Other potential players?

The Hai1a mutant line was found in a mutagenesis screen looking for skin abnormalities. Within this screen, other mutants were identified that display similar phenotypes to the Hai1a mutant. The m14/psoriasis mutant displays rounding and shedding keratinocytes starting around 3 days post fertilization; the Hai1a mutant shows a phenotype as early as 24 hpf. The mutated gene in psoriasis mutants has not yet been identified although it has been localized to chromosome 6 (Webb et al.; 2008); Hai1a is localized to chromosome 17 in zebrafish.

Other mutants were described from this screen that have been more completely studied. The penner mutant has a defect in the lethal giant larvae 2 (lgl2) gene, a protein involved in polarity of the epithelial cells. Penner mutants were shown to have keratinocyte rounding and shedding, similar to Hai1a. Penner mutants have a defect in hemidesmosome formation and enhanced epithelial to mesenchymal transition (EMT) (Sonawane et al., 2005). It would be interesting to determine if any of these described pathways play a role in the

Hai1a phenotype. We have failed to demonstrate enhanced EMT in Hai1a morphants and hemidesmosomes are not formed in the zebrafish larva until ~5 dpf; thus, it is unlikely that a disruption in hemidesmosome formation contributes to the Hai1a phenotype.

Does matriptase and/or Par2 directly regulate epithelial cell extrusion?

Our data suggests that gain of function of matriptase can trigger epithelial cell extrusion in the skin of zebrafish embryos in a Par2-dependent manner. However, it is currently unknown if either of these proteins play a direct role in cell extrusion under normal physiological conditions. We have identified active matriptase surrounding extruding apoptotic cells in culture, but we have yet to identify a necessary role in this process. We are currently testing the hypothesis that matriptase contributes to cell extrusion triggered by apoptosis or crowding using inhibitors and knockdown approaches in cultured epithelial monolayers treated with UV or staurosporine to induce apoptosis and manipulated on flexible membranes to induce crowding.

Materials and Methods

Zebrafish strains and husbandry

Morpholino studies were carried out in AB & TL zebrafish backgrounds.

Neutrophil invasion studies were carried out in MPO::GFP line.

Tg(krt4:Sce.Abp140-Venus)^{cy22} & Tg(krt4:nlsEGFP)^{cy34} were kind gifts from Dr.

Chung-der Hsiao (Chung Yuan Christian University, Taiwan). All animals were

housed in the zebrafish facility at the Cardiovascular Research Institute at the University of California, San Francisco.

Blind scoring of zebrafish embryos

Zebrafish morphants at 48hpf were scored by a lab member blinded to the experimental conditions. Embryos were given a score based upon severity of phenotype: normal, mild, moderate, or severe.

Cloning of zebrafish genes

Zebrafish St14a, Prss8, Par2a, Par2b were PCR cloned from cDNA from TL/AB strains of zebrafish. Primers were designed to the 5' and 3' ends of each gene, PCR was performed, and PCR products were cloned into the pC2+ plasmid. For cell culture experiments, genes were subcloned into pcDNA3.1(+).

Cell culture experiments

Human colorectal adenocarcinoma cells (Caco2), Madin-Darby canine kidney (MDCK) cells, or an immortal human keratinocyte cell line (HaCaT), and a mouse lung fibroblast cell line generated from Par1:Par2 knockout mice (KOLF) were cultured under standard procedures. MDCKs, HaCaTs, and KOLFs were cultured in DMEM containing 10% FBS. Caco2s were cultured in Eagle's MEM with 20% FBS, 1% non-essential amino acids. For transfections, KOLFs were cultured on gelatin-coated plastic dishware until ~75-85% confluency. Cells were then transfected using Trans-It LT1 transfection reagent (Mirus) at a ratio of 2:3 plasmid:reagent overnight.

PI Hydrolysis

Cells were transfected as described. The next day, the cells were washed and incubated in SFM (serum-free DMEM with 20 mM HEPES and 0.1% bovine serum albumin (BSA)) with 2 $\mu\text{Ci}/\text{mL}$ *myo*-[^3H]inositol overnight, then washed again and incubated with SFM for 2 hours prior to the addition of agonist and LiCl for 90 minutes. Cells were then extracted and released inositol phosphates measured ([Camerer et al., 2000](#)).

Sorting and preparation of mRNA from zebrafish keratinocytes

Zebrafish embryos were manually dechorionated ~24 hpf. Embryos were deyolked in Ringer's solution (116 mM NaCl, 2.6mM KCl, 5mM HEPES, pH 7.0) by pipetting with a P200 ~15-20 times. Embryos were transferred to pre-warmed protease solution (2.25mg/ml Collagenase P, 1X HBSS) for 15 min at 28C. 1X stop solution (5% calf serum, 1mM CaCl₂, 1X PBS) was added to stop the protease reaction. Cell suspension was centrifuged at 350 x g in the cold. Supernatants were removed and cells were resuspended in suspension buffer (1% calf serum, 0.8mM CaCl₂, 50U/ml penicillin, 0.05mg/ml streptomycin in DMEM). Cell suspensions were strained through 40-um cell strainers into FACS tube. Fluorescent cells were separated on a FACS-Aria cell sorter into TriZol. mRNA extraction was performed as described by manufacturer.

Taqman qRT-PCR

Taqman primer/probe sets (5'FAM/3'BHQ) for real-time PCR were designed using Primer Express software (Applied Biosystems) and cDNA sequences from the Ensembl database (see Appendix 5.1 for primer/probe set sequences). First strand synthesis, Taqman qRT-PCR, normalization of Ct data

to housekeeping genes using the Δ Ct method, and conversion to fold increase over gene levels in non-fluorescent cells using the $\Delta\Delta$ Ct method were as described (REGARD et al., 2008).

Staining of zebrafish embryos

Zebrafish embryos were fixed in 4% paraformaldehyde (PFA) overnight at 4C. The next morning, embryos were washed to dPBS and then stored in 100% methanol at -20C overnight. Embryos were rehydrated through successive washes of methanol/PBS solutions (70% MeOH, 50% MeOH, 25% MeOH, 100% PBS). Embryos were permeabilized in 1% Triton X-100 for 10 minutes, followed by another round of fixing in 4% PFA for 20 minutes. Embryos were washed 5 x 5 minutes in PBS containing 0.1% Tween-20 (PBS-T), then blocked for 1 hour at room temperature in 1X Western Blocking Reagent + PBS-T (Roche). For caspase-3 staining, embryos were incubated in anti-cleaved caspase-3 antibody (BD Biosciences) at 1:500 overnight at 4C. The next day, embryos were washed multiple times in PBS-T, followed by a 1 hour incubation in 1:500 goat anti-rabbit HRP-conjugated secondary antibody (BioRad). Secondary antibody was removed by washing with PBS-T and embryos were stained using the Tyramide Signal Amplification Kit (Invitrogen) with tetramethylrhodamine as the fluor (550 nm). For actin staining, embryos were incubated for 20 minutes with Alexa Fluore 488-phalloidin (Invitrogen) before imaging. For TUNEL staining, the In Situ Cell Death Detection Kit with TMR (Roche) was used according to manufacturer's recommendations. As a positive control, embryos were incubated for 30 min at 37C in 1500U/ml DNase I.

Immunofluorescence staining of cells

Caco2 cells were cultured on gelatin-coated coverslips to 100% confluency. Cells were serum-starved in serum-free media (Eagle's MEM + 20mM HEPES + 0.1% BSA) overnight and then subjected to short-wave UV irradiation at 120mJ/cm² in a Stratalinker UV Crosslinker (Stratagene). Cells were cultured for 2 hours and then fixed in 3.7% formaldehyde for 10 minutes. Cells were then washed with PBS, permeabilized in 1% Triton X-100 for 10 minutes followed by blocking in 10% goat serum for 1 hour. Cells were stained for caspase-3 (anti-cleaved caspase-3 Ab, 1:500, BD Biosciences), actin (Alexa Fluor 488-phalloidin, Invitrogen), active matriptase (M69, 1:100), or total matriptase (M24, 1:100) followed by the appropriate HRP-conjugated secondary antibody before imaging.

References

- Benaud, C., Dickson, R.B., and Lin, C.Y. (2001). Regulation of the activity of matriptase on epithelial cell surfaces by a blood-derived factor. *Eur J Biochem* 268, 1439-1447.
- Benaud, C., Oberst, M., Hobson, J.P., Spiegel, S., Dickson, R.B., and Lin, C.Y. (2002). Sphingosine 1-phosphate, present in serum-derived lipoproteins, activates matriptase. *J Biol Chem* 277, 10539-10546.
- Buzza, M.S., Netzel-Arnett, S., Shea-Donohue, T., Zhao, A., Lin, C.Y., List, K., Szabo, R., Fasano, A., Bugge, T.H., and Antalis, T.M. (2010). Membrane-anchored serine protease matriptase regulates epithelial barrier formation and permeability in the intestine. *Proc Natl Acad Sci U S A* 107, 4200-4205.
- Camerer, E., Barker, A., Duong, D.N., Ganesan, R., Kataoka, H., Cornelissen, I., Darragh, M.R., Hussain, A., Zheng, Y.W., Srinivasan, Y., *et al.* (2010). Local protease signaling contributes to neural tube closure in the mouse embryo. *Dev Cell* 18, 25-38.
- Carney, T.J., von der Hardt, S., Sonntag, C., Amsterdam, A., Topczewski, J., Hopkins, N., and Hammerschmidt, M. (2007). Inactivation of serine protease Matriptase1a by its inhibitor Hai1 is required for epithelial integrity of the zebrafish epidermis. *Development* 134, 3461-3471.
- Chen, C.F., Chu, C.Y., Chen, T.H., Lee, S.J., Shen, C.N., and Hsiao, C.D. (2011). Establishment of a transgenic zebrafish line for superficial skin ablation and functional validation of apoptosis modulators in vivo. *PLoS One* 6, e20654.
- Coughlin, S.R. (2000). Thrombin signalling and protease-activated receptors. *Nature* 407, 258-264.
- Coughlin, S.R. (2005). Protease-activated receptors in hemostasis, thrombosis and vascular biology. *J Thromb Haemost* 3, 1800-1814.
- Eisenhoffer, G.T., Loftus, P.D., Yoshigi, M., Otsuna, H., Chien, C.B., Morcos, P.A., and Rosenblatt, J. (2012). Crowding induces live cell extrusion to maintain homeostatic cell numbers in epithelia. *Nature* 484, 546-549.
- Frateschi, S., Camerer, E., Crisante, G., Rieser, S., Membrez, M., Charles, R.P., Beermann, F., Stehle, J.C., Breiden, B., Sandhoff, K., *et al.* (2011). PAR2 absence completely rescues inflammation and ichthyosis caused by altered CAP1/Prss8 expression in mouse skin. *Nat Commun* 2, 161.
- Godiksen, S., Selzer-Plon, J., Pedersen, E.D., Abell, K., Rasmussen, H.B.,

Szabo, R., Bugge, T.H., and Vogel, L.K. (2008). Hepatocyte growth factor activator inhibitor-1 has a complex subcellular itinerary. *Biochem J* 413, 251-259.

Hung, R.J., Hsu Ia, W., Dreiling, J.L., Lee, M.J., Williams, C.A., Oberst, M.D., Dickson, R.B., and Lin, C.Y. (2004). Assembly of adherens junctions is required for sphingosine 1-phosphate-induced matriptase accumulation and activation at mammary epithelial cell-cell contacts. *Am J Physiol Cell Physiol* 286, C1159-1169.

List, K., Haudenschild, C.C., Szabo, R., Chen, W., Wahl, S.M., Swaim, W., Engelholm, L.H., Behrendt, N., and Bugge, T.H. (2002). Matriptase/MT-SP1 is required for postnatal survival, epidermal barrier function, hair follicle development, and thymic homeostasis. *Oncogene* 21, 3765-3779.

List, K., Kosa, P., Szabo, R., Bey, A.L., Wang, C.B., Molinolo, A., and Bugge, T.H. (2009). Epithelial integrity is maintained by a matriptase-dependent proteolytic pathway. *Am J Pathol* 175, 1453-1463.

List, K., Szabo, R., Molinolo, A., Sriuranpong, V., Redeye, V., Murdock, T., Burke, B., Nielsen, B.S., Gutkind, J.S., and Bugge, T.H. (2005). Deregulated matriptase causes ras-independent multistage carcinogenesis and promotes ras-mediated malignant transformation. *Genes Dev* 19, 1934-1950.

Mathias, J.R., Dodd, M.E., Walters, K.B., Rhodes, J., Kanki, J.P., Look, A.T., and Huttenlocher, A. (2007). Live imaging of chronic inflammation caused by mutation of zebrafish Hai1. *J Cell Sci* 120, 3372-3383.

Rosenblatt, J., Raff, M.C., and Cramer, L.P. (2001). An epithelial cell destined for apoptosis signals its neighbors to extrude it by an actin- and myosin-dependent mechanism. *Curr Biol* 11, 1847-1857.

Sonawane, M., Carpio, Y., Geisler, R., Schwarz, H., Maischein, H.M., and Nueslein-Volhard, C. (2005). Zebrafish penner/lethal giant larvae 2 functions in hemidesmosome formation, maintenance of cellular morphology and growth regulation in the developing basal epidermis. *Development* 132, 3255-3265.

Szabo, R., Hobson, J.P., Christoph, K., Kosa, P., List, K., and Bugge, T.H. (2009). Regulation of cell surface protease matriptase by HAI2 is essential for placental development, neural tube closure and embryonic survival in mice. *Development* 136, 2653-2663.

Takeuchi, T., Harris, J.L., Huang, W., Yan, K.W., Coughlin, S.R., and Craik, C.S. (2000). Cellular localization of membrane-type serine protease 1 and identification of protease-activated receptor-2 and single-chain urokinase-type plasminogen activator as substrates. *J Biol Chem* 275, 26333-26342.

Webb, A.E., Driever, W., and Kimelman, D. (2008). psoriasis regulates epidermal

development in zebrafish. *Dev Dyn* 237, 1153-1164.

Xu, H., Echemendia, N., Chen, S., and Lin, F. (2011). Identification and expression patterns of members of the protease-activated receptor (PAR) gene family during zebrafish development. *Dev Dyn* 240, 278-287.

Chapter 4

Summary

Unraveling the role of Par2 in vivo

Efforts to unravel the precise function of Par2 in vivo have been hindered by the fact that Par2 knockout mice are grossly normal. Further studies have shown Par2 to have a more nuanced role: it appears to be important in challenged systems and in disease progression in mouse models. Our work fits within this idea as well as enhances our knowledge of roles for Par2 in animal models.

In Chapter 2, we describe a defect in neural tube closure in mouse embryos deficient for Par1 & Par2. Our efforts here focused on describing the role for Par2 in this model as well as a valiant attempt to identify the serine protease(s) responsible for Par2 function during neural development. Using a Taqman qRT-PCR approach, we screened over a hundred candidate serine proteases over numerous cell types and mouse tissues. Performing cluster analysis, we identified the proteases most likely to be Par2 activators based upon co-expression. This list narrowed our search down to a few likely candidates: matriptase, prostasin, & hepsin. Although this was a start to identifying the elusive Par2 activator, and despite our successful attempts to show a direct correlation between these proteases and Par2 in cell culture experiments, we were unable to show a direct correlation between any of these proteases and Par2 in vivo. Importantly, another group recently attempted to recapitulate our

neural tube closure defect in Par1:matriptase double knockout mice and was unsuccessful (Szabo et al., 2012). Thus, whether matriptase is the key regulator of Par2 in this model remains unknown.

In Chapter 3, we have identified a role for Par2 during skin development in zebrafish embryos. Importantly, we have successfully identified a direct contribution of matriptase catalytic activity on Par2. Hai1 morphants have severe skin defects including keratinocyte aggregation and shedding. We can rescue this phenotype with co-knockdown of Par2. To our knowledge, this is the first documentation of a direct role of matriptase on Par2 in vivo.

We went on to define the Hai1 morphant phenotype in great detail and found that keratinocytes appear to be undergoing epithelial cell extrusion, a phenomenon only recently appreciated and understood. We believe that live keratinocytes are extruding from the skin layer of the embryo and that this is matriptase and Par2 dependent.

Defining the matriptase protease cascade

Par2 is activated by serine proteases and thus, to understand Par2 function, it is critical to understand what proteases are responsible for triggering a Par2 signaling event. Our studies have focused specifically on the serine protease matriptase as an important regulator of Par2 in two models: during neural tube closure in the developing mouse embryo and in skin development in zebrafish embryos. In the first model, we have shown a correlation between matriptase and Par2 expression profiles but to date, have failed to identify a direct link between matriptase and Par2 in this system. However, in zebrafish

embryos, we believe we are the first group to demonstrate a direct link between matriptase and Par2 in vivo.

Matriptase regulation and activation are complex and not fully understood. We believe it is likely that a protease cascade exists that has yet to be identified completely. A protease cascade serves to amplify a proteolytic response and is a highly effective method to relay a molecular signal. There are an abundance of proteolytic cascades that have been described in the literature ranging from simple cascades involving a couple proteases to highly complex cascades with numerous proteases. Protease cascades can be linear or can be highly coordinated with feedback loops and negative regulation.

Our data, as well as from other groups, suggests that a protease cascade might exist between matriptase and prostasin. However, we do not completely understand the link between matriptase and prostasin. Data to unravel this cascade has been confusing and contradictory depending upon the context being studied. For instance, matriptase was originally described as an activator of prostasin due to similarities between knockout phenotypes and the absence of active prostasin in matriptase knockout mice (Netzel-Arnett et al., 2006). However, our lab demonstrated for the first time that prostasin, at least in cell culture, could activate matriptase. This prompted us to propose a positive feedback loop between matriptase and prostasin, to amplify an already robust signaling event. Further studies have validated our data suggesting that in some contexts (i.e. different tissues), prostasin might in fact be the positive regulator of matriptase (Szabo et al., 2012).

To be sure, matriptase and prostaticin do operate in a coordinated fashion. But might other proteases exist within this cascade? We are not confident that we have fully described the signaling events in either of our two models and it appears to be likely that other unidentified proteases might be important. One potential candidate is Tmprss4, another member of the type-II transmembrane serine protease family. Unpublished data from our lab has shown a potential interaction between Tmprss4 and Hai1 or Hai2 in cell culture and possibly an interaction between Tmprss4 and Hai1 in zebrafish embryos. Work on this front is currently ongoing.

Our data allows us to propose a possible (but perhaps incomplete) model of how matriptase might function through Par2 (Figure 4.1). We believe that our data has greatly expanded our knowledge of how these proteins function as well as opened new avenues of research.

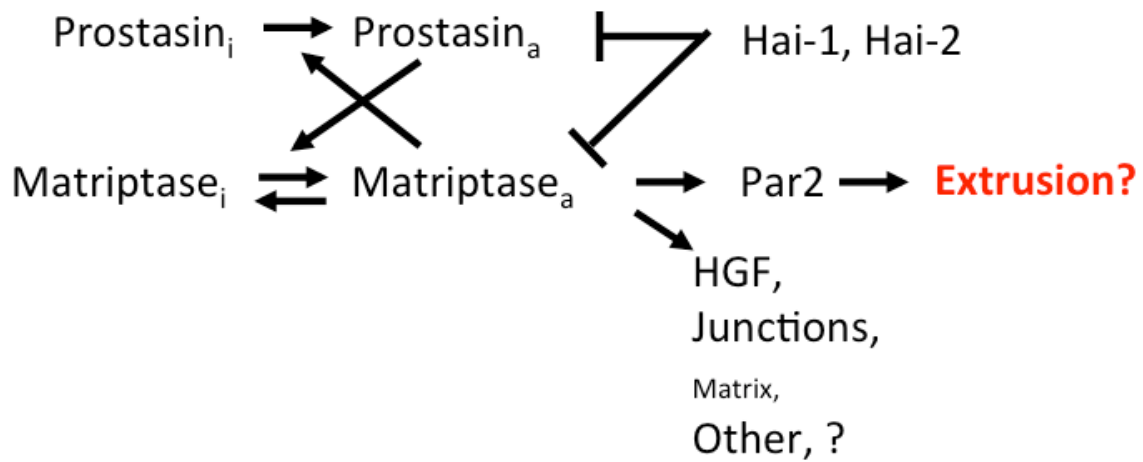


Figure 4.1 A proposed model of signaling pathway. Matriptase and prostatic are shown to activate one another leading us to propose a positive feedback loop that could serve to amplify the proteolytic signal. Hai1 & Hai2 are endogenous inhibitors that can negatively modulate the signaling event. Matriptase has numerous substrates including Par2 which we propose to be involved in epithelial cell extrusion.

References

Netzel-Arnett, S., Currie, B.M., Szabo, R., Lin, C.Y., Chen, L.M., Chai, K.X., Antalis, T.M., Bugge, T.H., and List, K. (2006). Evidence for a matriptase-prostasin proteolytic cascade regulating terminal epidermal differentiation. *J Biol Chem* *281*, 32941-32945.

Szabo, R., Uzzun Sales, K., Kosa, P., Shylo, N.A., Godiksen, S., Hansen, K.K., Friis, S., Gutkind, J.S., Vogel, L.K., Hummler, E., *et al.* (2012). Reduced prostasin (CAP1/PRSS8) activity eliminates HAI-1 and HAI-2 deficiency-associated developmental defects by preventing matriptase activation. *PLoS Genet* *8*, e1002937.

Appendix

Appendix 5.1. List of Taqman primer/probe sets

Gene	Name	Taqman Forward Primer	TaqMan Reverse Primer	Taqman Probe
1700074 P13Rik	Hypothetical serine protease	AGTCCAGCCCAGAGCC TTTG	TGGTAAAGAACAATGA GCAGCG	CTCTCATTGACCCTCAGTGG GTGCTCA
1700112 C13Rik	1700112C13Rik Protein, testis serine peptidase 6	TGGCGACCTGAAGTTT ACCAG	GAATGTAGCCAGTGAG GATGAATG	TGGCTGTCCCCTCCTTCCTG AGC
1810009J 06Rik	Trypsin IV, Trypsinogen 4	GGA CTCTGTGATGGT GATTCTG	ACTGAACCCCAAGGAGA CAATACC	TGGACCTGTCGTCTGCAATG GAGAGAT
1810009J 06Rik	Trypsinogen 5	AAGGACTCCTGTGATG GTGATTC	ACCCAGGAGACAATA CCCTG	TGGACCTGTCGTCTGCAATG GAGAGA
2210010 C04Rik	Trypsinogen 7	TTACCCAGGCAAGATC ACTAGCA	CAGAGTCACCCTGGCA GGAG	TCTGTCTGGGCTTCCTGGAG GGC
4931440 B09Rik	testis-specific serine protease 1	TTACA ACTGGATCGAGA CCATGAT	ATAGACAGCAGTGGCA GGGC	CCTCAATGGTGCAGTCAGGC GTGA
Acr	Acrosin	AGATGCTGCCAACTGT CGCT	ACGTGGTGTATCCTT GGCAA	TGCTGGTCTTGGCAGTGTCC GTG
BC03963 2	BC039632 protein, polyserase-3 (unit 1)	TGGAGCTTCTTGCTGG GC	GCGCAGATTCCGTAG GGTT	TGGGACCAGAACACCAGTGA TGTTTCC
C1r	Complement component 1, R subcomponent	GAAAATGCCCCGGTGT CTG	CCTCTGATGATGCGCT CCTT	CAGTGTGTGGGAAACCTGTC AACCCTG
C1rl	C1r-like protein	AGAGCTGGAGAACAGC CTATGG	CAAAGGAGCCACCA GCA	TCCCACCACAAGCTGCATGA GCA
C1s	Complement component 1, s subcomponent	CTGTAAGGCCTGAGGA CT ATGTTTT	CTGTCCCGTGACAGC TGT	CAACATGATCTGTGCTGGCG AGAAAGG
C2	Complement component 2	ACCTCCCTCACCAACCT GC	ATCTTACGGCCCAAAC TTTTGG	AGCCACCAATCCCACCCAGA ACCTT
cfb	Complement factor b, C3/C5 convertase	CGGCAACAGCTGGTAC CC	CCTTTAGCCAGGGCAG CA	CGGGACTTCCACATCAACCT CTCCAG
cfD	Complement Factor D (Adipsin)	AATGCCTCGTTGGGTC CC	CGGGTTCCAATTCTTT GTCC	ACGTGAGACCCTACCCTTG CAATACG
cfi	Complement factor i	AGAATCACCTGTGGTG GCATTT	ACTGGGTCTGACACAG TGCG	CGGTGGCTGTTGGATTCTGA CTGCT
Cma1	Mast cell protease 5, Mast cell chymase 1	AACTTCAACTTTATCCC ACCCG	TGGCTCATTACGTTT GTTCTG	AGAATGTGCAGGGCAGTTGG CTGG
Cma2	Chymase 2	GGGTGGCCCATGGTAT TG	GGGAGATTGGGTGA AGATTG	TCTGGACGCGAAATGCAAA GCC
corin	Corin	GGAAGA ATGCTCTCCGAGTCA	CCTGGCCGTCACATCT CC	CCGCTCGGGACGATGCGTTCT
Ctrb1	Chymotrypsin B1, chymotrypsin B	CCGATGTGGTGGTAGC TGG	AAACCTGAGCGATTTT CAGGAC	TCAGGGCTCCGATGAAGAGA ATGTCC
Ctrl	Chymopasin	CACCATGAACAATGAC CTGACTCT	AGACTGGTGAGACTTG TGCTGTG	CTGAAGCTTGCCTCGCCAGC CC
Ctsg	Cathepsin G	ACCCTCCAGCTGTATTC ACCAA	GTGCAAAGCGTCTCAT TGTTCT	TCCAGAGCTTCATGCCCTGG ATCAA
Cyp4v3	Cytochrome P450, family 4,	AAGCACAGTGCAAGCG GAA	AGGACTTCAGTGAGAA TCCAGACA	CCCACCAGCATAAAGTCAGC GGACAAC

	subfamily v, polypeptide 3 / Plasma kallikrein B1			
EG43652	Trypsinogen	TCTTAGCTTTGGTGTCA	TCACAGTCAGCCTGAG	TGCTCCAGTGCCTGGATGCC
3	12, trypsin 12	GTGAACC	GCAG	C
Ela1	Elastase 1	CTGCATGGTGAACGGT	CTGGCGACATTACAGC	CTGTCCACGGAGTGACCAGC
		CAGTAT	CCA	TTTGTG
Ela2	Elastase 2, Neutrophil elastase	GAGCGCACTCGACAGA	CAGCAGTTGTGATGGG	TGTGCAGCGGATCTTCGAGA
		CCTT	TCAAA	ATGG
Emr4	EGF-like module containing mucin-like hormone receptor-like 4	GAATGTTGATGGGAGC	ACCAGATAAGCAGCAT	AAGCAGGTGCCTTCTGCATG
		AACTAGAGA	TCCAGG	CCTC
F10	Coagulation Factor X	CTACATCCTCACTGCTG	TCCGATCACCTACCCT	TGTCTCCATCAGGCCAGGCC
		CCCA	CACC	ATTC
F11	Coagulation factor XI precursor	AATGCTCGAGAATGCC	TACCCTGTTGCGTATG	ATGCACAGACGATGCCCACT
		AGGA	TGAAAAAC	GCC
F12	Coagulation factor XII, Hageman factor	TTATCCTTCCCTCCTTG	TAGTTCACCTGTGACC	TTGGGATGGGACGATGAATG
		TGTGC	CAGCA	TGGC
F2	Coagulation factor II, thrombin	GAACTTCACTGAGAATG	TCAACATTCCGCTCAT	TGCGCATTGGCAAGCATTCC
		ACCTCCTG	ATCTGG	C
F7	Coagulation factor VII	TCTGCGCTGGCTACAT	TAGTGCGTGGCATGTG	ACCAAGGACGCCTGCAAGG
		GG	GG	GTGA
F9	Coagulation factor IX	TCCAGTTCCAACCTACC	GTCAGTTGGCCATTTG	CATGTCTCTCACAGCAGGCT
		TAAGGG	CAATG	CAAGGCT
Fap	fibroblast activation protein alpha subunit	CTAAGAATCCGGTTGTT	CTGGCACTTCCATTGG	TTGACACCACCTACCCTCAC
		CGTGTT	GC	CACGTG
Gm1019	Epidermis- specific serine protease-like protein precursor, epidermis- specific SP- like putative peptidase	TCATCGGTCAATTCTGCC	CCCAGCAAGAAGCTG	TGCTTGCCCAATATCTCAAA
		CA	GAACT	GCAGCTG
Gm249	Novel protein, Mername- AA184 peptidase	GAAGAGCGCCATCGTA	ACAGATTGATGAGGTA	TTTGTGCTCCCAATTTGCTTG
		TTTTCT	CAAGTCGGA	CCA
Gzma	Granzyme A	GGGATTCTGGCAGCCC	ATCGGCGATCTCCACA	TGATGGTATTTTGGCAGGCA
		TC	CTTC	TCACCTCTTT
Gzmb	Granzyme B	CTGCAAAGACTGGCTT	GGCAGAAGAGGTGTT	TTCACAAGGACCAGCTCTGT
		CATGTC	CCATTG	CCTTGGC
Gzmc	Granzyme F	CCGCTTGTGTGTA AAA	TTGTGAAGACTTGTGG	CAGGCATCGTCTCCTACGGG
		GAGCAG	AGCTGATC	CAAAC
Gzmd	Granzyme D	AGGAATCTTCACTAAGG	CACGGGTGGTTTAACT	TGCCGTGGATAAGCTGGAAC
		TTGTGCAC	CCTGTT	ATGAAGT
Gzme	Granzyme E	CAAAAGCCATTCCCCAT	CTTGGCCTTACTCTCC	AATGCCACTGCCTTCTTCAG
		CC	AGCTTTAA	TGACATCA
Gzmg	Granzyme G	GTTAAACCACCCGTGC	TTCATTCTTTGCTGCC	TGTCCGACCTCAGGCAAGAA
		CTGA	CAGTC	CCACA
Gzmk	Granzyme K	CATCCCATTCTCAGGAC	GCAGCAGTGCGAAGC	CCGGTCCGCATCGCATGAC
		TTCAG	TTTATC	AT
Gzmm	Granzyme M	AGAGGCCTGCCACCAA	AGGATGACTCACAGG	AGCACAGGACCTACACGGCT
		GC	GTCAGTTC	CAAGGA
Gzmn	Granzyme N	TAAACCACCCGTGCCTT	TTCATTCTTTGCTGCC	TGTCCGCCCTCAGGCAAGAA
		ACC	CACTC	CC
Habp2	Hyaluronan- binding protein	CCCAGAAGCACCCCTA	CGGAAGCACTTTGGAG	CCTGCAAATACCCTTACAGG
		CTACC	CAG	GGACCAG

	2			
Hgfac	Hepatocyte growth factor activator	ACAGCATCACAGTGGT ACTGGGT	TTCTCAATGCCAAATG TCTGTGTC	CACTTCTTCAACCGCACCAC GGATG
Hpn	Hepsin	GCATGGTGACTCAGCC CTG	GACCAACTCTGACTCT GGATGCTA	TCATCTCGCTGCTCCGTGCT GC
Htra1	Serine protease HTRA1	ACACTTGTCTCCGAGT CGG	TCTCAGAAGCCAGGGT CACC	AGAGGAATTTGATGCCCCGA GACCAC
Htra3	High-temperature requirement factor A3 (Pregnancy-related serine protease)	GTCCGGATCTCAGCCT TGAC	ACATCAGGAGCATCTG GTCCA	AGC TCCAGTAGAGGAAGCACAGC GTCC
Klk10	Kallikrein 10	GACCTTCTACCCAGGT GTGATCA	TCTGGCAAGAGTCTTG GTTTCC	CAACAGCATGATTTGTGCTG AGGCAGA
Klk11	Hippostasin/Kallikrein11	GATGGCCACTGAGTCC TTCC	ATGTCATTCCGGTGGT CTTTG	CCGACTTCAACAACAGCCTC CCCA
Klk14	Kallikrein 14	CCCCTGCTCTGCAGT GTGT	TGATTCAGGGTAGGC TCGAT	TGTCAACATCATGTCGGAGC AGGCAT
Klk15	Kallikrein 15, Prostin	CGCCTGGGTGAGCACA AT	GATGCGAGAGACGGA GCG	CGCAAGTTCGATGGTCCAGA GCAAC
Klk1b1	kallikrein 1-related peptidase b1	AAAAGCTTCCTTACCC TTGCTA	CTGTAGTCGTCTGAG GATTTTGG	TGAGCCTCCATCGGAACCGC A
Klk1b11	Kallikrein 1-related peptidase b11, Tissue	CTGAGGACGATGAGAG CAATGA	GCTTACAGCATCTGT GATGTCA	TGATGTTACTACGCCTCAGC GAGCCAG
Klk1b16	kallikrein-11 Kallikrein 1-related peptidase b16, Tissue	CAAGCAGAGAGTCCAC CTCTGTC	TCCCCTGTCTGTTGC CA	CAAGGGCAGGGCTTAGTCAG CATCTG
Klk1b21	kallikrein 16 Kallikrein 1-related peptidase b21, Tissue	CACCCTGACTACAACAT GAGCCT	AACATCAGGTCATTGC TGATGTCATC	ATGAATGACCACACCCCA TCCTGA
Klk1b22	kallikrein 21 Epidermal growth factor-binding protein type A	CAAGATGAACCCTCTG CTCAGC	TGGAGGAGGCTCATGT TGAAGT	TTGGTCAGCAAAAGCTTCCC TCATCCT
Klk1b24	Kallikrein 1-related peptidase b24, Tissue	AGAGATGGGTGGAGGC AAAGA	CCGTGGAGAATACCAT CACAGA	ACTTGTGCGGGTGACTCAGG AGGC
Klk1b26	kallikrein 24 Kallikrein 1-related peptidase b26, Prorenin-converting enzyme 2	TGCAGTTCCTGGACAC CTGTTA	GCATCAATCCCTCCTA GGGAC	TGGTTCCTGATCCTGTTCCC AGCC
Klk1b27	Kallikrein 1-related peptidase b27, Tissue	TGACACCAGCCAGCAT AATGTT	CCATCGGTGCTGAGCA GAG	TGGGCAAAAACAAGCTATTC CAACGTG
Klk1b3	kallikrein 27 Kallikrein 1-related peptidase b3, 7S nerve growth factor gamma chain	GTTCTCCAAGGTATCAC ATCATGG	TTAAGTTTGGTGTAGA CGCCTGG	CCATACCCCATGCGGTGAAC CTGA
Klk1b5	Kallikrein 1-related	CCCTGACTTCAACATGA GCCTC	CATCAGGTCATTGCTG TAGTCGTC	TGAATGAGCACACCCCA CCTGA

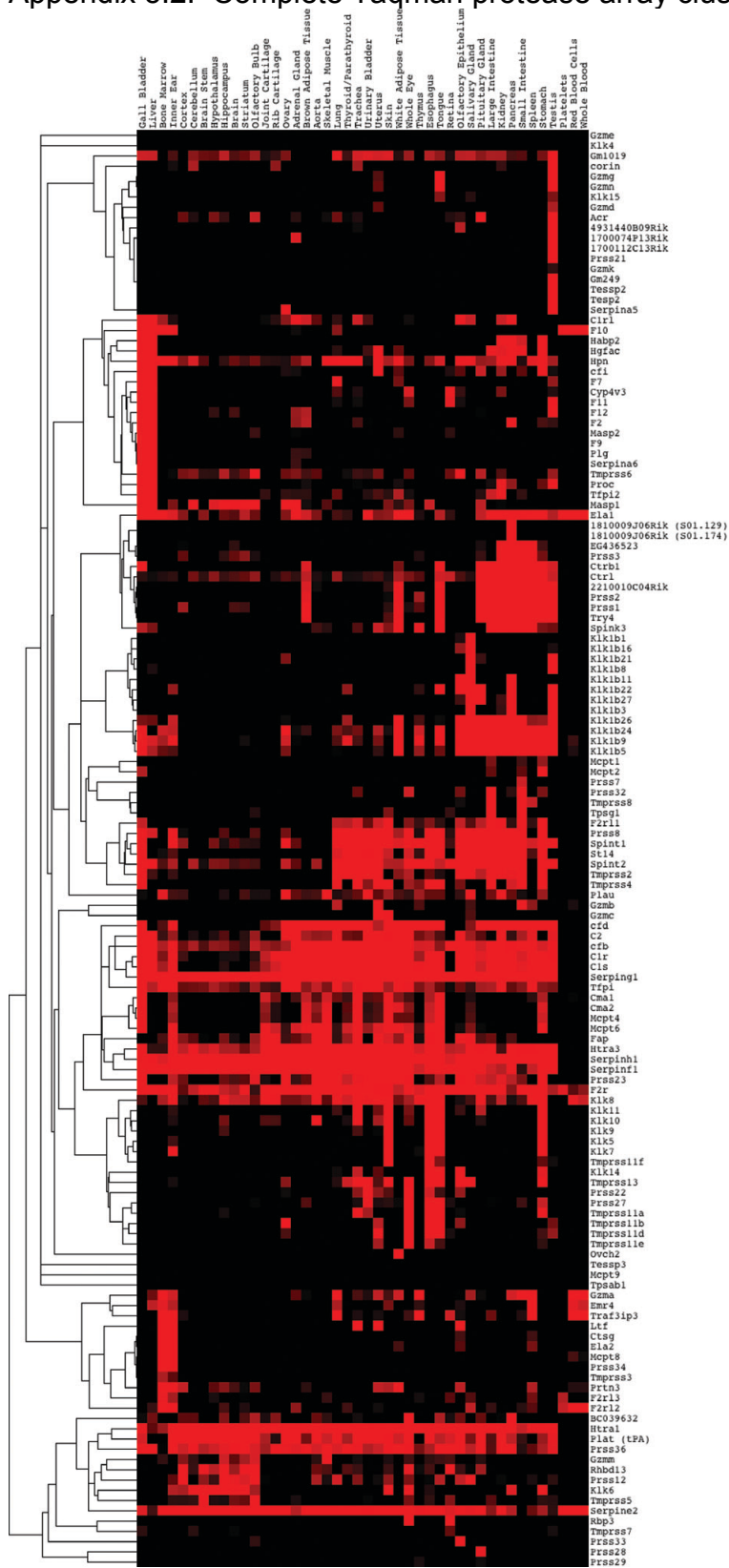
Klk1b8	peptidase b5 precursor Kallikrein 1-related	CAAGCCTGCTGACATC ACAGA	CTAGGCATGTGCTCCC CAGT	CCATCACCCCTGCCACGAAG GAGT
Klk1b9	peptidase b8 Kallikrein 1-related	TGCTGACATCACAGAT GTTGTGA	TGAGGCAAGGCATGT GCTC	CCTGCCTACTGAGGAGCCCA AGCTG
Klk4	peptidase b9, Tissue kallikrein 9 Enamel matrix serine proteinase 1	ACAAGGCCAGGACTGC TCC	AAAACCGTCTTCTGAG AACAGTGC	CACACTCGCAACCCTGGCAG GC
Klk5	Kallikrein 5	CAGGAACCACGGAACC AGTG	ATCTTCAGCA TTCTCAGAGAGGGA	CACCCAACGGCAATGAGGAG CACT
Klk6	Neurosin, Kallikrein 6	CCTGGCAAGATCACCC AGAG	TGACAGGAATCGTTGC CTTCT	CATGTCGCCTGCGCACACCA T
Klk7	kallikrein 7 (chymotryptic, stratum corneum)	CGAGCTGTGAGCCTTT GAGG	CCAGGCAGGACTTTAC AGGG	TGCCACGATGTCCTTACTCC ATGATCA
Klk8	Kallikrein 8, Neuropsin	AGAACAAGTGTGAGAG AGCCTATCC	AGCTCCATTGCTGCTG CC	TCACCGAGGGCATGGTCTGT GC
Klk9	Kallikrein 9	CTGGAGAGGAAGACGG ATGTAGAA	TGACACGCATCAGAGA AGCTG	AGAGGATGCTGCAGGATTCC AGAGCC
Ltf	lactoferrin	CATGGTGCCATTGAC CTG	TCTCTATGTGAAGAAA CCAGATCCC	ACAACCACGTGATGTTTCTG TCCCCA
Masp1	mannan-binding lectin serine peptidase 1, MBL-associated serine protease-3	AGAATCATCGGAGGTC GCAAT	TGTCTTCCACCACTAT GAGGGC	TGAGCTTGGCCTCTTCCCAT GGC
Masp2	Mannan-binding lectin serine protease 2	GGCGGCTACTATTGCT CCTG	ACAAAGGGCTGAGCA CGTGT	AGAGCGGGCTACGTTCTCCA CCAGAA
Mcpt1	Mast cell protease 1	CATAAATGGCAAGTAG CTGAGAAGTCT	GTTGAACACAAAGAGT ACCAGAGAGC	ACCAGCCTGAGACAGATTCT CCAAGCC
Mcpt2	Mast cell protease 2	GTGGCCCATGGTATTG CATC	TCCAGGGCAGGTAATA GGAGATT	AAGCAAAGGCCCTGCAGTC TTCAC
Mcpt4	Mast cell protease 4	CCTTCTGACTTTATCAA GCCGG	TGAGGTAGGTTCTGTC ACTCCAGTT	AGATGTGCCGGCAGCTGG CT
Mcpt6	Mast cell protease 6	TTCCGTCTTGAGTCCCT AGC C	AGGGACCCACACAAT GCAA	TCCGGTTCCCTCTTGCCTCC CA
Mcpt8	Mast cell protease 8	ACTTCCTCGGTATTCA CCAGA	AGGGTTGTTGCAGGA GTTTCA	CCAGCTTTATGCCTTGGATT CGGAAAA
Mcpt9	Mast cell protease 9	CCTTCCTCCTGGGAAC TACTTTG	TTGAATCTGTGGCCTG ATCATG	CAGTCACCACCTCATCATGG GATCCA
Ovch2	Oviductin	AGTTCCTCCAGTGTGAT GCTCAT	GAAATGTCAGCCTGGA AGCC	CCAATCAGATGAAAATGGCA CTGCCAG
Plat (tPA)	Plasminogen activator, tissue	GAGAGAGCTGCTGTGT GTACTGCT	AACCTCCCATGTATTC CCTGG	TTGTGGACTGGCTTTCCCAT TGCCCT
Plau	Urokinase-type plasminogen activator, uPA	CGATTCTGGAGGACCG CTT	GGCCCCAGCTCACAAAT CC	TGTAACATCGAAGGCCGCC AACTCT
Plg	Plasminogen	GTCCTGGGCAGCTATG TTTCC	TAGTTCATCTCCAAGC CAGCATC	CAGGCATTCGAAGACCCAG AGAACTTC
Proc	Protein C precursor	AACTACACCCGGAGCA GCAGT	TTTGGAGAGAGTGGCT GGCT	CGACATTGCTCTGCTCCGC CTAGC
Prss1	Trypsinogen 16	TGTGGCTCTGCCCAGC TC	AGCTAAGAGTGTGGCC CCAGC	TGCACCTGCTGGCACTCAGT GTCTC
Prss12	Neurotrypsin, Motopsin, Brain-specific serine	CCGATAAGCATGCAGC TG TG	AATAAGCCATAGTCCT TGCTCTGG	ACCCTTATAGCCAAGCTGCC GGCA

	protease 3			
Prss2	Serine protease 2, Trypsinogen 20	GCAATGGTGTGAACAA CCCAG	CCTCACAGTCAGCCTG AGGC	TGCTCCAGTGTGTTGATGCC CCAGT
Prss21 (testisin)	Testisin, Tryptase 4	CAACAACAGCATGTGTA ACCATATG	CCAGCGCAAACCATGT CTC	AAAAGCCAGACTTCCGCACG AACATCT
Prss22	Brain-specific serine protease 4	TGAAGGTGCCCATCAT CGA	TCCGTGATGGCTTCCT GAC	TCCGAACCTGCAAAAGCTT GTACTGGC
Prss23	Serine protease 23 precursor, umbelical vein peptidase	GGACAAAGATAGGAGG ACTGATGGT	GCCTTATTCTCTGTA GCAAAGTCTC	TTGCTGGCTTCTGGCCCAAC TCC
Prss27	Serine protease 27, Marapsin	CGTGAAGCAGGTGAAA AGCA	GCAGCTCCACCAGAG CCA	CTCAGTACCAAGGCATGGCC TCCAGTG
Prss28	Implantation serine proteinase 1	CAAGCCAGTGGGCATT GTG	ACATTCTTAGGCTGAC CTGCCA	ATGTACCCACCAGGGAAGT GGCC
Prss29	Serine protease 29, strypsin 2, implantation serine protease 2	CATCAGATGAGGATAG GTCGGC	CCTACACTCCAGAGCC TAAACCC	TCACGATTCCAGAGTGGACG GCC
Prss3	Serine Protease 3	CTCTTAGCTTTGGTGTC AGTGAACC	TCACAGTCAGCCTGAG GCAG	CTCCAGTGCCTGGATGCCCC AC
Prss32	Tryptase 5	AATCAACCGCTCCCAC CAC	ATTGCAGGTCTCAGCA TCAATG	CCTGCAGGAGTTGCAGGTGC CTC
Prss33	Tryptase 6	CGGGATGCTCAGGATG GA	CTCCGCACACATGGG CTC	TGGCAAACAAGCATTAGCA CCGT
Prss34	Mast cell protease-11	CGGTTCCCTCATCCATC CT	CTCCATAGGCCTCCAC CTCTT	TGCTAACTGCTGCTCACTGT GTGAGGC
Prss36	Polyserase 2	AGGTCACTGCTCTGCTT CTGC	GGTGTGAATAGGAGC CGGG	TGGCTCCACTGATCCCTCGC TGAG
Prss7	Enteropeptidase, enterokinase	AGAAAGTCAGCCCAAA GATCGT	GATACAAAGCCACAAC CCAGG	TGGAAGTGACGCCCAGGCA GG
Prss8	Prostasin	AGACCCATCTGCCTCC CTG	CCATCCCCTGACAGTA CAGTGA	CCAATGCCTCCTTTCCCAAC GGC
Prtn3	Myeloblastin precursor (Proteinase-3)	TTGTGACAGTGGTGCT GGGT	GGTGAACCTCTGCTGC TCAGG	CCCACGACCTGCTGAGCTCG GA
Rbp3	interphotoreceptor retinoid-binding protein, unit 1	ACCTATGATCGCCGCA CC	ACTCCACGCTGGTTAC CATAGC	GGCCTAGCAACTCCCGATGG CTG
Rhbd13	ventrhold transmembrane protein	CTGGACCCACACAAAA AGGAG	AGGTTGACAAAGTCCT GGTAGCA	CCTGGCTCTCGCAGACAGCC ATG
St14	Suppressor of tumorigenicity protein 14 (Epithin/matrilipase)	AGGGCAACCCTGAGTG TGAT	AAGGATCGCAGCCCA CAGT	CGGACTGTAGCGATGGCTCC GATG
Tesp2	Testicular serine protease 2	AAGCCACCTCACTGAG CACTGT	TGTTTTGCCTGGCCTA GGG	TCATGCCTCCATCAGTGTGC CACTC
Tessp2	Testis serine protease 2	GTGAGCGTTCGGGTCA GG	CGGCAGTCAGCACCC ACT	TGCATGTCTGTGGAGTTCC CTCATC
Tessp3	Testis specific serine proteinase 3	GAGGCATCCAACATCTT CGG	CTCGTGCAGGTGCCTT CC	TCAGGACCACAGCCGTCCTG CC
Tmprss1 1a	Transmembrane serine protease 11a	GGAAACCCTGCAGCTA AGGG	CCCCACACTGATGGAT GTTG	CCGTGGCAAGTTTCCCTTCA GCG
Tmprss1 1b	Transmembrane serine	TACGACAGAATCACGG GAGGT	ACCATTCACTCTGAGA CTCGCTT	TGCTCACAAAGGAGAGTGGC CATGG

	protease 11b			
Tmprss1 1d	Transmembrane serine protease 11d, Airway trypsin-like protease	ATTCAGGTGGCCCCGT AGTAC	ATATCCCCAGCTCACA ATGCC	AGACTCAAGGCGGCTTTGGT TTGTTGT
Tmprss1 1e	DESC1, transmembrane serine protease 11e	CCCAGAATAACCTTCG GCAAG	GCTCCGTTGTAAGATT GAGGCT	ACAGGTGGACTACATAGATA CCCAGACCTGCAA
Tmprss1 1f	Transmembrane protease, serine 11f, Mername-AA181	TGAGGTGCTCTACGTT GCATCT	CCAACATCAGTCATGC CCAG	AACTACGAGCACACAGAGGT CATGTCTGGTC
Tmprss1 3	Transmembrane serine protease 13	CCAGGAAAGCCTCTAT AGGTCG	GCTCTCAAACCACAGT GGGAA	CCTTCCCGCGGTATGTCTC CC
Tmprss2	Transmembrane serine proteinase 2, Epitheliasin	GAGCTACCCATTGCCT GTGG	CCATGTTACCCAGGC TGTTA	ACCAGCCCAACCTGCACAGC AGATTTA
Tmprss3	Transmembrane serine protease 3	GGGCAATGACATAGCC CTCA	GGCAGACAGATGGGC TGG	TCCGAGC CACTCACCTTTGACGAGAC
Tmprss4	Transmembrane serine protease 4, mCAP	ACTGCAGGCATCAGTC CAGG	TCACTTCCCCTTCGTA GGCA	CAGCACACGGTGCAATGCAG AGG
Tmprss5	Transmembrane serine protease 5, spinesin	TCATTCCCCACCCTTTG TACA	ATTGGTGTCCGGAGCT GC	TGCCCAGAACCATGACTATG ATGTGGC
Tmprss6	Matriptase 2	TCCAGGCCAAGTTCAG GGT	AAACAGGCCTTAGCAG GGTCA	TCCACCCAGCCAGGACACAA GTATTCTG
Tmprss7	Transmembrane serine protease 7, Matriptase-3	TCCATGGAAACAGGCT GTCTG	CTCACTGGAGAGATAA ACTTGCCA	ACATACATCCCAAGGTGAGC AGTCCATGG
Tmprss8	Transmembrane serine protease 8, Distal intestinal serine protease,	GGACATGCTCTGTGCA GGC	ACGAGCGGTCCTCCA GAGT	CGTAGAAGGCCAGAAGGACT CCTGCC
Tpsab1	Tryptase alpha/beta 1	GTGAGCCTGCGTGCCA AT	GCACCCACTGTGGGT GGA	CTACTGGATGCATTTCTGCG GTGGCTC
Tpsg1	Tryptase gamma 1	TGTGTGCCTCCAGAG GC	CTCCCCTGTATAGCCC CAGC	TTCTACCCTGGGATGCAGTG CTGGG
Traf3ip3	TRAF3 interacting protein 3	GATCCAAGCAGCTGTT CAAGG	GACCTCGAGTCTGAGC TGATCA	AGCCAAACACAACAGGTGCT CGGG
Try4	Tesp4 protein, Trypsinogen 9, trypsin 9 (mouse numbering)	TGGCTTCTGGAGGGA GG	GAGCTGTCCATTGCAA ACCA	CTGCCAGGGTGACTCTGGTG GTCC
Serpina5	protein C inhibitor	TGGGTATTCCTACTACC TGGACCA	ATAGAGCGATGGCATT GCCTT	AACATCTCTGCACGGTGGT GGG
Serpina6	corticosteroid-binding globulin	ATTCCCTTCTCCAGCAG TCTGAC	CAGCTTTAGGTTCTGG AGGAGG	TGGCTTGGAGATGAACATGG GCAA
Serpine2	protease nexin-1	GGGTTTGTGGAAGTCT CGGTT	GTACTTGGTAGGATTT CCCATCACC	AGCACAAAGAAACGGACATT CGTGCC
Serpinf1	pigment epithelium derived factor	ATCACCCGACTTCAGC AAGATTAC	TCCACTCGAAAGCAGC CCT	ACCCGTGAAGCTCACCCAAG TGGA

Serping1	C1 inhibitor	CCTCTTCCTGCTCTGG GACC	TACCCAAGCCTGTCTC AACCC	CAGGTTCCAGTCTTCATGG GTCGTGT
Serpinh1	colligin 1	GCGAGATGAGTTGTAG AGTCCAAG	ATAGCACCCATGTGTC TCAGGA	TGGCACGGCAGGAAGTAGC CAAA
Spink3	SPINK1	CTAAGGTGACTGGAAA AGAGGCTAGTT	GTCAGTCCCACACACA GGATCA	CCATGATGCAGTGGCGGGAT GTC
Spint1	hepatocyte growth factor activator inhibitor 1	GGTCTTCGGAGGGAAG GC	GCAGATGACCAGAAAT ACAGCAATA	TTCCCACTGTAGGCTCCGCT GAGGTA
Spint2	hepatocyte growth factor activator inhibitor 2	CTGATGGGTCCTGCCA GC	CACTCCTCCTTGCTCT GGTAGTTAT	TTTATGGAGGCTGTGAAGGC AATGGC
Tfpi	inhibitor unit 1 tissue factor pathway inhibitor-1	ATTCGTGTACGGTGGC TGC	ACTGGATTCTCACAGA TCTTCTTGC	TGGGCAACCGCAACAACCTTT GAAAC
Tfpi2	inhibitor unit 1 tissue factor pathway inhibitor-2 inhibitor unit 2	ACTTTTATTACCTGGAT GCTTGCC	TCACCTATCTTCCATCT CTTGGG	CCGTGCCTGCGTTAAAGGCT GG

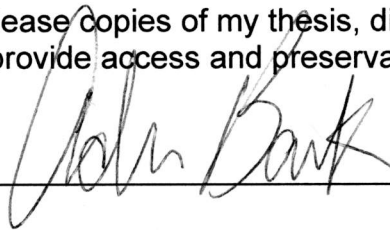
Appendix 5.2. Complete Taqman protease array cluster analysis



It is the policy of the University to encourage the distribution of all theses, dissertations, and manuscripts. Copies of all UCSF theses, dissertations, and manuscripts will be routed to the library via the Graduate Division. The library will make all theses, dissertations, and manuscripts accessible to the public and will preserve these to the best of their abilities, in perpetuity.

I hereby grant permission to the Graduate Division of the University of California, San Francisco to release copies of my thesis, dissertation, or manuscript to the Campus Library to provide access and preservation, in whole or in part, in perpetuity.

Author Signature



Date

12/12/13